# TRIBOLOGICAL PERFORMANCE OF HYBRID COMPOSITES BASED ON PALM KERNEL ACTIVATED CARBON AND ALUMINA BLEND

CHEN WEI WEI

UNIVERSITI TEKNIKAL MALAYSIA MELAKA

# TRIBOLOGICAL PERFORMANCE OF HYBRID COMPOSITES BASED ON PALM KERNEL ACTIVATED CARBON AND ALUMINA BLEND

**CHEN WEI WEI**

**A report submitted**
**in fulfillment of the requirements for the degree of**
**Bachelor of Mechanical Engineering**

**Faculty of Mechanical Engineering**

**UNIVERSITI TEKNIKAL MALAYSIA MELAKA**

**2018**

# DECLARATION

I declare that this report entitled "Tribological Performance Of Hybrid Composites Based On Palm Kernel Activated Carbon And Alumina Blend" is the result of my own research except as cited in the references. The report has not been accepted for any degree and is not concurrently submitted in candidature of any other degree.

Signature    :  ...........................................

Name       :  CHEN WEI WEI

Date        :  ...........................................

# APPROVAL

I hereby declare that I have read this report and in my opinion this report is sufficient in terms of scope and quality for the award of degree of Bachelor of Mechanical Engineering.

Signature            : ...........................................

Supervisor Name     :    PROF. MADYA DR. MOHD FADZLI BIN ABDOLLAH

Date                : ...........................................

# DEDICATION

Dedicated to my beloved father and mother,

my friends and family members

for their encouragement and supports throughout the research.

# ABSTRACT

Nowadays, it is expected the demand of new composites with optimum tribological performance is growing in industry applications. Hybrid composites are finding increased applications because of the improved mechanical properties and wear resistance and hence are better substitutes for single reinforced composites. On the recent global green technology trend, innovative and sustainable raw materials are becoming a priority choice for manufacturer. Agricultural wastes may consider as potential sustainable materials such as carbon consisting wastes to be treated as new reinforcement substitutes in enhancing tribological properties. There are limited tribology studies regarding to reinforcement of agricultural wastes carbon with good wear properties metal. The objectives of this study were to determine optimal composition and tribological properties of blended hybrid composite sample of Palm Kernel Activated Carbon (PKAC) with Aluminium Oxide/ Alumina, $AL_2O_3$ and to compare its wear performance with conventional composites, SK2 carbon steel disc by conducting ball-on-disc tribometer dry sliding test. Basically, PKAC and $AL_2O_3$ were measured according to the set compositions and pressed into disc shaped with size of 74mm diameter using hot compaction technique. Some basic mechanical tests were done when the disc specimens were ready such as surface roughness and hardness tests. Then, specimens were tested through ball-on-disc tribometer test under unlubricated condition at room temperature and surface morphology of specimens were studied by using 3D Surface Profilometer. Collected data were analyzed through qualitative and quantitative approaches. This study has found that friction coefficient and wear rate are highly affected by composition percentages with respect to weight of samples due to the amount of content of PKAC, $AL_2O_3$ and epoxy. Through the comparison between two hybrid composites, PKAC+AL/E (60/40) exhibit lower friction coefficient than PKAC+AL/E (50/50) with difference of 0.057 while for specific wear rate, PKAC+AL/E (60/40) is slightly higher than PKAC+AL/E (50/50) with insignificant difference of $8.530 \times 10^{-8}$ $mm^3$/Nmm. Hence, PKAC+AL/E (60/40) was suggested as optimal composition hybrid composites which exhibited better wear performance in this study.

# ABSTRAK

*Pada masa kini, permintaan komposit baru dengan prestasi tribologi optimum telah berkembang dalam aplikasi industri. Aplikasi komposit hibrid meningkat kerana sifat-sifat mekanikal dan rintangan haus yang lebih baik. Oleh itu hibrid dianggap sebagai pengganti yang baik berbanding dengan komposit bertetulang tunggal. Mengenai trend teknologi hijau global baru-baru ini, bahan mentah yang inovatif dan mampan menjadi pilihan utama bagi industri. Bahan buangan agrikultur boleh dipertimbangkan sebagai bahan berpotensi yang mampan terutamanya bahan buangan yang mengandungi karbon dianggap sebagai pengganti tetulang baru dalam meningkatkan sifat-sifat tribologi. Berdasarkan kajian-kajian sebelum ini, kajian tribologi masih terhad tentang pengukuhan antara bahan buangan agrikultur yang mengandungi karbon dengan logam yang mempunyai prestasi tribology yang baik. Objektif kajian ini adalah menentukan komposisi optimum dan sifat-sifat tribologi tentang campuran komposit hibrid antara kernel sawit diaktifkan karbon (PKAC) dengan aluminium oksida / alumina, $AL_2O_3$ serta membandingkan prestasi tribologinya dengan komposit konvensional, disk keluli karbon SK2 dengan menggunakan tribometer "ball-on-disc" dalam keadaan yang tiada pelinciran. Pada asasnya, PKAC dan $AL_2O_3$ diukur mengikut komposisi yang ditetapkan dan ditekan ke bentuk disk dengan diameter 74mm menggunakan teknik pemadatan panas. Beberapa ujian mekanikal asas telah dilakukan seperti ujian kekasaran permukaan dan ujian kekerasan. Kemudian, spesimen diuji melalui tribometer "ball-on-disc" di bawah keadaan tiada pelinciran pada suhu bilik dan morfologi permukaan spesimen telah dikaji dengan menggunakan 3D Surface Profilometer. Data yang dikumpulkan dianalisiskan melalui cara kualitatif dan kuantitatif. Kajian ini mendapati bahawa faktor yang mempengaruhi pekali geseran dan kadar haus ialah peratusan komposisi yang berdasarkan berat sampel, jumlah kandungan PKAC, $AL_2O_3$ dan epoksi. Melalui perbandingan antara dua komposit hibrid, PKAC + AL / E (60/40) mempunyai pekali geseran yang lebih rendah daripada PKAC + AL / E (50/50) dengan perbezaan 0.057 manakala untuk kadar haus spesifik, PKAC + AL / E (60 / 40) lebih tinggi daripada PKAC + AL / E (50/50) dengan perbezaan yang tidak signifikan $8.530 \times 10^{-8}$ $mm^3$ / Nmm. Oleh itu, PKAC + AL / E (60/40) dicadangkan sebagai komposit hibrid yang mempunyai komposisi optimum dan memaparkan prestasi tribologi yang paling baik dalam kajian ini.*

# ACKNOWLEDGEMENTS

**TABLE OF CONTENTS**

# LIST OF TABLES

# LIST OF FIGURES

# LIST OF APPENDICES

# LIST OF ABBREVIATIONS

| | |
|---|---|
| 2D | Two Dimensional |
| 3D | Three Dimensional |
| Al | Aluminium |
| AL | Alumina |
| $Al_2O_3$ | Alumina / Aluminium Oxide |
| AMC | Aluminum Matrix Composite |
| ASME | American Society of Mechanical Engineers |
| ASTM | American Society for Testing and Materials |
| $B_4C$ | Boron Carbide |
| CoF | Coefficient of Friction |
| DIN | Deutsches Institut für Normung (German Institute for Standardization) |
| E | epoxy |
| EFB | Empty Fruit Brunches |
| FIB | Focused Ion Beam |
| GDP | Gross Domestic Product |
| Gr | Graphite |

| LST  | Low Surface Temperature      |
|------|------------------------------|
| OPF  | Oil Palm Fronds              |
| OPMF | oil palm mesocarp fibre      |
| OPS  | oil palm shell               |
| OPT  | Oil Palm Trunks              |
| PKAC | Palm Kernel Activated Carbon |
| PKS  | Palm Kernel Shells           |
| POME | Palm Oil Mill Effluent       |
| PPF  | Palm Pressed Fibers          |
| PSAC | Palm Shell Activated Carbon  |
| PSM  | Projek Sarjana Muda          |
| RHA  | Rice Husk Ash                |
| SiC  | Silicon Carbide              |
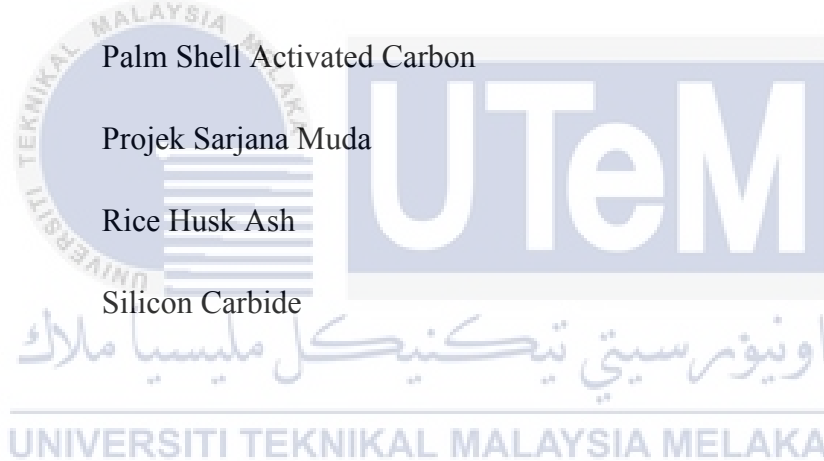
# LIST OF SYMBOLS

| | | |
|---|---|---|
| F | = | Frictional Force |
| H | = | Hardness of Rubbed Surface |
| K | = | Wear coefficient |
| k | = | Specific Wear Rate |
| L | = | Sliding Distance |
| $M_a$ | = | Mass after sliding test |
| $M_b$ | = | Mass before sliding test |
| $M_{loss}$ | = | Loss of Mass |
| r | = | Radius of Disc Sample |
| t | = | Thickness of Disc Sample |
| t | = | Time |
| $t_s$ | = | Time to reach steady state |
| V | = | Wear Volume |
| $V_{loss}$ | = | Loss of Volume |
| W | = | Applied Load |
| ρ | = | Density |

# CHAPTER 1

# INTRODUCTION

## 1.1     Background of Study

During the previous decade, the need for the new wear resistant material for high performance tribological applications has been one of the major driving forces for the tribological development. Importance of tribological properties influenced many researchers to study friction and wear behavior of lubricant materials and at the same time to identify the best composition of composites for various industrial applications (Kathiresan and Sonarkumar, 2010). This is due to the rapid growth of automotive, aerospace and biomedical fields which cause the growing demand of generating improved composites with optimum wear performance for certain harsh industrial applications (Jost and Peter, 1966). Previous tribology studies have introduced a few methods to enhance wear properties such as coating, alloying and composites reinforcement. In this study, the method used to test and enhance the wear properties of hybrid composites is composites reinforcement. Hybrid composites are finding increased applications because of the improved mechanical and wear resistance and hence are better substitutes for single reinforced composites (Slobodan et al., 2011). Hybrid materials are composites consisting of two constituents at the nanometer or molecular level. Commonly one of these compounds is inorganic and the other one organic in nature. The hybrid composites used in this study consist of palm kernel activated carbon-epoxy (PKAC-E) and alumina (with the chemical formula of $Al_2O_3$) which are the organic and inorganic compound respectively. Nowadays, activated carbon started emerged in

1

tribological applications due to its high porosity which provide large surface area. By referring to Yusoff et al. (2010), graphite and porous carbon such as palm shell activated carbon exhibited its potential to act as a self-lubricating material when reinforced in aluminum alloy, which significantly improved wear resistance by increasing palm shell activated carbon (PSAC) content up to 10 wt.% (Yusoff et al., 2010). Due to the potential of PSAC, PKAC has become an interesting research material in tribology field. Based on the previous studies, researchers stated a hypothesis that the excellent performance shown by the materials (PSAC) were obtained through residual oil from the palm fruit. Hence, the hypothesis supported the possibility of PKAC may also carry the residual oil from palm oil fruit (Tahir et al., 2017). Zamri (2012) found the content of reinforcement (PSAC and slag) had significant effect on wear resistance of aluminum matrix composite. The results showed the wear resistance of hybrid composite is better than un-hybrid composite due to the good bonding of slag particles in aluminum matrix causing improved the ability in supporting load. Prasad and Shoba (2014) have studied the dry sliding wear behavior of unreinforced alloy and hybrid composites through pin-on-disk wear test and the result showed the hybrid composite (aluminium, Al/ rice husk ash, RHA/ silicon carbide, SiC) exhibit higher wear resistance than the unreinforced alloy. Thus, a few of these previous studies proved that there are possibilities and potentials exhibited for activated carbon (PSAC/PKAC) and aluminum as one of the major research materials in tribological applications development. Last but not least, the global awareness of promoting the sustainable and environmental friendly products had influenced the increasing of demand in replacing synthetic composites materials with natural-based or secondary source of materials such as wastes or biomass products. Hence, this is one of the motivations for researchers to investigate the new reinforcement substitutes from agriculture wastes in order to be used in fabrication of composites which able to be classified as one of the effective self-lubricating materials.

2

## 1.2 Problem Statement

The global impact of friction and wear on energy consumption, economic expenditure, and carbon dioxide emissions are still considerable (Jost and Peter, 1966). Based on "Influence of tribology on global energy consumption, costs and emissions" which published by Holmberg and Erdemir (2017), they considered four main energy consuming sectors which are transportation, manufacturing, power generation and residential. In these four sectors, 23% of the world total energy consumption originates from tribological contacts. Of that 20% is used to overcome friction and 3% is used to remanufacture worn parts and spare equipment due to wear and wear-related failures. Lubrication technologies for reduction of friction and wear in automation and machinery can reduce energy losses by 40 % in 15 years and by 18% in 8years. These savings would amount to 1.4% of GDP (Gross Domestic Product) per year and 8.7% of the long term total energy consumption on a global scale (Holmberg and Erdemir, 2017). Although there were many researches about tribological studies, few of them focused on friction and lubricants of hybrid composites. A clear understanding of effect of the composites' compositions on wear behavior is very essential for maximized the work efficiency. Therefore, a basic awareness of tribology in wear is important to increase the work performance efficiency of machinery without wasting valuable resources, reduce the cost of maintenance and avoid common manufacturing issues.

Previously, there are several studies on wear behavior of hybrid composites which undergoes hard reinforcement by using silicon carbide or soft reinforcement by using carbon. However, the studies and information available recently for natural-based material reinforcement such as PKAC is limited. Yusoff (2012) has done a similar research on physical and wear properties of hybrid biomass by-product particulates reinforced aluminum matrix composite (AMC) which the reinforcement is using PSAC and slag. His study's result showed that hybrid composite (undergoes PSAC and slag reinforcement) has better wear

resistance than un-hybrid composite. Hence, PKAC similar with PSAC as one of the palm oil extraction wastes is chosen in this study because it may be a potential self-lubricating material as well.

Malaysia palm oil production is the world's second-largest producer of the commodity after Indonesia. The biomass produced by Malaysia oil palm industries has created severe disposal problems. The solid wastes produced are empty fruit brunches (EFB), oil palm trunks (OPT), oil palm fronds (OPF) palm pressed fibers (PPF) and palm kernel shells (PKS) and palm oil mill effluent (POME). POME digestion gas which consists of methane will cause the ozone depletion and reduce the air quality. Incineration of EFB can be used for power generation and PKS is potential to be used as self-lubricating materials by transforming it into activated carbon. However, current practice is actually wasting the potential renewable energy resources. Moreover, by looking into the conventional hybrid composites recently, there is limited creation of the renewable sources-based hybrid composites which able to turn the biomass wastes residues into wealth.

In conclude that maximizing the usage of secondary resources and renewable energy is desirable for both economic and environmental reasons. In this study, an attempt is made in developing a new reinforced hybrid composite as one of the alternative self-lubricating material which is sustainable, effective and environmental friendly.

4

## 1.3 Objectives

Objectives of this study are:

a) To determine the optimal composition of the hybrid composites based on palm kernel activated carbon and alumina blend;

b) To investigate the tribological properties of the hybrid composite samples under dry sliding conditions;

c) To compare the tribological performance of the hybrid composites with the conventional composites, SK2 carbon steel disc;

## 1.4 Scope

Scope of this study:

1. Materials : Palm Kernel Activated Carbon, Alumina and Epoxy

2. Samples compositions : Shown in Table 1.1 below

3. Machine : Ball-on-disc Tribometer

4. Load : 49.05N (5kg)

5. Sliding Speed : 400rpm

6. Sliding Distance : 3000m

7. Surrounding Temperature : Room temperature

8. Sliding Test Standards : ASTM G99-95a

Table 1.1: Composition percentages of testing composites

| Sample | Palm Kernel Activated Carbon (PKAC), % | Alumina (Al$_2$O$_3$), % | Epoxy, % |
|---|---|---|---|
| PKAC+AL/E | 25 | 25 | 50 |
| PKAC/E | 50 | - | 50 |
| AL/E | - | 50 | 50 |
| PKAC+AL/E | 30 | 30 | 40 |
| PKAC/E | 60 | - | 40 |
| AL/E | - | 60 | 40 |
| PKAC+AL/E | 35 | 35 | 30 |
| PKAC/E | 70 | - | 30 |
| AL/E | - | 70 | 30 |

# CHAPTER 2

# LITERATURE REVIEW

## 2.1    Introduction

There is an increasing worldwide need for high wear performance materials such as hybrid composites. Recently, many researches have been conducted in the development of materials to investigate suitable materials with broad spectrum of properties combinations which to fulfill the demand of wide range engineering applications. For example, those combinations are high specific strength, low coefficient thermal expansion and high thermal resistance, good damping capacities, superior wear resistance, high specific stiffness and satisfactory levels of corrosion resistance (Ravindran et al., 2012). Previous studies have found that the hybridization of two reinforcements able to improve wear resistance, to reduce wear loss and have a lower friction coefficient which are the major topics in tribology (Bodunrin et al., 2015; Guo and Tsao, 1999; Ravindran et al., 2012).

## 2.2    Tribology

### 2.2.1    Friction

Tribology is a term which defined based on Greek word and including three keys topics which are friction, wear and lubrication. Friction is a resistance to attempted motion of two objects which moving relative to another. Based on Amonton's and Coulomb's Law of Friction which known as classical laws of friction which not fundamental stated that friction is proportional to normal load, friction is independent of the apparent area of contact, friction is independent of sliding velocity, friction is independent of temperature and friction is independent of surface roughness. These classical laws of friction are not applicable for ceramics and polymers. In years 1930-1970, Philip Bowden and David Tabor conducted analysis of contact mechanics and they concluded that friction consists of adhesion force and deformation of ploughing force at micro contact level. Adhesion force associated with real contact area at asperity level while ploughing is the force needed for harder surfaces' asperities to plough through softer surface. Normally metal-ceramic and metal-polymer contacts exhibit elastic deformation at asperity level. Polymers considered as viscoelastic material with strong time dependence of mechanical properties. In addition, friction of polymers is highly affected by surface roughness due to the ploughing effect which contribute to high friction if high surface roughness detected. Presence of tribofilms or generated debris will affect the friction of polymers as well. Operating temperature is important to be taken into account in friction analysis of polymers because the mechanical properties of polymers is sensitive to temperature and an elevated temperature will result in softening the polymer material. Frictional behavior of materials often represented by coefficient of friction which can be obtained from equation below, where $\mu$ is coefficient of friction, $F$ is frictional force (N) and $W$ is applied load (N) (Tahir et al., 2015).

8

$$\mu = \frac{F}{W} \qquad\qquad (2.1)$$

### 2.2.2 Wear

Wear happened due to sliding and cause loss of materials. Wear is crucial to be studied as it may lead to components failure, system malfunction, shorten components' performance lifetime, reduce work efficiency and produce unwanted noise. For example, loss of materials from the sliding surfaces will reduce the dimension of the component and cause the clearance increases between the two moving parts. This may further be leading to catastrophic failure due to fatigue fracture of the components. In addition, the wear debris produced may cause contamination especially in food manufacturing industry. The wear debris which trapped in machines will block the vessels, pipelines, affecting the normal function of the system. Maintenance cost of wear is enormous thus wear is vital to be studied and eliminated since the early ages of industry. Possible parameters which affect the dry sliding wear are speed, load and time. A general formula used to calculate wear rate is as shown below (Agunsoye et al., 2013).

$$\text{wear rate} = \frac{\text{wear volume loss}}{\text{sliding distance} \times \text{applied load}} \qquad (2.2)$$

There are two types wear which are adhesive and abrasive wear. Adhesive wear occurred between two surfaces which rub together and cause removal of material from softer material surface especially when the load applied is high enough and both surfaces adhere to each other and form micro-joints. The continuous sliding motion will cause the rupture of

the micro-joints and the fragment of the softer material is transferred and adhered to countersurface. Figures 2.1 and 2.2 shows the adhesive wear between two surfaces.
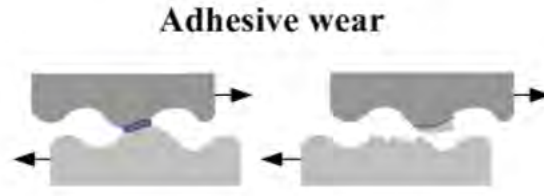


Figure 2.1: Adhesive wear between two surfaces (Kopeliovich, 2017)

By referring to Archard wear model, the calculation of adhesive wear under sliding condition is by using the equation below where $V_{adh}$ is the adhesive wear volume, $K$ is the wear coefficient, $P$ is the normal load, $H$ is the hardness of material, and $L$ is the wear stroke distance (Yunxia et al., 2016).

$$V_{adh} = K \frac{P}{H} L$$ 

(2.3)

Study by Li (n.d.) stated that enhancing hardness and strength of materials and conducting surface engineering to change the surfaces' chemical nature will effectively minimize the adhesive wear rate. On the other hand, abrasive wear may occur under two situations which are either three body abrasion or two body abrasion. Two body abrasion normally occur in metal to metal contact situation when harder material abrading against the softer material which hardly to be eliminated through polishing. While three body abrasion consists third rigid particles which trapped in between two surfaces and rubbing against the soft surface. Both two body abrasion and three body abrasion are demonstrated in Figure 2.2 and 2.3.

Figure 2.2 Two body abrasive wear (Kopeliovich, 2017)
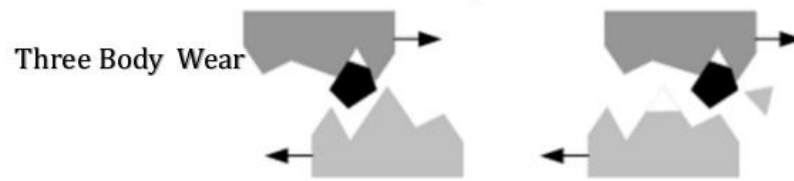


Figure 2.3: Three body abrasive wear (Kopeliovich, 2017)

There is an alternative way of prediction of abrasive wear rate is h, the depth of hard particles penetrates the material surface is linearly proportional to applied load, *P* and inversely proportional to hardness of surface being rubbed, *H*. With the sliding distance of *L*, wear volume of *V* and wear coefficient of *k*, the formula or the Archard's wear equation can be expressed in the form which shown at below (Velickovic et al., 2017).

$$K = \frac{V \times H}{W \times L} \qquad (2.4)$$

By referring to formulae of abrasive wear rate, the hardness of material, H is a most adjustable parameter if the function of a machine is needed to be maintained. Surface hardness can be changed by changing materials, undergoes heat treatment and surface engineering to prevent abrasion wear in machines.

11

### 2.2.3 Lubrication

Lubrication referred to as "lube" that a substance introduced in between two contacting bodies to reduce friction between them, improving efficiency and reducing wear. Lubricant helps to avoid direct contact between objects and is also act as cooling agent and to carry away contaminants other than only to reduce friction and wear. It can be in solid, semisolid, liquid or gaseous form (Shaffer, 2013). Solid lubricant characteristics of hybrid composites is important to be studied in this current research. A few typical harsh applications require solid lubricant instead of liquid because liquid lubricant will squeeze out especially during the sliding or reciprocating motion. Solid lubricant often used in applications with high loads applied to sliding surfaces in boundary or mixed lubrication regimes, over wide range or elevated temperature conditions (Bart et al., 2013). Solid lubricants are classified as structural lubricants, mechanical lubricants, soaps and chemically active lubricants. Lubricating properties of structural lubricants such as graphite and metal dichalcogenides are depends on their layered lattice structures. Previous study of frictional wear stability mechanisms of an activated carbon composite derived from palm kernel by phase transformation study supported that PKAC transferred layer is an effective medium contribute to low friction and low wear at certain applied loads (Mahmud et al.,2017). The study analyzes that phase transformation of PKAC changed from carbon-like-structure to graphite-like-structure ($sp^2$) which also known as layered structure during sliding motion. Low shear strength bonds of $sp^2$ rich structure consistently produced a low friction coefficient (Abdollah et al., 2010).

## 2.3 Hybrid Composites

As the ways of improvement of wear which mentioned above, both adhesive and abrasive wear can be minimized through changing materials and improving the surface hardness. According to previous studies, the results shown that hybrid composites will exhibit higher wear resistance than unreinforced alloy (Prasad and Shoba, 2014; Surendran et al., 2017; Yusoff, 2012). Composites is produced by hybridization of two or more different materials with different properties. The different materials blended together to provide a unique property. A material is classified as composite when the blended materials show significant property changes, constituents content is more than 10% and property of one of the constituents is five times greater than the other.

### 2.3.1 Definition of Hybrid Composites

There are several definitions for hybrid composites materials. The first definition by Fukuda (1984), hybrid composites defined as materials which made by mixing two or more type of fibers or constituents in a matrix (Fukuda, 1984). It is a weighed sum of different materials where there is a balance between the strength and weakness of both materials so the strength of one of the fibre can complement what lacking in the other fibre (Jacob et al., 2014). Hybrid composites defined consists of organic and inorganic hybrid materials or inorganic biomaterials. They stated that hybrid materials are less than 103 nanometers and the materials and composites are classified according to the scale levels as shown in Figure 2.4 below.
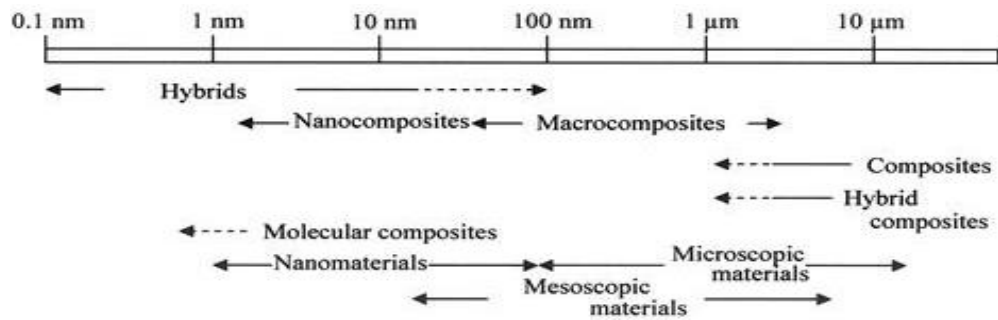
Figure 2.4: Classification of materials according to different scale levels (Nanko and

Makoto, 2009)

Other than that, "hybrid" in hybrid composite materials means hybridization of composites materials which also known as the composites that reinforced with fibers or material consisting reinforced metals and thin foil metals (Nanko, 2009). Composites consists of matrix and reinforcement. Matrix typically has good shear properties and low density which suitable to be used to hold the reinforce fibres together in positions, protect fibres from surrounding disturbances or abrasion and distributes the loads evenly between fibres. Whereas reinforcement is commonly in high strength, high stiffness which able to help in maintain the strength of matrix, withstand load and to provide desired properties.
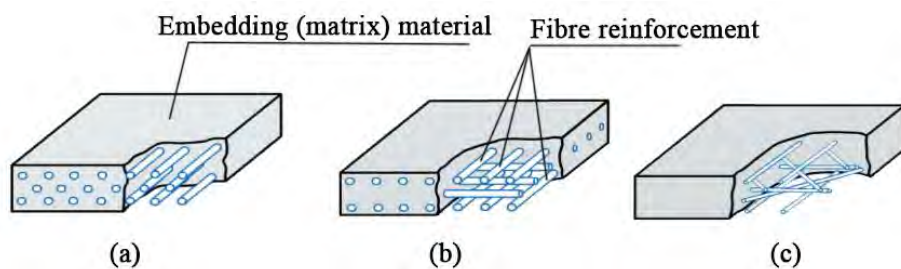


Figure 2.5: Fibre reinforcement composites (Tamas and Turcsan, 2016)

14

**2.3.2 Classification and Applications of Hybrid Composites**

Classification of composites materials is shown in the Figure 2.6 (Kumar and Kuppan, 2017). There are two categories under composites materials which are either fiber-reinforced or particle-reinforced composites. Particle- reinforced is separated into two types which are random or preferred orientation while fibre-reinforced is separated into single or multi- layer composites. Single layer composites consist of continuous or discontinuous fibres. Continuous fibres consist unidirectional or bidirectional reinforcement and discontinuous fibres consist of random or preferred orientation. Multi-layer composites separated into laminates or hybrid composites.
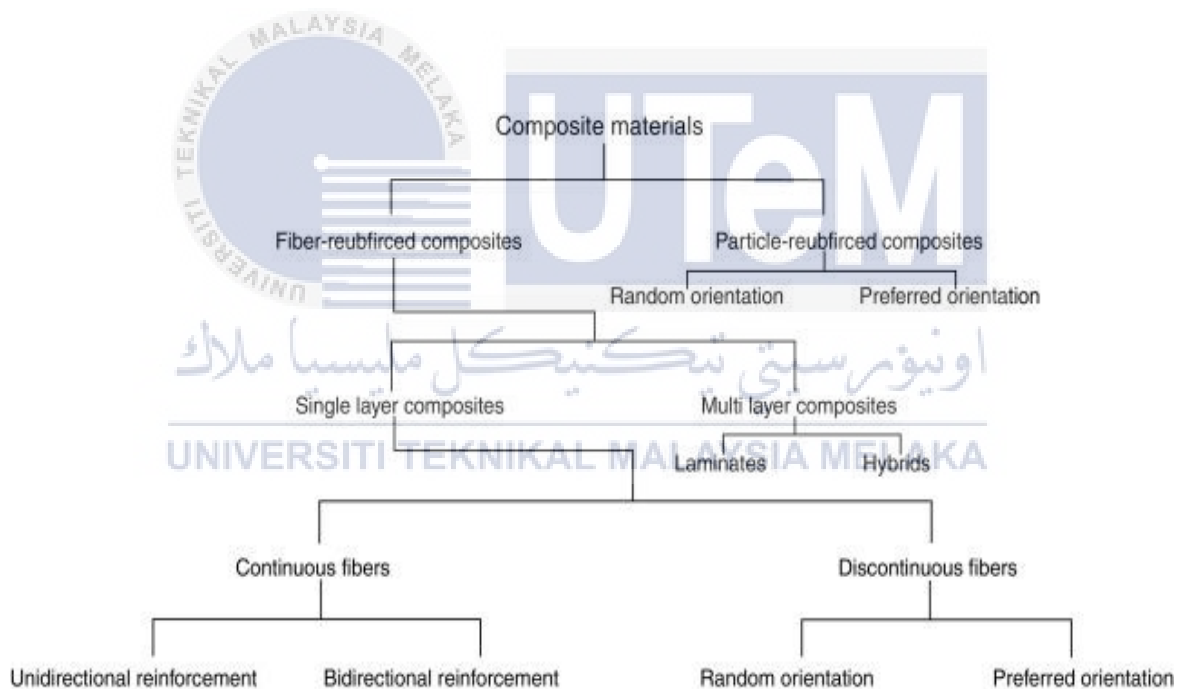


Figure 2.6: Classification of composites materials (Kumar and Kuppan, 2017)

There are a few types of composites exist in the world and one of it is known as natural composites. Example of natural composites such as wood, it is made from long cellulose fibres that held together by lignin. Lignin is a complex organic polymer deposited

15

in the cell walls of many plants, making them rigid and woody. Lignin and cellulose fibres are both weak materials and they merged together to form a strong wood trunk. Besides, human bone is also considered as a composite which combine hydroxyapatite and collagen which is strong enough to provide sufficient support to human body. Hydroxyapatite is a brittle material and mainly is calcium phosphate while collagen is only a soft and elastic material which can found in hair and nails. Early man-made composite example is mud bricks. Mud bricks have good compressive strength and poor tensile strength. By combining mud and straw, a brick which resistant to both compressing and cracking can be achieved. Concrete is a compound of small stones, cement and sand with good compressive strength. It can be reinforced by adding metal rods or wires to increase its tensile strength which is good for construction purpose. The first modern composite is fiberglass which widely used in aeronautics, automotive and ocean engineering applications. Matrix is a plastic which reinforced by glass fine threads which often woven in sort of cloth. Glass is strong and brittle so the plastic matrix able to hold the glass fibres together without damage by helping to evenly distribute out the forces acted on them. A more advanced composite is using carbon fibres or carbon nanotubes instead of glass because it is stronger and lighter than glass fibres. It is commonly found to be used in aircraft structures or sports equipment due to its lightness and strength which promote the possibilities for developing lighter transportation vehicle or aircraft which will use lesser fuel compare to recent transportation in the world. The world's largest passenger airliner, Airbus A380 is a double-deck with four engine jet aircraft which manufactured by European manufacturer Airbus. More than 20% of the structures are made up of modern composites materials such as plastic reinforced with carbon fibres. In addition, a new glass-fibre reinforced aluminium composites is being used and it is 25% stronger and 20% lighter weight than conventional aircraft structures. Hybrid composites has special abilities to be used to fulfill different design requirements in a more economical way. For

example, the more expensive substances such as boron and graphite can be substitute by glass fibres and Kevlar. Comparison between hybrid composites with the common composites is result in hybrid composites exhibit balanced strength and stiffness, balanced bending, balanced thermal distortion abilities reduced weight, improved fracture toughness and improved impact resistance (Chamis and Lark, 1977). Hybrid composites are the potential composites to be used in this study due to its combination properties that cannot be found in single type of composites materials. Hybrid composites generally considered promoting low density, high strength, high stiffness and high wear resistance. This is the main reasons that the investigations of hybrid composites have been one of the deep interest for researchers to be developed in order to fulfill the demand of industry. Those industries which bring up the trend of examination of hybrid composites are such as automotive industries, electronic components industry, aeronautics and transportation industry.

### 2.3.3 Researches and Studies of Hybrid Composites

Previous researches have concentrated on tribological potential or wear behavior on different hybrid composites materials (Mitrovic, 2012; Prasad and Shoba, 2014; Ravindran et al., 2012; Surendran et al., 2017; Uthayakumar et al. 2012; Yusoff, 2012). The investigations by all these researchers have presented that hybrid composites possess better tribological behavior, better mechanical properties and higher wear resistance than un-hybrid composites. This is also proved that hybrid composites considered as an outstanding potential material where high strength, light weight and wear resistant materials are the major demand in aerospace, automotive and engineering sectors in recent times. Moreover, some effort should be done to carry out a low-cost reinforcement to produce a high-quality hybrid composites by using secondary source materials or biomass wastes products

17

(Pruthviraj, 2014). Prasad and Shoba (2014) found that the composites hardness increased, wear rate decreased, and the wear resistance increased with the increasing of reinforcement percentages of rice husk ash content (Prasad and Shoba, 2014). Blaza and Lozica (2015) proposed that the hybrid composites compounded is aimed to enhance the structural, tribological, thermal, chemical and material properties of it. Besides, the hybrid composites with aluminium matrices are having higher wear resistance, higher specific stiffness and higher fatigue resistance (Blaza and Lozica, 2015).

Rajesh and Kaleemulla (2016) conducted an experimental investigation on mechanical behavior of aluminium metal matrix composites. Table 2.1 shows the sample specimen composition used in the experiment which are pure aluminium alloy 7075 (Al-7075), aluminium oxide or alumina (Al2O3) and silicon carbide (SiC) (Rajesh and Kaleemulla, 2016). Hardness test is carried out by using Vickers hardness tester and results of hardness against samples composition variation is shown in Figure 2.7.

Table 2.1: Composition of sample specimen of Al-7075-$Al_2O_3$- SiC (source: Rajesh and Kaleemulla, 2016)

| Specimen Code | AL -7075 | $Al_2O_3$ | SiC |
|---|---|---|---|
| 1 | 100% | 0 | 0 |
| 2 | 90% | 5% | 5% |
| 3 | 80% | 10% | 10% |
| 4 | 70% | 15% | 15% |
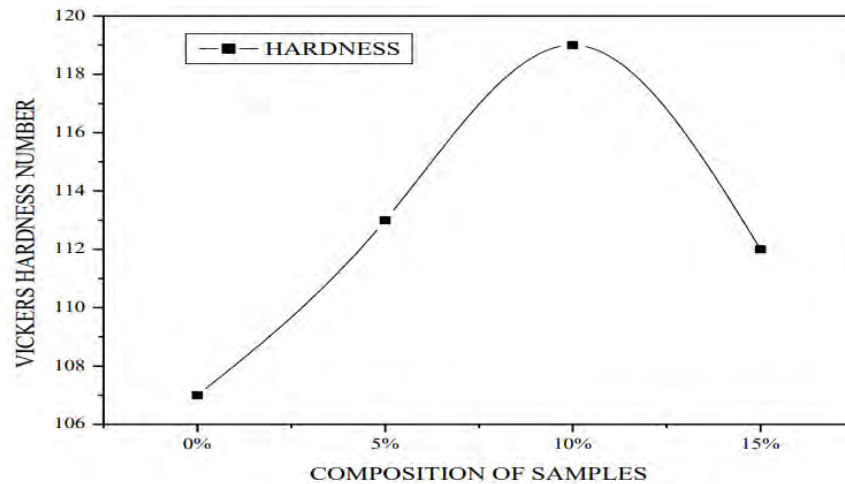
Figure 2.7: Vickers hardness test against variation of composition of specimen samples

(Rajesh and Kaleemulla, 2016)

Experiment result reveals that the addition of silicon carbide and alumina particles in aluminium matrix improved the mechanical properties with the prove of wear rate decreased after reinforcement of composites. The optimal composition obtained from the experiment analysis to have the highest hardness property is 80%-10%-10% for Al 7075-SiC-Al2O3 (Rajesh and Kaleemulla, 2016).

Previous study by Surendran et al. (2017), they had examined the wear behavior of aluminium casting alloy LM25 reinforced with various weight ratios of alumina, $Al_2O_3$. The alumina weight ratios are 1%, 1.5%, 2% and 2.5%. Wear behavior of hybrid composites are investigated by using pin-on-disc machine under load and unload conditions. The results obtained are similar to other studies where the wear rate is decreased and wear performance is improved with the increase of reinforcement content, alumina in LM25. The best performance achieved for the composition of 97.5% LM25 and addition of 2.5% of alumina (Surendran et al., 2017).

Hitnesh (2011) proved that microhardness and wear resistance of the composites increases after the addition of silicon carbide, alumina and red mud. Wear rate decreases as the weight percentages of silicon carbide and alumina increases up to 2.5-10% (Hitnesh, 2011).

According to Ravindran et al. (2012), they investigated tribological properties of powder metallurgy that processed aluminium self-lubricating hybrid composites with SiC additions. The researchers have tested both hard reinforcement and soft reinforcement which are silicon carbide, SiC and graphite, Gr to produce Al-SiC-Gr hybrid composites. Wear mechanism is examined through the worn surface, wear track and wear debris analysis. Hard ceramic in SiC helps in enhancing wear resistance and increase friction coefficient at the same time. They found that Al-SiC-Gr hybrid composites exhibit higher wear resistance and higher friction of coefficient than matrix. This proved that wear resistance increases with the increasing of reinforcement SiC content due to hardness of composites increased (Ravindran et al., 2012).

The research study by Uthayakumar et al. (2012) also conducted similar investigation about the wear performance of Al-SiC-$B_4C$ (aluminium- silicon carbide- boron carbide) hybrid composites under dry sliding conditions. Intention of the researchers is trying to improve wear performance of aluminium matrix with hard reinforcements. Researchers emphasize the dry sliding wear test on aluminium matrix with 5% of SiC and 5% of $B_4C$. The effect of reinforcement on wear mechanism is examined through detailed metallurgical and energy dispersive analysis. The experiment is done with different normal load and sliding speed with the use of pin-on-disc machine. They proposed the result of hybrid composites able to maintain wear resistance properties up to 60N with the sliding speed range of 1 to 4 meter per second. Besides, wear rate and friction coefficient are decreased up

to 4 meters per second and the result is reversed in sliding speed which higher than 4 meters per second. Worn surface of the composites is study by using FIB (Focused Ion Beam) technique to examine the subsurface deformation. Deformation is increased with increasing of normal load applied. The lower the deformation of subsurface, the lower the wear debris formation. Plastic deformation of the wear mechanism is driven by abrasion at sliding speed ranges of 1 to 4 meter per second and load ranges of 20 to 60 N and 80 to 100N. High order of local stress due to higher sliding speed and higher applied load causes melt wear occurred (Uthayakumar et al., 2012).

Furthermore, a research with the topic of the physical and wear properties of hybrid biomass by-product particulates reinforced aluminium matrix composite by Yusoff (2012) concluded that the bulk density, hardness and wear resistance of hybrid composites is better than un-hybrid composites with 7.5 wt.% Slag/7.5 wt. %PSAC content in aluminium matrix. This is due to the high strength of slag which help in withstanding the load and presence of smear debris particle in between the sliding surface which help to reduce wear rate.

Velickovic et al. (2016) have carried out optimization of tribological properties of aluminum hybrid composites using Taguchi design. The study analyzed the effect of reinforcement of graphite on A356 aluminium matrix composites with various load and sliding speed by taking the constant sliding distance. Taguchi method is used in the experiment to figure out the optimal composition by investigating the wear mechanism and performance with the use of block-on-disc tribometer to perform dry sliding test. Al-SiC-Gr (aluminium-silicon carbide-graphite) is used in the experiment and the optimal composition and parameters obtained are 3wt% of graphite, 10N load and 0.25 meters per second sliding speed after carried the ANOVA analysis and Taguchi method. The impact on the specific wear rate is represent in percentages where impact from load is 69.16% and impact from

sliding speed is 14.43%. Researchers concluded that the optimal composition of the composite which exhibit the best tribological properties is A356/10SiC/3Gr. The wear mechanism in this study is justified as adhesive wear due to the formation of pits which discovered after conducted the worn surface analysis by using SEM (scanning electron microscope) (Velickovic et al., 2016).



(a)           (b)           (c)
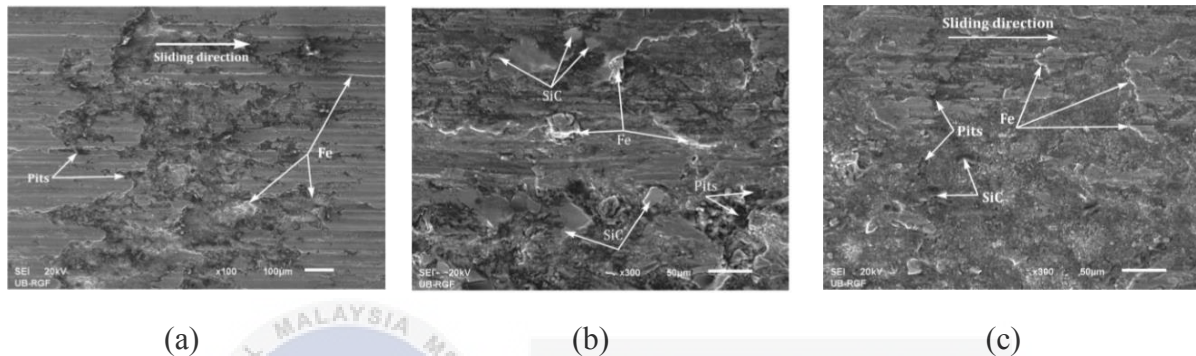
Figure 2.8: SEM analysis: (a) A356/10SiC; (b) A356/10SiC/3Gr; (c) A356/10SiC/5Gr with load of 10N (Velickovic et al., 2016)

It appears from the aforementioned investigations that numerous investigations have been conducted the tribological studies on hybrid composites. The studies validated the desirable properties of reinforcement are high strength, low cost, chemically stable, low density, well distribution and easy to fabricate. Most of the published literatures recently were focused mainly on the wear behavior of reinforcement aluminium matrix with graphite or carbides. However, there is no attempt was made to investigate wear performance of hybrid composites based on alumina and palm kernel activated carbon (PKAC). There are limited studies which indicated and revealed the potential of alumina and carbon in tribological application studies so this was the motivation behind the present study.

22

## 2.4 Alumina / Aluminium Oxide ($Al_2O_3$)

Alumina is also known as aluminium oxide (aluminium and oxygen compound) with the molecular formula of $Al_2O_3$. It appears as a white odorless crystalline powder. Naturally in mineral corundum form and protected by aluminium oxide layer from corrosion. Alumina is produced from refining process of bauxite, an aluminium ore. Alumina is extracted from bauxite through bayer process which including crushing and milling, filtration, precipitation and calcination. Hot solution of sodium hydroxide and calcium oxide is used to differentiate alumina from bauxite. The mixture is heated in high pressure container and precipitation of alumina from saturated solution is dissolved by sodium hydroxide. It is being heated to remove water and make it dry. Then, alumina is being washed to recover the sodium hydroxide solution and the filtrate obtained after filtration is dried into powder form. Figure 2.9 show the flow chart of the alumina extraction process.
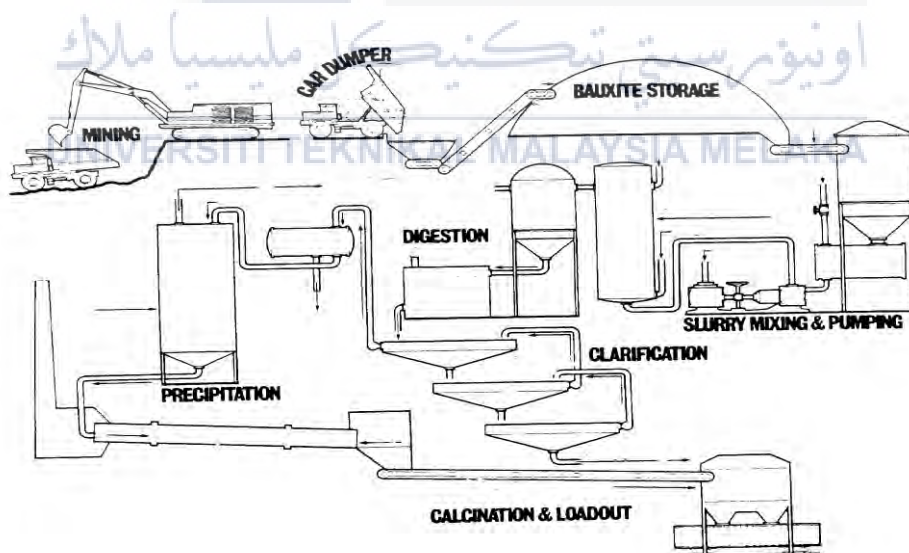


Figure 2.9: Operations principle in Bayer process to extract alumina through refining process of bauxite (Lancashire, 2014)

Molecular weight of alumina is 101.96 g/mol, 2980℃ of boiling point and 2000℃ of melting point. Alumina has no reaction with air and no rapid reaction with water. It is insoluble in water, an electric insulator but a thermal conductor. Alumina is selected as reinforcement in this study due to its interesting combined properties, hardness, light weight and able to withstand elevated temperature. It can be considered as one of the most widely used materials in tribological research. Properties of alumina are shown in the Table 2.2. Characteristics of alumina which make it to be a potential reinforcement composite are shown in Table 2.3.

Table 2.2: Properties of auminium oxide ($Al_2O_3$) (source: Adams, 2013)

| | Properties | Aluminium Oxide ($Al_2O_3$) |
|---|---|---|
| 1. | Hardness (kg/mm$^2$) | 1175 |
| 2. | Density (g/cm$^3$) | 3.69 |
| 3. | Coefficient of thermal expansion ($\mu$m/m℃) | 8.1 |
| 4. | Fracture toughness (MPa-m$^{1/2}$) | 3.5 |
| 5. | Poisson's ratio | 0.21 |

Table 2.3: Characteristics of reinforcement composites of aluminium oxide ($Al_2O_3$)

(source: Adams, 2013)

| | Characteristics of Auminium Oxide ($Al_2O_3$) / Alumina |
|---|---|
| 1. | High hardness |
| 2. | High wear resistance |
| 3. | Inert / no chemical reaction with acids or alkali at high temperature |
| 4. | High thermal conductivity |
| 5. | Excellent forging ability |
| 6. | High stiffness |

Composites which reinforced with alumina is better than unreinforced composites in terms of greater abrasion and adhesion wear resistance, greater strength, greater stiffness, lower density (light weight) and improved properties at elevated temperatures. The provided chemical, physical and mechanical properties of alumina have revealed the reasons of great attention given by researchers on alumina in tribological researches (Hitnesh, 2011; Surendran et al., 2017).

## 2.5 Palm Kernel Activated Carbon (PKAC)

There have been several studies in the literature reporting about the oil palm wastes produced will cause the wastes of energy, pollutions and some of the other environmental issues in all around the world such as Indonesia, Malaysia, Thailand, Nigeria and Columbia. Oil palm wastes consists of oil palm trunks (OPT), empty fruit bunch (EFB), oil palm fronds (OPF), oil palm mesocarp fibre (OPMF), oil palm kernel (OPK) and oil palm shell (OPS) which shown in the Figure 2.10 below.



Figure 2.10: Types of biomass in oil palm (source: palm biomass waste pellet production line, n.d.)
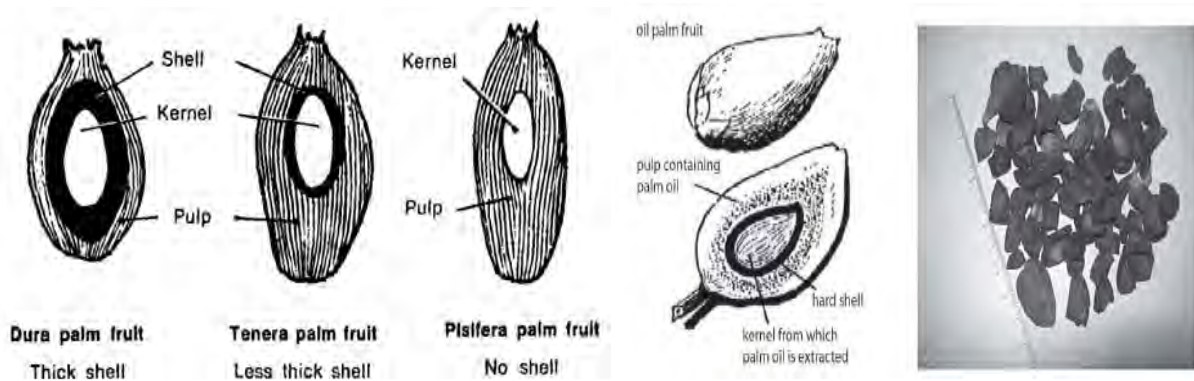
Figure 2.11: Oil palm fruit structures (source: modern oil palm cultivation, n.d.)

Palm kernel shell is one of the oil palm biomass residues which possesses potential applicable characteristics to serve as bio-fuels, bio-oils bio-gas and solid lubricant by converting in activated carbon form. After the oil is extracted from oil palm kernel, the palm kernel cake consists of 42.73% of carbon, 67.71% of volatile matter and 4031 Kcal /kg of calorific value. The Figure 2.12 shown the composition of wastes which used in composting process. Carbon content in palm kernel cake is about 96.21% which is the highest compared to other wastes (Kolade et al., 2005).

Table 2.4: Wastes composition in composting process (source: Kolade et al., 2015)

| Waste | Moisture content, % | Carbon (C %) | Nitrogen (N %) | Phosphorus (P) | Potassium (K) |
|-------|---------------------|--------------|----------------|----------------|---------------|
| Palm Kernel Cake | 58.92 | 96.21 | 2.88 | 0.60 | 0.19 |
| Goat dung | 29.79 | 75.94 | 3.62 | 0.51 | 0.18 |
| Poultry droppings | 49.11 | 78.83 | 2.83 | 3.29 | 0.16 |

By referring the references above, palm kernel consists of high amount of carbon which can be fully utilized in tribological applications. Nevertheless, there have been relatively few recent studies on wear properties or tribological applications of Palm Kernel Activated Carbon (PKAC) (Chua et al., 2014; Mohmad et al., 2017; Tahir et al., 2015; Tahir, 2016).

Study by Chua et al. (2014) on potential of palm kernel activated carbon epoxy (PKAC-E) composite as solid lubricant with the diferent variable parameter which is effect of load on friction and wear properties. Pin-on-disc machine is used to run dry sliding test on specimen with different load applied. Result of specific wear rate, k (mm$^3$/Nmm) against normal load (N) is shown in Figure 2.13.
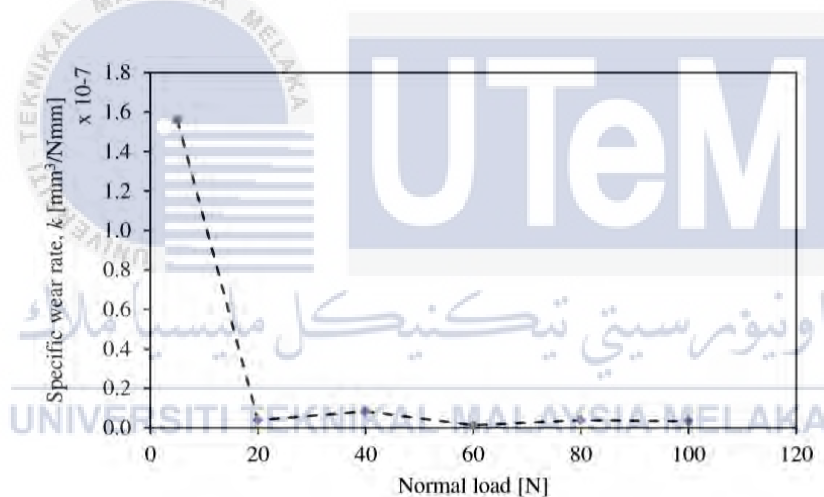


Figure 2.12: Graph result of specific wear rate against normal load (Chua et al., 2014).

Researchers have observed the worn surface of PKAC specimen after dry sliding test and discovered adhesive and abrasive wear occurred on the surface. The finding of the study proposed that friction coefficient of specimen will decrease with the increasing applied load and suggested PKAC as solid lubricant at low load, dry sliding conditions (Chua et al., 2014).

A similar investigation is conducted by Tahir et al. (2015) to study about the effect of the temperature on the tribological properties of palm kernel activated carbon-epoxy composite. The investigation is carried out by using pin-on-disc dry sliding test and the

27

PKAC specimen is prepared in pin formed. The variation of temperatures in this test is from 27°C to 150°C. The results of the test showed that frcition coefficent increases as the temperatures increases and significantly increases after 90°C because of the epoxy bond failure. Besides, wear rate is also inreases as the temperature increases due to the reduction in hardness of PKAC specimen. The results of specific wear rate, steady state of coefficient of friction and hardness against temperatures are represent in two graphs and bar chart respectively which shown in Figure 2.13, Figure 2.14 and Figure 2.15.
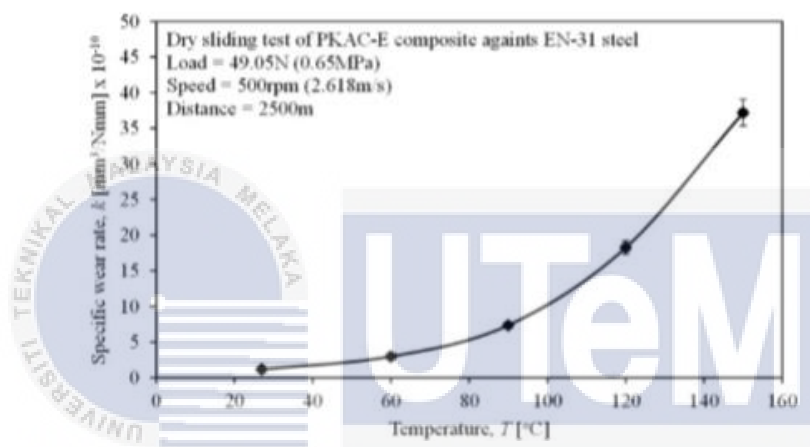


Figure 2.13: Graph of specific wear rate against temperatures (Tahir et al., 2015)
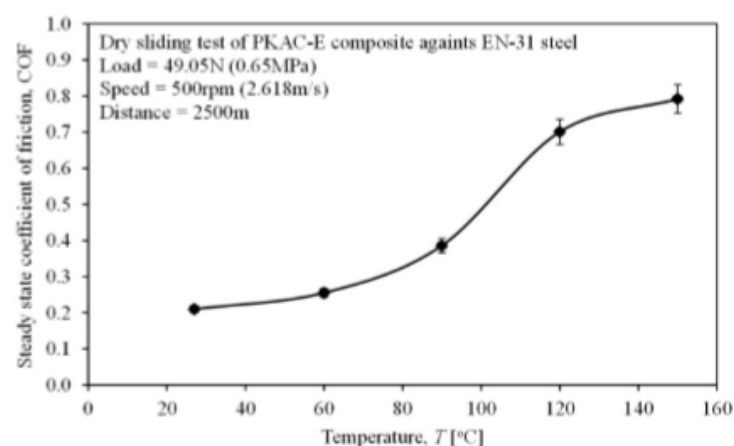


Figure 2.14: Graph of Steady state coefficient of friction (Tahir et al., 2015)
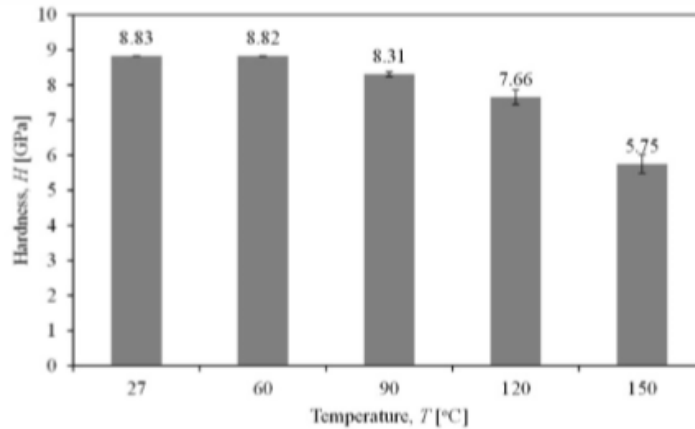
Figure 2.15: Bar chart of hardness against temperatures (Tahir et al., 2015)

The wear mechanism of the spcimen is being observed after the sliding tets and crack formation is discovered on the worn surface and it is classified as abrasive wear (Tahir et al., 2015).

In addition, same group of researchers investigated about the effect of sliding distance at different temperatures on tribological properties of palm kernel activated carbon (PKAC). The examination on friction coefficient and wear rate of PKAC is carried out by using pin-on-disc machine to run the dry sliding test. The results show that sliding distance will not affect the friction coefficient significantly whereas critical operating temperature will significantly increse wear rate and friction coefficient of the composite specimen. Based on the collected data shown in Table 2.5, friction coefficient and specific wear rate of PKAC are lower than the other composites. They concluded that PKAC is a potential self-lubricating carbon under temperature of 90℃ (Tahir et al., 2015).

Table 2.5 Result and data for friction coefficient and specific wear rate for synthetic and

agriculture wastes- based polymeric composites under dry sliding test at room temperature

(source: Tahir et al., 2015)

| Materials | Testing apparatus | Sliding speed [m/s] | Load [N] | Sliding distance [km] | COF | Specific wear rate [mm$^3$/Nmm] $\times 10^{-5}$ | Ref. |
|---|---|---|---|---|---|---|---|
| Polyester | Block-on-disc | 2.8 | 30 | 0.84–4.2 | 0.9–0.95 | 14–16 | [31] |
| Coir/Polyester | Block-on-disc | 2.8 | 30 | 0.84–4.2 | 0.6–0.8 | 11–17 | [31] |
| Betelnut/Polyester | Block-on-disc | 2.8 | 30 | 1–6 | 0.45–0.65 | 2–22 | [32] |
| Glass/Polyester | Block-on-disc | 2.8 | 50 | 1–14 | 0.2–0.6 | 0.4 – 0.6 | [33] |
| Epoxy | Pin-on-disc | 2.8 | 50 | 1–5 | 0.75 | 17–23 | [34] |
| Kenaf/Epoxy | Pin-on-disc | 2.8 | 50 | 1–5 | 0.4–0.65 | 3–6 | [34] |
| Bambo/Epoxy | Pin-on-disc | 2.8 | 30 | 1–4 | 0.55–0.85 | 5.5–9 | [35] |
| Glass/Epoxy | Pin-on-disc | 2.5 | 60 | 1–4.2 | 0.44 | 1.2–3 | [36] |
| PKAC/Epoxy (27 °C) | Pin-on-disc | 2.7 | 49 | 0.5–2 | 0.21–0.24 | 0.05–0.085 | This study |
| PKAC/Epoxy (90 °C) | Pin-on-disc | 2.7 | 49 | 0.5–2 | 0.30–0.34 | 0.08–0.14 | This study |
| PKAC/Epoxy (150 °C) | Pin-on-disc | 2.7 | 49 | 0.5–2 | 0.55–0.74 | 0.2–0.395 | This study |

# CHAPTER 3

# METHODOLOGY

## 3.1 Introduction

The general process flow of the study is shown in Figure 3.1. The study begins with identifying objectives, sample preparation, tribometer testing, surface morphology, results validations, analysis and discussion and documentation of report writing.

## 3.2 Sample Preparation

First, palm kernel activated carbon (PKAC) coarse powder is being crushed into fine powder by using crusher. Then, the fine PKAC powder with the size of 250 micrometer can be obtained by using sieve. For the first trial of composition test, the prepared PKAC and Alumina ($Al_2O_3$) fine powder are weighed at 25 wt.% each and mixed with 50 wt.% high density epoxy (E) with the ratio of 4:1 for resin and hardener respectively (West system 105 epoxy resin (105-B) and West system 206 slow hardener (206-B)). PKAC was obtained from manufacturer and the preparation is confidential. The $Al_2O_3$-PKAC-E mixture is placed in a mold, hot-pressed at approximately 80°C with pressure of 1.839 MPa for approximately 40 minutes. This process is known as hot compaction technique or hot compression molding process. Then the composites mixture together with the mold is left to cool at room temperature for approximately 15 to 20 minutes before being expressed from the mold. The disc is taken out from the mold after cooled and left to cure for one week. Observation on

disc's surface conditions is needed after cured to make sure that the disc is at suitable and acceptable conditions (good and flat surface condition without ruptures or pits). Next, all the cured specimen samples are polished evenly with sandpaper. The polishing process is conducted gradually started from 1000 grit, 1500 grit, 2000 grit and followed by 3000grit size of sandpapers. The polished samples are subjected to surface roughness and hardness tests. A ground surface roughness of arithmetic average 0.8 $\mu$m (32 $\mu$in.) or less is usually recommended by ASTM G99 testing standards for specimen. Table 3.1 shows composition percentages of testing composites, Table 3.2 shows optimum range of values of fixed testing parameters and Table 3.3 shows mechanical properties of ball and disc samples. Figure 3.2 shows the disc samples after curing process and before polishing and laser cutting process.

```
                    ╭─────────────╮
                    │    START    │
                    ╰──────┬──────╯
                           │
                           ▼
                  ┌──────────────────┐
                  │ Identify objectives │
                  └─────────┬────────┘
                            │
                            ▼
                  ┌──────────────────┐◄──────────────┐
                  │  Sample Preparation │              │
                  └─────────┬────────┘              │
                            │                       │
            PKAC            ▼                       │
  ┌────────────┐◄────◆ Materials ◆                  │
  │   Crush    │                                    │
  └─────┬──────┘       │ Alumina                    │
        │              ▼                            │
        ▼        ┌──────────────┐                   │
  ┌────────────┐──►│  Hot Press  │                  │
  │   Sieve    │   └──────┬──────┘                  │
  └────────────┘          │                         │
                          ▼                         │
                  ┌──────────────────┐              │
                  │  Cure (one week) │              │
                  └─────────┬────────┘              │
                            │                       │
                            ▼      NO (Surface rupture)
                      ◆ Observe ◆───────────────────┘
                      ◆ & Check ◆
                            │
                            │ YES (Good Surface Condition)
                            ▼
                  ┌──────────────────┐
                  │ Tribometer Testing │
                  └─────────┬────────┘
                            │
                            ▼
                  ┌──────────────────┐
                  │ Surface Morphology │
                  └─────────┬────────┘
                            │
                            ▼
                  ┌──────────────────┐
                  │ Result Validations │
                  └─────────┬────────┘
                            │
                            ▼
                  ┌──────────────────┐
                  │ Analysis & Discussion │
                  └─────────┬────────┘
                            │
                            ▼
                  ┌──────────────────┐
                  │  Documentation   │
                  └─────────┬────────┘
                            │
                            ▼
                    ╭─────────────╮
                    │     END     │
                    ╰─────────────╯
```
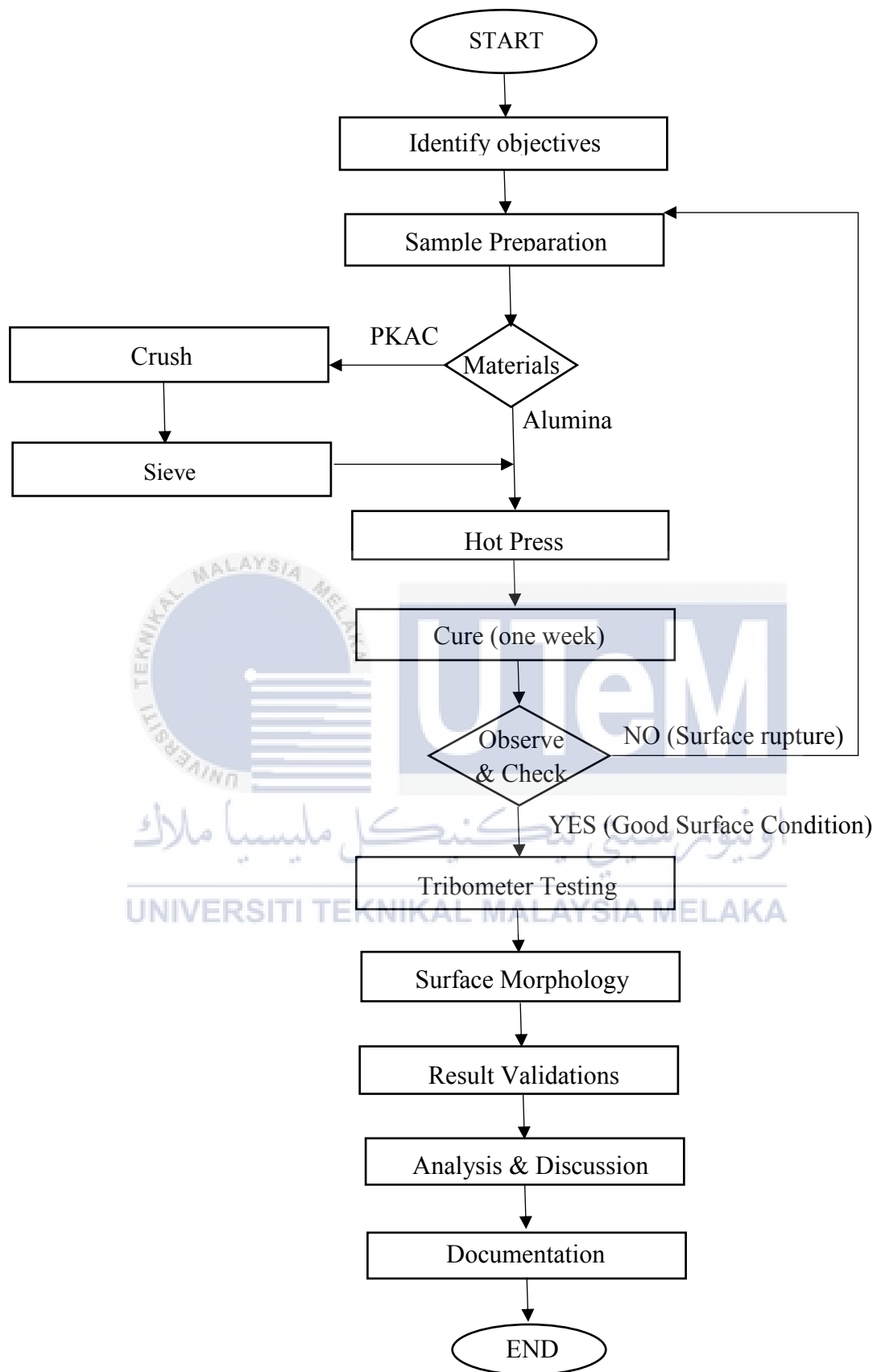
Figure 3.1: General methodology flow chart

Table 3.1: Composition percentages of testing composites

| Sample | Palm Kernel Activated Carbon (PKAC), % | Alumina (Al$_2$O$_3$), % | Epoxy, % |
|---|---|---|---|
| PKAC+AL/E | 25 | 25 | 50 |
| PKAC/E | 50 | - | 50 |
| AL/E | - | 50 | 50 |
| PKAC+AL/E | 30 | 30 | 40 |
| PKAC/E | 60 | - | 40 |
| AL/E | - | 60 | 40 |
| PKAC+AL/E | 35 | 35 | 30 |
| PKAC/E | 70 | - | 30 |
| AL/E | - | 70 | 30 |

Table 3.2: Optimum values of fixed testing parameters

| Fixed Parameters | Optimum Values |
|---|---|
| Sliding Speed (rpm) | 400 |
| Sliding distance (m) | 3000 |
| Load (N) | 49.05 |
| Hot Press Temperature (°C) | 80 |
| Hot Press Pressure (MPa) | 1.838746 |

Table 3.3: Mechanical properties of ball and disc samples (source: Mohmad et al., 2017; Adam, 2013)

| Properties | PKAC-E disc | Carbon-Chromium steel ball | Alumina, $Al_2O_3$ |
|---|---|---|---|
| Hardness (GPa) | 8.36 | 7.45 | 14.12 |
| Density (g/cm$^3$) | 1.40 | 7.81 | 3.89 |
| Arithmetic surface roughness (µmRa) | 0.40 | 0.02 | - |



(a)                                         (b)
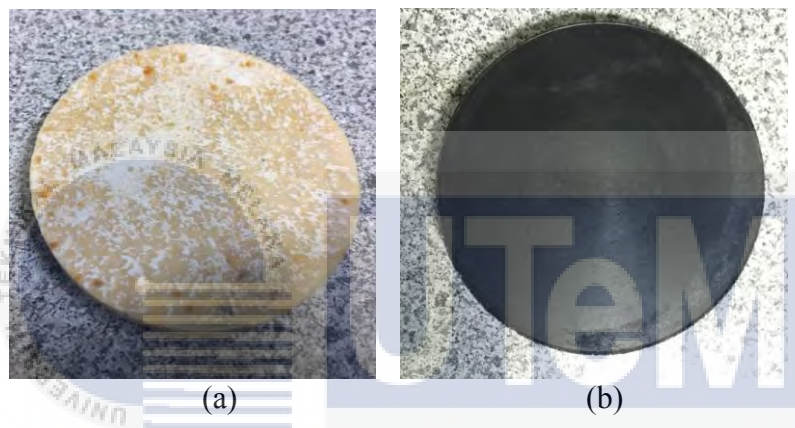
Figure 3.2: a) Alumina-Epoxy (60%-40%) disc before polishing and laser cutting b) PKAC-Epoxy (60%-40%) disc before polishing and laser cutting

## 3.3 Ball-On-Disc Tribometer Test

Carbon chromium steel ball is clean with ultrasonic cleaner at temperature of 40°C by immerse it into hexane for duration of five minutes before running the test. The composites disc is ready for ball-on-disc tribometer testing after four holes are created by laser cutting with $CO_2$ LST machine. The tribometer test is carried out by using DUCOM Ball-On-Disc Tribometer with the constant sliding speed of 400rpm, sliding distance of 3000m and applied loads of 49.05N which shown in Table 3.2. Test standards provided by

DUCOM are shown in Table 3.4 and ASTM (G 99 – 95a) Standard Test Method for Wear Testing with a Pin-on-Disk Apparatus is also used in this tribometer test. Tribometer test is carried out two times for each sample with different track diameters, 40mm and 30mm or 20mm in order to obtain the average readings of coefficient of friction and frictional force. The average coefficient of friction can be obtained by using the equation 3.1. Where $\mu$ is coefficient of friction, $F$ is frictional force (N) and $W$ is applied load (N) (Tahir et al., 2015).

$$\mu = \frac{F}{W} \tag{3.1}$$

The steps from sample preparation to tribometer testing are repeated 8 times for the following different compositions percentages as shown in Table 3.1. Figure 3.3 is schematic diagram of ball-on-disc tribometer machine. Figure 3.4 shows the disc samples after conducted the tribometer test. Specimens after test, materials used and ASTM (G 99 – 95a) Standard Test Method for Wear Testing with a Pin-on-Disk Apparatus are shown in Appendix D1 and D2.

Table 3.4 Testing standards used in testing (source: Celis and Ponthiaux, 2012)

| Standard codes | Evaluations |
| --- | --- |
| ASTM G 133-95 | Standard test method for linear reciprocating ball-on-flat sliding wear |
| DIN 50324 | Tribology; testing of friction and wear model test for sliding friction of solids (ball-on-disc system) |
| DIN 51834-1 | Testing of lubricants- Tribological test in the translator oscillation apparatus- Part 1: general working principles |
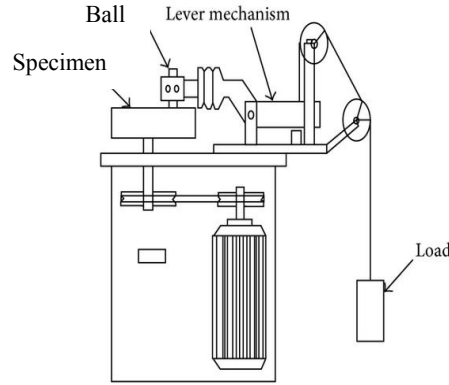
Figure 3.3: Schematic Diagram of Ball-On-Disc Tribometer Machine (source: Miramontes et al., 2016)



(a)         (b)
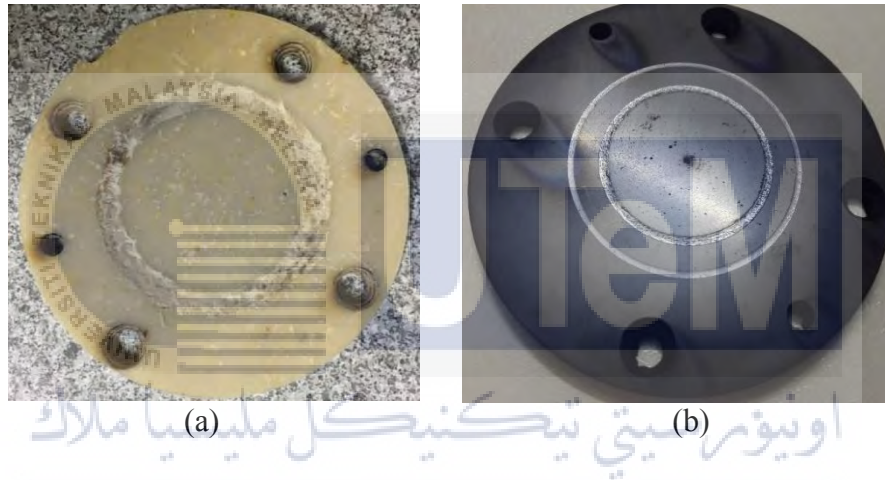
Figure 3.4: a) Alumina-Epoxy (50%-50%) disc after laser cutting and sliding test b) PKAC-Epoxy (50%-50%) disc after laser cutting and sliding test

## 3.4 Calculation of Specific Wear Rate

Specific wear rate is calculated with Equation 3.2 and 3.3, where $V_{loss}$ is loss of volume (mm$^3$), $M_{loss}$ is loss of mass after tribometer test (kg), $\rho$ is density (kg/mm$^3$), $k$ is specific wear rate (mm$^3$/ Nmm), $L$ is sliding distance (m) (Tahir et al., 2015). Values needed for specific wear rate calculation are mass before sliding test, $M_b$ (g), mass after sliding test, $M_a$ (g), radius of disc sample, $r$ (mm), thickness of disc sample, $t$ (mm), load applied, $W$ (N)

and sliding distance, $L$ (mm). Weights of samples are measured before and after the test. Loss of mass is measured and converted to volume loss (in cubic millimeters) using an appropriate value for the specimen density.

$$V_{loss} = \frac{Mloss}{\rho} \qquad (3.2)$$

$$k = \frac{Vloss}{W \times L} \qquad (3.3)$$

## 3.5 Surface Morphology Observation

The wear topography of the worn surface will be conducted by using 3D Surface Profilometer to observe the tracks' surfaces on the disc and carbon chromium steel ball after the ball-on-disc tribometer test. The surface morphology will be presented in data of 2D view camera zoom image. Types of dominant wear mechanism can be justified as either adhesive wear or abrasive wear through surface morphology observation.

## 3.6 Result and Data Collection

Results and data such as surface roughness, hardness readings, coefficient of friction (CoF), specific wear rate and worn surface morphology images are collected and average values of the readings are calculated. The collected readings are presented in tables. Bar charts are used to visually compare average readings across all samples. Line graph is used to demonstrate the trends of frictional force and coefficient of friction, CoF against time.

# CHAPTER 4

## RESULTS AND DISCUSSION

Surface roughness analysis, hardness test analysis, ball-on-disc tribometer testing, specific wear rate calculations and wear morphology of samples are all conducted in this study. Samples PKAC+AL/E (70/30) are broken after removed from the mold. AL/E (70/30) sample is cracked after the curing process and before the ball-on disc tribometer test is carried out. It is assumed that both samples are fragile and brittle due to the small proportion of epoxy (30%) for embedding the two materials. Hence, surface roughness and hardness data in Table 4.1 are not including sample PKAC+AL/E (70/30) and data results of coefficient of friction, specific wear rate and wear topography study are not including sample PKAC+AL/E (70/30) and AL/E (70/30). The images of specimens for PKAC+AL/E (70/30) and AL/E (70/30) are shown in Appendices.

**4.1 Physical Mechanical Properties**

The surface roughness and hardness test are done for all specimens by repeating five times for each in order to obtain average readings which shown in Table 4.1. Data collected for surface roughness and hardness are presented in bar chart form in Figure 4.1 and Figure 4.2 respectively for comparison purpose. From the Figure 4.1, it shown that PKAC+AL/E (50/50) is the smoothest and PKAC/E (70/30) is the roughest among all the samples. The surface roughness for samples 1, 2 and 3 which have 50% of epoxy content is relatively lower than samples with the epoxy content of 40% and 30%. The conclusion from the bar chart is the higher the content of epoxy, the lower the surface roughness. However, the data shown is approximation data because all the cured specimen samples are polished with sandpapers manually. The polishing process is conducted gradually started from 1000 grit, 1500 grit, 2000 grit and followed by 3000grit size of sandpapers. Based on ASTM G99 testing standards, a ground surface roughness of 0.8 μm (32 μin.) arithmetic average or less is recommended for specimen in tribometer tests. Hence, the surface roughness data shown above is not the exact smoothest surface roughness can be achieved for the hybrid composites in real. This is because the polishing process of the samples is considered done when the surface roughness of the samples met the ASTM G99 testing standards which less than 0.8 μm. Thus, surface roughness shown below are the acceptable values fall in the standard range for purpose of conducting ball-on-disc dry sliding test.

The hardness readings obtained are converted into unit of GPa by using conversion chart shown in Appendix B. The hardness readings in GPa are shown in Table 4.1 and presented in the form of bar chart in Figure 4.2. The readings obtained show that PKAC+AL/E (60/40) has the highest hardness value, 8.493GPa whereas AL/E (70/30) has the lowest hardness value of 6.645 GPa. The overall readings for all the samples are quite similar which in the range of 8.14 to 8.493 GPa except AL/E (70/30). AL/E (70/30) is the

specimen which consists the highest alumina content but exhibits the lowest hardness property and this reflects the findings of Rajesh and Kaleemulla (2016), the optimum composition to have highest hardness property is not the highest alumina content composites (Rajesh and Kaleemulla, 2016). AL/E (70/30) sample fractured after the curing process and before the ball-on disc tribometer test is conducted. It is assumed that the sample are fragile and brittle which supported with the low hardness value shown in Table 4.1 and Figure 4.2. This might due to the small proportion of epoxy (30% which consists 4:1 resins and hardener) for embedding particles and insufficient epoxy for adhesive system in sample.

Table 4.1: Average surface roughness and hardness for specimens

| Sample | Composition | Average surface roughness (µmRa) | Average hardness (GPa) |
|---|---|---|---|
| PKAC+AL/E | 50/50 | 0.201 | 8.218 |
| PKAC/E | 50/50 | 0.274 | 8.140 |
| AL/E | 50/50 | 0.319 | 8.267 |
| PKAC+AL/E | 60/40 | 0.205 | 8.493 |
| PKAC/E | 60/40 | 0.337 | 8.306 |
| AL/E | 60/40 | 0.301 | 8.258 |
| PKAC+AL/E | 70/30 | Sample broken (No data obtained) | |
| PKAC/E | 70/30 | 0.677 | 8.473 |
| AL/E | 70/30 | 0.612 | 6.645 |
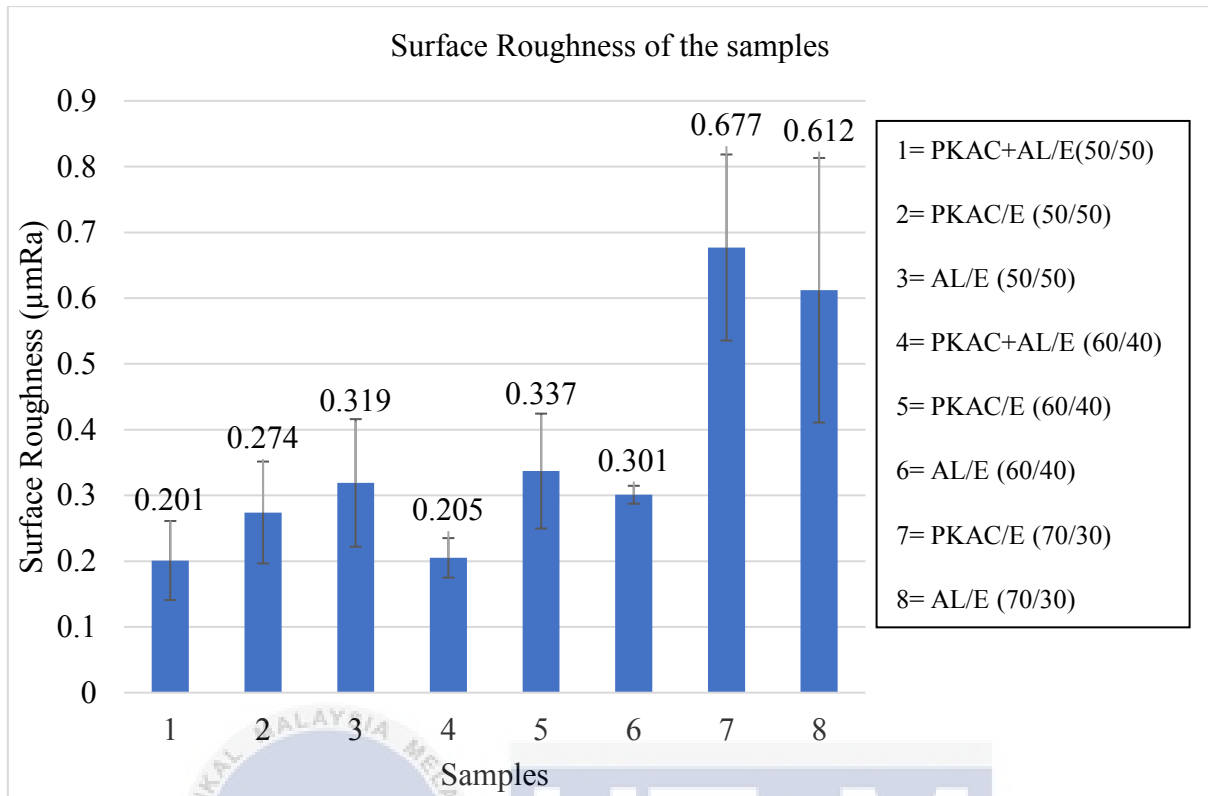
Figure 4.1: Average surface roughness of samples
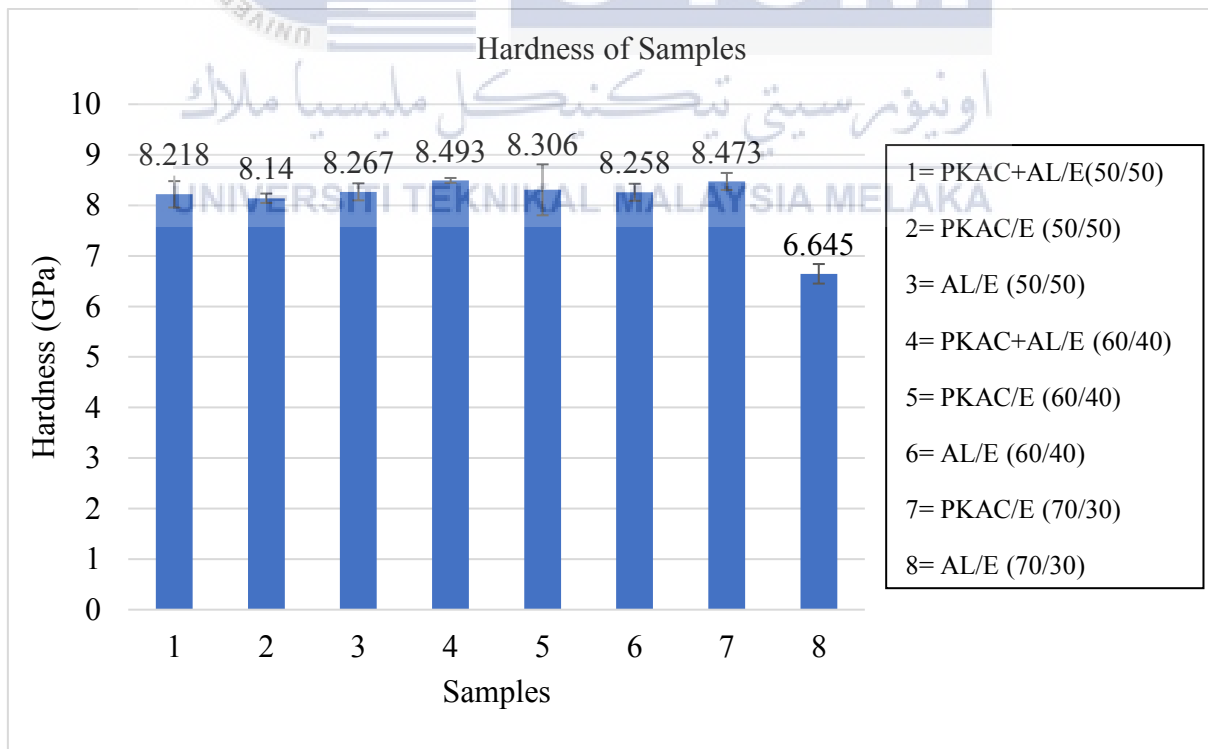


Figure 4.2: Hardness of samples

## 4.2 Coefficient of Friction (CoF)

In Appendix E, coefficient of friction against time for all the specimens including conventional SK2 disc are shown in line graph form. Most of the graphs are increasing abruptly at initial stage in a short time and slowly decreasing to reach the steady state at the end of the graph. Some of the samples experienced a short term of fluctuation during the test. Fluctuation may cause by the increasing sliding temperature due to high speed and high load which applied in this ball-on-disc dry sliding test. Throughout the test, the ball and disc temperatures were slightly increased due to the high sliding speed with long sliding distance of 3000m. At higher temperature, it will thermally affect the epoxy layer due to resin softening and reduction of matrix adhesion. This producing larger contact area and higher friction of coefficients which lead to the occurrence of fluctuation during the test.

By referring to Table 4.2 and Figure 4.3, the results suggest that composition percentages of 60/40 (60% composites and 40% epoxy) contribute to lower CoF because the overall CoF values for PKAC+AL/E (60/40), PKAC/E (60/40) and AL/E (60/40) are lower compare to PKAC+AL/E (50/50), PKAC/E (50/50) and AL/E (50/50) respectively. While for both composition of 60/40 and 50/50 in Figure 4.3, the data show the same ascending order for CoF values of the samples which PKAC/E exhibit lowest CoF follow by PKAC+AL/E and AL/E. This trend pointed out the higher the PKAC content, the lower the friction coefficient of the samples or the higher the alumina content, the higher the friction coefficient.

The friction was found to depend on surface roughness where the rougher surfaces gave higher friction coefficients (Svahna et al., 2003). Friction refers to the forces that resist the relative motion of two sliding surfaces. A rougher surface means the average irregularities on the surface higher. This requires higher abrasive force to break over or to

43

move up and down over the surface which may lead to abrasive wear. However, this is not relevant in this study because the surface roughness of specimens are approximate values which met standard of testing less than 0.8 μm and not the exact smoothest surface roughness can be achieved for the hybrid composites in real. PKAC was justified as a good self-lubricating carbon as stated in previous researches (Tahir et al., 2015). PKAC play a dominant role as self-lubricating material in this tribometer test. The study revealed that the hybrid composites of PKAC+AL/E (60/40) exhibit lower CoF compare to PKAC+AL/E (50/50) which proved that 60/40 is the optimum composition for hybrid composite to achieve lowest friction in this study. This is because PKAC+AL/E (60/40) reinforced with higher percentage of PKAC than PKAC+AL/E (50/50) which are 30% PKAC and 25% PKAC respectively.

Moreover, for 60/40 composition, PKAC/E (60/40) has lower CoF than PKAC+AL/E (60/40) because of former sample has 60% of PKAC and 40% of epoxy whereas the latter consist of 30%PKAC, 30%AL and 40% epoxy. The lower PKAC content in PKAC+AL/E (60/40) hybrid composite minimizing self-lubricating properties of the sample and hence contribute to higher CoF.

SK2 Carbon Steel is conventional disc which used in the study as comparison specimen with hybrid composites. It is a carbon tool steel that used in wide range of fields from hard applications that require elasticity and toughness. SK2 disc was tested under the same condition with same testing parameters and the result indicates that CoF of SK2 is higher than CoF of all specimens (PKAC+AL/E, PKAC/E and AL/E) for both composition of 50/50 and 60/40. PKAC+AL/E (60/40) hybrid composite is justified as better lubricating material compare to SK2 Carbon Steel in this study. Hybrid composites exhibit lower friction coefficient can be supported with wear morphology shown in section 4.4, micrograph of PKAC+AL/E (60/40) shows that PKAC transferred layer is formed at counter

44

surface of carbon chromium steel ball. This is supported with previous study that PKAC undergoes phase transformation changed from carbon-like-structure to a graphite-like structure ($sp^2$) with lower shear strength bonds and adhere to counter surface during sliding motion. Transferred layer would help to break adhesive joints between asperities and leads to low friction (Mahmud et al., 2017; Abdollah et al., 2010).

This CoF result conclude that 60/40 (60% composites and 40% epoxy) is the optimum hybrid composites composition also the result reveals that alumina exhibit highest CoF and PKAC exhibit lowest CoF which contribute to the ascending CoF trend of PKAC/E, PKAC+AL/E and AL/E for both 50/50 and 60/40 compositions.

Table 4.2: Average coefficient of friction of samples

| Samples | Composition | Average Coefficient of Friction, $\mu$ |
|---|---|---|
| PKAC+AL/E | 50/50 | 0.270 |
| PKAC/E | 50/50 | 0.202 |
| AL/E | 50/50 | 0.514 |
| PKAC+AL/E | 60/40 | 0.213 |
| PKAC/E | 60/40 | 0.111 |
| AL/E | 60/40 | 0.505 |
| PKAC+AL/E | 70/30 | Sample broken (No data obtained) |
| PKAC/E | 70/30 | 0.858 |
| AL/E | 70/30 | Sample broken (No data obtained) |
| SK2 Carbon Steel | - | 0.515 |
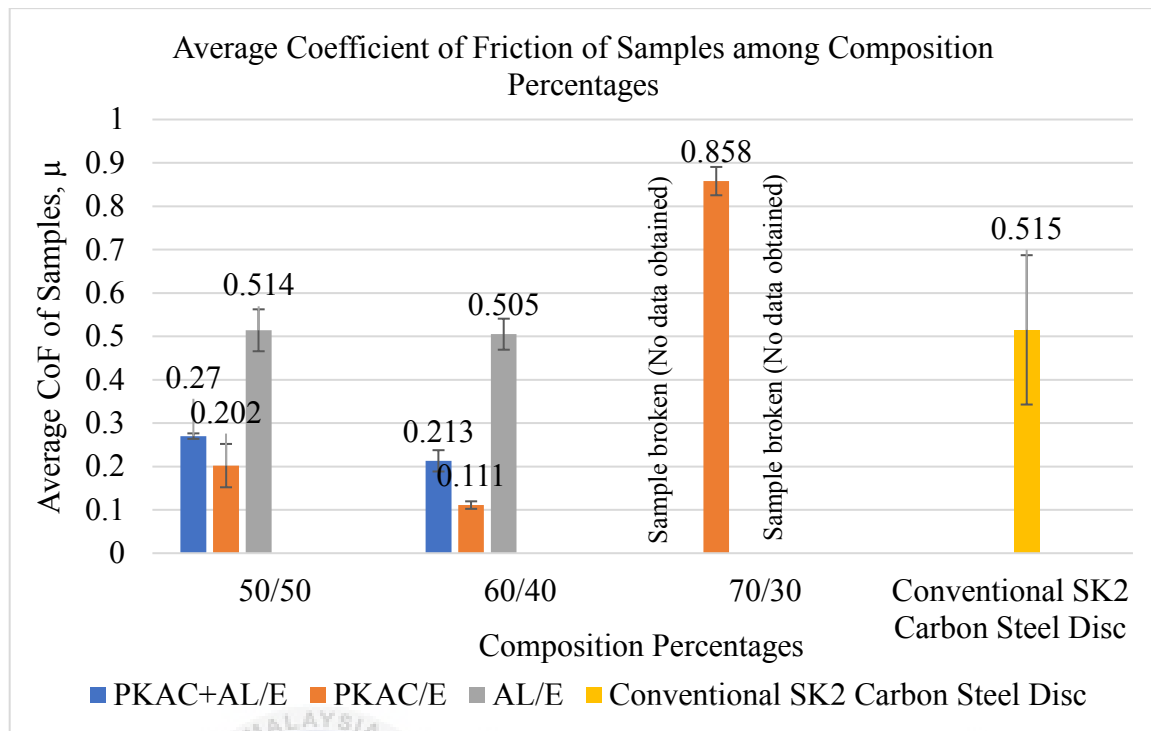
Figure 4.3: Average coefficient of friction of samples among composition percentages under dry sliding condition at room temperature with applied load of 49.05N, sliding speed of 400rpm and sliding distance of 3000m.

## 4.3 Specific Wear Rate

Table 4.3 shows the specific wear rate of samples and it is illustrated in Figure 4.4 for comparison purpose. The result clearly shows that samples composition of 50/50 exhibit lower specific wear rate compare to samples with 60/40 composition.

By comparing the hybrid composites of both composition of 50/50 and 60/40, specific wear rate, k of PKAC+AL/E (60/40) is $5.125 \times 10^{-7}$ mm$^3$/Nmm which is slightly higher than PKAC+AL/E (50/50) with k value of $4.272 \times 10^{-7}$ mm$^3$/Nmm. The difference is insignificant with value of $0.853 \times 10^{-7}$ mm$^3$/Nmm. Specific wear rate, k is volume of material removed per unit load and sliding distance. Percentage of epoxy content is decisive in contributing to high or low specific wear rate of samples. Trend of results show higher epoxy content contributes to lower specific wear rate. Sample with 50/50 composition consists of 50% of composites (PKAC, AL or PKAC+AL) and 50% of epoxy whereas sample with 60/40 composition consists of 60% composites and 40% of epoxy. There have been several tribological studies of self-lubricating and wear resistant of epoxy and its coatings in dry sliding applications which proved that epoxy is one of the self-lubricating materials that desired to prevent and minimize the wear (Khun et al., 2013; Kumar et al., 2015). Hence, these previous findings agree and giving support on higher content of epoxy in 50/50 composition samples will contribute to lower specific wear rate. Furthermore, epoxy consists of 4:1 of resin and hardener which act as an epoxy bonding and adhesive systems in the samples. Samples with 50/50 composition has higher epoxy content of 50% which able to form more thorough joint connection between composites particles such as PKAC crushed powder or AL nano-powder compare to 60/40 composition samples which have only 40% epoxy content. Since the bonding or connection of particles is better in 50/50 composition samples, the particles will not easily pull out during the dry sliding test and less likely to occur two body and third body abrasion thus contribute to low specific wear rate.

In addition, alumina is significantly harder than PKAC particles which means it may act as third body abrasive increasing the composite wear rate when the alumina debris are generated during the sliding motion (Godet, 1984). The chemical properties of alumina exhibit poorer adhesion to epoxy matrix which caused the easy pull out under high contact pressure and sliding speed. Vasconcelos et al. (2005) justified that the lower material integrity where interface resistance affects the large production of debris derived from particles pullout during the sliding test (Vasconcelos, Lino, Baptista, and Neto, 2005). Hence, a trend of higher alumina content contribute to higher wear rate was presented in this study. For samples of both 50/50 and 60/40 composition, AL/E exhibit highest wear rate follow by PKAC+AL/E and PKAC/E with lowest wear rate.

SK2 Carbon steel possess good steel tools properties of high hardness, wear resistance and toughness which cause it has the lowest specific wear rate among the samples. Besides, all the disc samples or specimens were prepared manually started from initial stage of powder crushing process to the final stage of hot press process to form a disc whereas SK2 Carbon Steel disc was provided by faculty in good condition. For the comparison between hybrid composites PKAC+AL/E (60/40) and PKAC+AL/E (50/50) with SK2 Carbon Steel disc, experimental limitation needed to be considered throughout the samples preparation processes especially mixing process which will affect wear rate result. Complete mixing of powders or microparticles is needed to prevent the formation of lumps which results in incomplete recombination of materials. Complete mixing defined as complete break-up and uniform distribution of materials and this is incapable perform by low-shear device (Hogg, 2009). Hence, the agglomeration of materials or formation of lumps may occur in mixture due to the lower mixing speed and low-shear mixing tools used during the manual samples preparation process in this study. Once after the outmost smoothest surface layer worn out during the sliding test, carbon chromium ball will penetrate deeper into

samples, uneven mixtures and agglomerated particles in the samples will be pulled out easily and contribute to higher mass loss, higher volume loss and higher specific wear rate to the samples (PKAC+AL/E (60/40) and PKAC+AL/E (50/50)). Images of worn surface of these samples shown in Figure 4.5 in section 4.4 are providing evidence for this justification. It is clearly shown the uneven mixtures and lumps formations are present on the worn part of samples whereas the unworn surface is smooth and fine.

Conclusions of specific wear rate results are the optimum hybrid composites composition for lowest specific wear rate is PKAC+AL/E (50/50) with minor difference with PKAC+AL/E (60/40) and higher epoxy content contribute lower specific wear rate whereas higher alumina content contribute higher specific wear rate.

Table 4.3: Specific wear rate of samples

| Samples | Composition | Loss of mass, $M_{loss}$ (g) | Loss of Volume, $V_{loss}$ (mm$^3$) | Specific wear rate,k ($\times 10^{-7}$ mm$^3$/Nmm) |
|---|---|---|---|---|
| PKAC+AL/E | 50/50 | 0.098 | 62.861 | 4.272 |
| PKAC/E | 50/50 | 0.028 | 19.872 | 1.350 |
| AL/E | 50/50 | 0.200 | 129.032 | 8.769 |
| PKAC+AL/E | 60/40 | 0.162 | 75.419 | 5.125 |
| PKAC/E | 60/40 | 0.039 | 29.208 | 2.036 |
| AL/E | 60/40 | 0.260 | 146.182 | 9.934 |
| PKAC+AL/E | 70/30 | Sample broken (No data obtained) | | |
| PKAC/E | 70/30 | 0.035 | 30.568 | 4.794 |
| AL/E | 70/30 | Sample broken (No data obtained) | | |
| SK2 Carbon Steel | - | 0.120 | 15.699 | 1.067 |
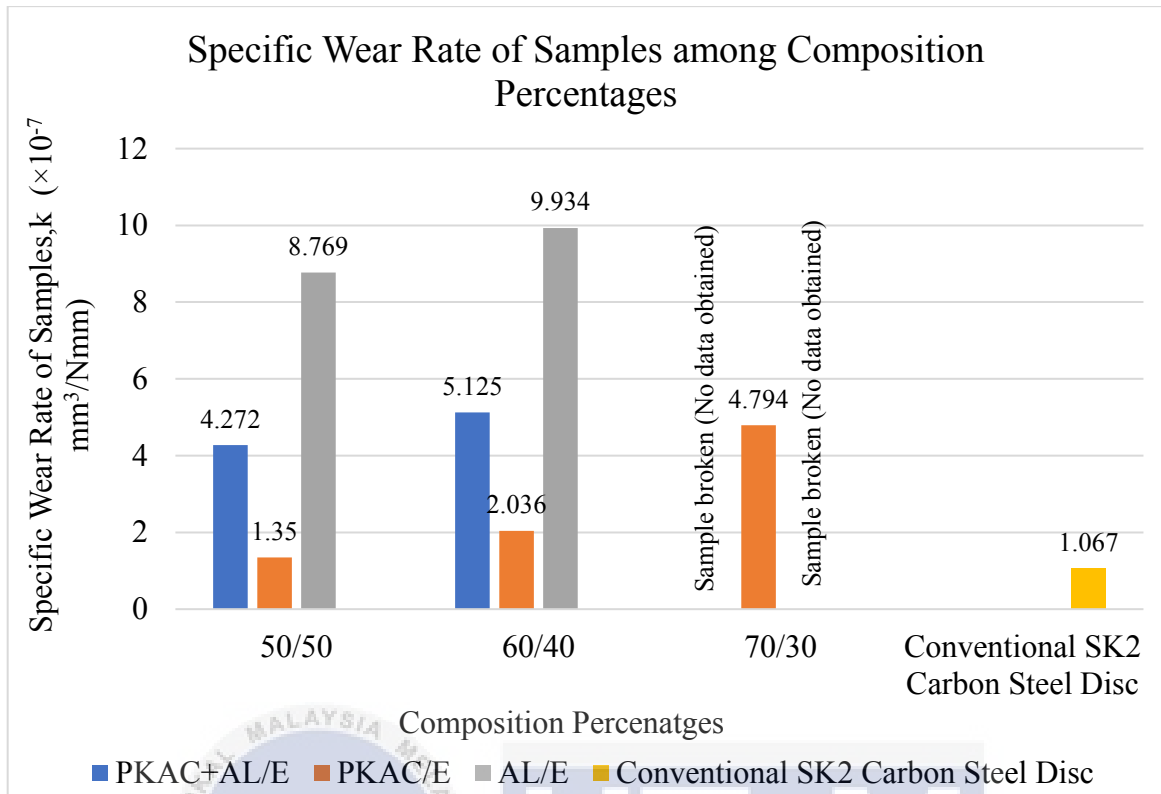
Figure 4.4: Specific wear rate of samples among composition percentages

**4.4 Surface Wear Morphology**
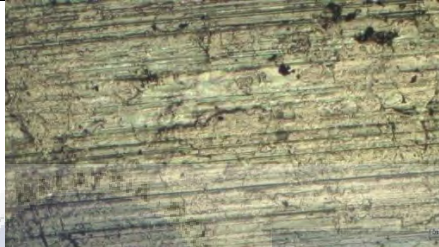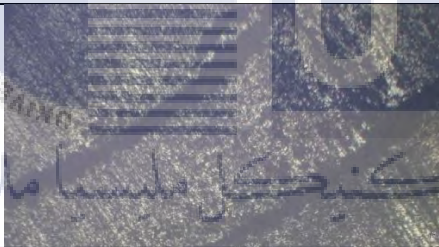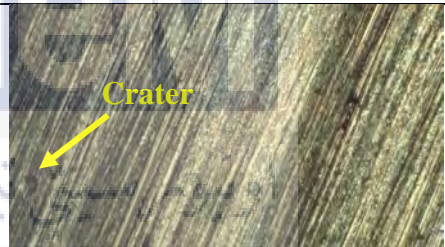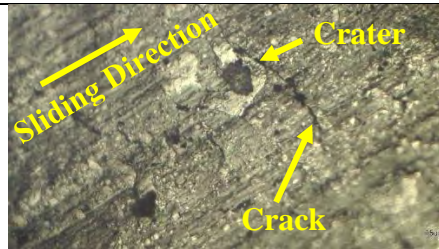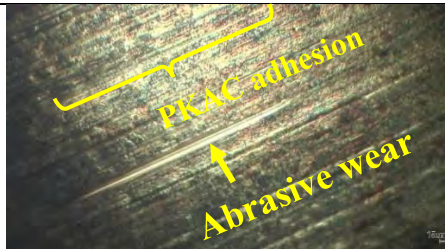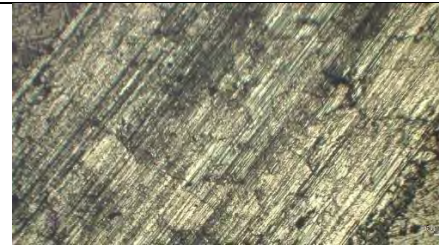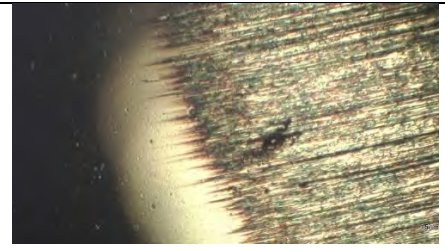
Morphology of wear track and worn surfaces of samples were conducted by using 3D surface profilometer.  By referring to Table 4.4 (g), the micrograph reveals the presence of cracks and crater on the wear track of PKAC+AL/E (60/40) which is more obvious compare to PKAC+AL/E (50/50) in Table 4.4 (a). Besides, it is clearly shown in Figure 4.5 (d) there is more debris generated on the wear track of PKAC+AL/E (60/40) compare to PKAC+AL/E (50/50) in Figure 4.5 (a) and the wear track width of PKAC+AL/E 60/40 (4.5mm) is wider than PKAC+AL/E (50/50) (4mm). This could imply that the lower content of epoxy in the samples, the weaker the joint connection between the particles. Hence, more particles in PKAC+AL/E (60/40) being pulled out easily and more debris are formed on the wear track surface. This could have contributed for higher specific wear rate with lower coefficient of friction for PKAC+AL/E (60/40). The pulled-out particles contribute to higher wear rate due to higher mass loss and volume loss. While a formation of transfer film was observed on the counter surface of carbon chromium steel ball in Table 4.4 (h) which helps to stabilize friction due to the surface contact changes from carbonized-steel to carbonized-carbonized materials. The adhering film breaks adhesive joints between asperities and contribute to low friction coefficient (Mahmud et al., 2017).
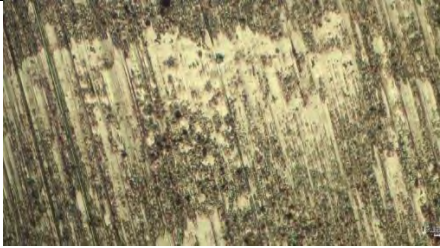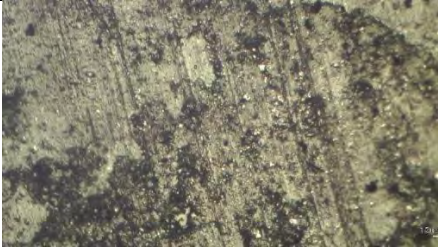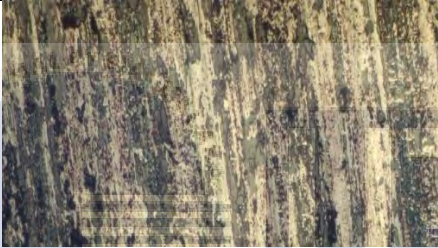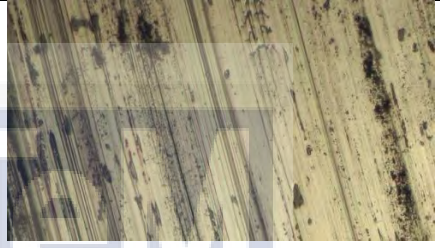
For the wear track worn surface comparison between hybrid composites PKAC+AL/E (50/50), PKAC+AL/E (60/40) and conventional SK2 Carbon disc which shown in Table 4.4 (a), Table 4.4 (g) and Table 4.4 (o) respectively, there is no cracks and craters observed on SK2 Carbon Steel Disc track surface. Wear track width of SK2 Carbon Steel Disc (Figure 4.5 (h)) is obviously narrower than PKAC+AL/E (50/50) (Figure 4.5 (a)) and PKAC+AL/E (60/40) (Figure 4.5 (d)). Thus, SK2 Carbon wear rate is much lower among all the specimens. However, there is no formation of transfer layer observed in Table 4.4 (p) for carbon chromium ball of SK2 Carbon Steel disc. It is believed that with the

absence of carbon transfer layer formed on the counter surface would contribute to higher friction coefficient when compare with PKAC+AL/E (50/50) and PKAC+AL/E (60/40).

Worn surface of wear track for hybrid composites PKAC+AL/E for both 50/50 and 60/40 composition (Figure 4.5 (a) and Figure 4.5 (b) respectively) are obviously rougher and wider compare to PKAC/E (Figure 4.5 (b) and Figure 4.5 (e)). This may due to the alumina particles inside the hybrid composites have increased the overall shear modulus of samples and cause the hybrid composites exhibit higher wear rate. This is contradicted with the good wear resistant properties of alumina which able to minimize wear. As mentioned in previous studies, PKAC is a good self-lubricating material. It is believed that in this case, the addition of alumina will increase wear rate of sample although alumina is excellent with its wear resistant properties because PKAC is exhibit better wear resistant and contribute lower wear rate than alumina. This is also proven in previous wear rate result discussion which shown in Figure 4.4, pure AL/E exhibit higher wear rate than pure PKAC/E samples for both composition which justified that alumina exhibit higher wear rate than PKAC.

Table 4.4: Micrographs of worn surface of samples and carbon chromium steel ball

| Samples | Micrograph of the worn surface on the wear track of samples | Micrograph of the worn surface on the carbon chromium steel ball |
|---|---|---|
| PKAC+AL/E (50/50) | (a) | (b) |
| PKAC/E (50/50) | (c) | (d) |
| AL/E (50/50) | (e) | (f) |
| PKAC+AL/E (60/40) | (g) | (h) |
| PKAC/E (60/40) | (i) | (j) |

| | | |
|---|---|---|
| AL/E (60/40) | <br>(k) | <br>(l) |
| PKAC/E (70/30) | <br>(m) | <br>**Abrasive Wear**<br>(n) |
| SK2 Carbon Steel Disc | <br>(o) | <br>(p) |
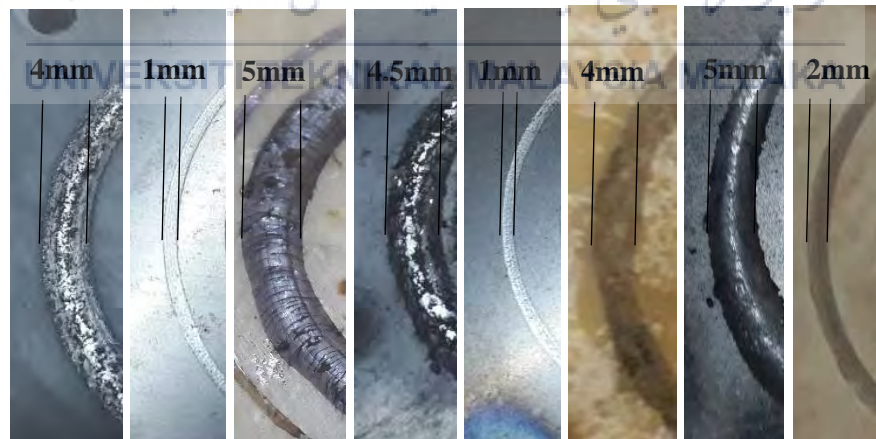


**(a)**  **(b)**  **(c)**  **(d)**  **(e)**  **(f)**  **(g)**  **(h)**

Figure 4.5: Wear track images of (a) PKAC+AL/E (50/50), (b) PKAC/E (50/50), (c) AL/E (50/50) (d) PKAC+AL/E (60/40), (e) PKAC/E (60/40), (f) AL/E (60/40), (g) PKAC/E (70/30), (h) SK2 Carbon Steel Disc

## 4.5 Discussions Summary

Table 4.5 is the summary of data and results of this study. The finding highlights 60/40 is the optimal composition for hybrid composite PKAC+AL/E because it exhibits lower friction coefficient compare to 50/50 hybrid composition and conventional SK2 Carbon Steel disc. Although PKAC+AL/E (60/40) exhibited slightly higher specific wear rate than PKAC+AL/E (50/50) and SK2 Carbon Steel, but the differences of the values are minor and insignificant so PKAC+AL/E (60/40) is a preferable choice in this case. For the new generation of hybrid composites which involve the agriculture waste, PKAC improved the performance of hybrid composites in terms of friction and wear. Whereas a further study should be conducted on how much improvement of hybrid composites in terms of tribological performance is obtained by adding alumina in samples. In summary, the optimum composition of hybrid composite PKAC+AL/E is 60/40 and it is suitable to be treated as a solid lubricating material under unlubricated condition at room temperature.

Table 4.5 Collected data for surface roughness, hardness, coefficient of friction, specific wear rate and wear track width of samples under dry sliding ball-on-disc test at room temperature.

| Samples | Composition | Surface Roughness (μmRa) | Hardness (GPa) | Coefficient of Friction, μ | Specific Wear Rate, k ($\times 10^{-7}$ mm$^3$/Nmm) | Wear Track Width (mm) |
|---|---|---|---|---|---|---|
| PKAC+AL/E | (50/50) | 0.201 | 8.218 | 0.270 | 4.272 | 4.0 |
| PKAC/E | (50/50) | 0.274 | 8.140 | 0.202 | 1.350 | 1.0 |
| AL/E | (50/50) | 0.319 | 8.267 | 0.514 | 8.769 | 5.0 |
| PKAC+AL/E | (60/40) | 0.205 | 8.493 | 0.213 | 5.125 | 4.5 |
| PKAC/E | (60/40) | 0.337 | 8.306 | 0.111 | 1.985 | 1.0 |
| AL/E | (60/40) | 0.301 | 8.258 | 0.505 | 9.934 | 4.0 |
| PKAC+AL/E | (70/30) | Sample broken after cured | | | | |
| PKAC/E | (70/30) | 0.677 | 8.473 | 0.858 | 4.794 | 5.0 |
| AL/E | (70/30) | 0.612 | 6.645 | Sample broken before tribometer test | | |
| SK2 Carbon Steel Disc | - | - | - | 0.516 | 1.067 | 2.0 |

55

# CHAPTER 5

## CONCLUSION AND RECOMMENDATION

### 5.1 Conclusion

Generally, the research is conducted in order to identify the optimal composition and investigate the tirobological properties of the blended hybrid composite sample (PKAC+AL/E) under dry sliding ball-on-disc tribometer test. Tribological performance of the samples which obtained from the tribometer test is taken to compare with conventional composites, SK2 Carbon Steel Disc. There are nine samples with different composition percentages with respect to weight were prepared for this study. The composition percentages for hybrid composites (PKAC/Alumina) used with respect to weight are 50%, 60% and 70% whereas for epoxy are 50%, 40% and 30% respectively. Coefficient of friction (CoF), specific wear rate, k and wear morphology of worn surface are the three essential elements in studying wear performance of hybrid composites. However, there are two specimens PKAC+AL/E (70/30) and AL/E (70/30) became brittle and ruptured after hot press process and curing process which believed that it may due to lack of epoxy for embedding the particles. Hence, these two specimens are unable to run under the test, no friction coefficient and specific wear rate results shown, and no comparison can be done for 70/30 composition.

The results from tribometer test revealed that among all specimens, PKAC/E (60/40) exhibit lowest coefficient of friction and PKAC/E (70/30) exhibit highest friction coefficient.

While for comparison between hybrid composites, PKAC+AL/E (60/40) exhibit lower friction coefficient than PKAC+AL/E (50/50). The result proved that 60/40 is the optimal composition for hybrid composites of PKAC+AL/E in this dry sliding test at room temperature. In addition, friction coefficient of PKAC+AL/E (60/40) is much lower than conventional disc SK2 Carbon Steel which also supported that PKAC+AL/E (60/40) is considered a good self-lubricating material in this study.

Specific wear rate of samples was calculated based on mass loss after performed tribometer tests. The results suggested that specimen of 50/50 composition exhibited lower specific wear rate than 60/40 composition with minor differences. From the wear rate results shown in both composition provide the evidence that higher PKAC content contribute lower wear rate whereas higher alumina content contribute higher the wear rate. It is proven that although alumina has been justified as a good wear resistant material in previous tribological studies and applications but PKAC exhibited better wear resistant than alumina. This is the reason alumina being treated as high wear material in this study. Specific wear rate of PKAC+AL/E (50/50) is slightly lower than PKAC+AL/E (60/40) which suggested that 50/50 composition is optimal composition for hybrid composites to achieve lower wear rate. SK2 Carbon Steel Disc exhibited lower specific wear rate than hybrid composites in this study which it is believed that the wear rate difference between PKAC+AL/E (50/50 and 60/40) and SK2 Carbon Steel disc was affected by experimental limitations during sample preparation process of hybrid composites.

Wear morphology of specimens shown that wear tracks of AL/E are the widest and roughest with the significant microcracks and irregularities on the surface compare to PKAC/E and PKAC+AL/E. It is believed that presence of alumina will increase wear rate of sample although alumina is excellent with its wear resistant properties because PKAC is exhibit better wear resistant and contribute lower wear rate than alumina. Hence, AL/E has

highest wear rate follow by PKAC+AL/E and PKAC/E. Moreover, wear morphologies for PKAC+AL/E (50/50) and PKAC+AL/E (60/40) are consistent with specific wear rate results. PKAC+AL/E (60/40) exhibit higher wear rate, wider wear track and more cracks, craters are shown in micrograph compare to PKAC+AL/E (50/50). The results suggested that the higher epoxy content contribute to lower wear due to the better adhesive bonding system in samples prevent the particles being pulled out easily during the high-speed sliding motion.

In summary, the current study reveals that for hybrid composites of PKAC+AL/E, 60/40 composition is the optimal composition which exhibit low friction coefficient, 0.213 and low specific wear rate, $5.125 \times 10^{-7}$ mm$^3$/Nmm. Although PKAC+AL/E (50/50) exhibit lower wear rate compare to PKAC+AL/E (60/40) but PKAC+AL/E (60/40) is chosen as optimal hybrid composites composition because the difference of the wear rate, k values is $0.853 \times 10^{-7}$ mm$^3$/Nmm which is minor and insignificant. So, lower friction coefficient specimen is chosen in this study. PKAC improved the performance of hybrid composite in terms of friction and wear. Whereas a further study should be conducted on how much improvement of hybrid composites is obtained by adding alumina in samples in terms of higher operating temperature. The overall findings suggested that the PKAC+AL/E (60/40) is suitable to act as solid lubricating material under unlubricated condition at room temperature.

**5.2 Recommendation for Future Study**

I. Methodology of samples preparation process for future study is recommended to use the laboratory mixer or blender and grinding and polishing machine. Laboratory mixer use to break-up and mix the materials or powders completely to prevent formation of lumps in the specimens. Grinding and polishing machine is used to polish the specimens automatically with even distributed force on the samples to avoid the uneven grinding force applied on the surfaces and to ensure to obtain reliable surface roughness analysis.

II. PKAC was proven as a good self-lubricating material and it contributed in improvement of wear performance of hybrid composites. Alumina exhibit excellent characteristics of high hardness, high wear resistance and high thermal conductivity. However, improvement contributed by alumina is insignificant in this study where the tribometer test operate at room temperature. Hence, the future study for the effect of different temperatures on tribological performance of hybrid composites based on PKAC and alumina blend is suggested for investigate the improvement of hybrid composites in terms of different operating temperatures. Table 5.1 shows the composition percentages of testing composites suggested for future study. Since composition of 60/40 is the optimal composition found in this study and it is consistent with optimum composition used in previous researches (Mohmad et al., 2017), hence these compositions are suggested for future research to investigate the more specific optimal composition under different operating temperatures. The results of this suggested study will help to reveal a more specific composition of how many % of PKAC combine with how many % of AL with 40% epoxy will give a best tribological performance of low friction and low wear under different sliding temperatures. The example of CoF result could be obtained is shown in Figure 5.1.

Table 5.1: Composition percentages of testing composites suggested for future study

| Sample | Palm Kernel Activated Carbon (PKAC), % | Alumina ($Al_2O_3$), % | Epoxy, % |
|---|---|---|---|
| PKAC+AL/E (1:5:4) | 10 | 50 | 40 |
| PKAC+AL/E (2:4:4) | 20 | 40 | 40 |
| PKAC+AL/E (3:3:4) | 30 | 30 | 40 |
| PKAC+AL/E (4:2:4) | 40 | 20 | 40 |
| PKAC+AL/E (5:1:4) | 50 | 10 | 40 |
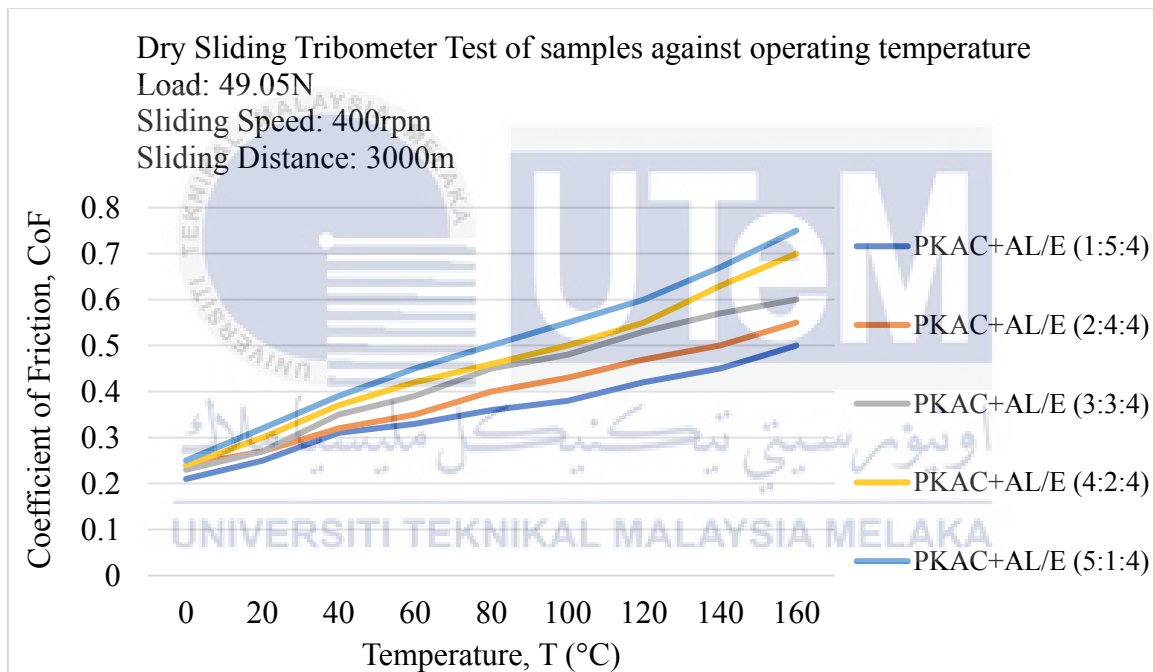


Figure 5.1: Example of CoF result for future study

III.   Scanning Electron Microscopy (SEM), Energy Dispersive X-ray spectroscopy (EDX) and Raman spectroscopy analysis are suggested to examine the worn surfaces, chemical composition and phase transformation of the specimens respectively.

# REFERENCES

Adam, M. (2013). Aluminium oxide ceramic properties. *Accuratus*. Retrieved from http://accuratus.com/alumox.html

Agunsoye, J. O., Isaac, T. S., Awe, O. I. and Onwuegbuzie, A. T. (2013). Effect of silicon additions on the wear properties of grey cast iron. *Journal of Minerals and Materials Characterization and Engineering*, *1*(02), 61.

Bansal, H., Singla, Y. K. G. and Kalra, A. G. (2011). *Wear behaviour of aluminium based metal matrix composites reinforced with red mud, SiC and Al2O3* (Doctoral dissertation).

Bart, J. C., Gucciardi, E. and Cavallaro, S. (2013). Chemical transformations of renewable lubricant feedstocks. *Biolubricants Science and Technology*, 249-350.

Bodunrin, M. O., Alaneme, K. K. and Chown, L. H. (2015). Aluminium matrix hybrid composites: a review of reinforcement philosophies; mechanical, corrosion and tribological characteristics. *Journal of Materials Research and Technology*, *4*(4), 434-445.

Celis, J. P. (2017). *Testing tribocorrosion of passivating materials supporting research and industrial innovation: A Handbook*. Routledge.

Chamis, C. and Lark, R. (1977). Hybrid composites-State-of-the-art review: Analysis, design, application and fabrication. In *18th Structural Dynamics and Materials Conference* (p. 415).

Chua, K. W., Abdollah, M. F. B., Ismail, N. and Amiruddin, H. (2014). Potential of palm kernel activated carbon epoxy (PKAC-E) composite as solid lubricant: Effect of load on friction and wear properties. *Jurnal Tribologi*, *2*, 31-38.

Prasad, D. S. and Shoba, C. (2014). Hybrid composites–a better choice for high wear resistant materials. *Journal of Materials Research and Technology*, *3*(2), 172-178.

Fukuda, H. (1984). An advanced theory of the strength of hybrid composites. *Journal of materials science*, *19*(3), 974-982.

Godet, M. (1984). The third-body approach: a mechanical view of wear. *Wear*, *100*(1-3), 437-452.

Guo, M. T. and Tsao, C. Y. (2000). Tribological behavior of self-lubricating aluminium/SiC/graphite hybrid composites synthesized by the semi-solid powder-densification method. *Composites Science and Technology*, *60*(1), 65-74.

Holmberg, K. and Erdemir, A. (2017). Influence of tribology on global energy consumption, costs and emissions. *Friction*, *5*(3), 263-284.

John, M. J., Anandjiwala, R. D., and Thomas, S. (2014). *Hybrid Composites*, 15.

Jost, H. P. (1966). *Lubrication: Tribology; Education and Research; Report on the Present Position and Industry's Needs (submitted to the Department of Education and Science by the Lubrication Engineering and Research) Working Group*. HM Stationery Office.

Kathiresan, M. and Sornakumar, T. (2010). Friction and wear studies of die cast aluminum alloy-aluminum oxide-reinforced composites. *Industrial lubrication and tribology*, *62*(6), 361-371.

Kolade, O. O., Coker, A. O., Sridhar, M. K. C. and Adeoye, G. O. (2006). Palm kernel waste management through composting and crop production. *Journal of Environmental Health Research*, *5*(2), 81.

Kopeliovich, D. (2017). Mechanisms of wear. *SubsTech*. Retrieved from http://www.substech.com/dokuwiki/doku.php?id=mechanisms_of_wear

Kumar, V., Sinha, S. K. and Agarwal, A. K. (2015). Tribological studies of epoxy and its composite coatings on steel in dry and lubricated sliding. *Tribology-Materials, Surfaces & Interfaces*, *9*(3), 144-153.

Lancashire, R. J. (2014). The Chemistry and Processing of Jamaican Bauxite. Retrieved from http://wwwchem.uwimona.edu.jm/lectures/bauxite.html

Li, C. X. (n.d.). Surface Engineering. *Wear and Wear Mechanism*. Retrieved from http://emrtk.uni-miskolc.hu/projektek/adveng/home/kurzus/korsz_anyagtech/1_konzultacio_elemei/wear_and_wear_mechanism.htm

Rajesh, A. M. and Kaleemulla, M. (2016). Experimental investigations on mechanical behavior of aluminium metal matrix composites. In *IOP Conference Series: Materials Science and Engineering* (Vol. 149, No. 1, p. 012121). IOP Publishing.

Mahmud, D. N. F., Abdollah, M. F. B., Masripan, N. A. B., Tamaldin, N. and Amiruddin, H. (2017). Frictional wear stability mechanisms of an activated carbon composite derived from palm kernel by phase transformation study. *Industrial Lubrication and Tribology*, *69*(6), 945-951.

Abdollah, M. F. B., Yamaguchi, Y., Akao, T., Inayoshi, N., Umehara, N. and Tokoroyama, T. (2010). Phase transformation studies on the aC coating under repetitive impacts. *Surface and Coatings Technology*, *205*(2), 625-631.

Miramontes, J. C., Tiburcio, C. G., Tellez, A. V., Salas, C. P. and Calderón, F. A. (2016). Wear resistance of thermal spray WC-Co-VC nanostructured coatings. In *Advances in tribology*. InTech.

Mitrović, S., Babić, M., Stojanović, B., Miloradović, N., Pantić, M. and Džunić, D. (2012). Tribological potential of hybrid composites based on zinc and aluminium alloys reinforced with SiC and graphite particles. *Tribology in Industry*, *34*(4), 177-185.

Modern oil palm cultivation. (n.d.). The Oil Palm. Retrieved from http://www.fao.org/docrep/006/t0309e/T0309E01.htm

Mohmad, M., Abdollah, M. F. B., Tamaldin, N. and Amiruddin, H. (2017). The effect of dimple size on the tribological performances of a laser surface textured palm kernel activated carbon-epoxy composite. *Industrial lubrication and Tribology*, *69*(5), 768-774.

Nanko, M. (2009). Definitions and categories of hybrid materials. *AZojomo*, *6*, 1-8.

Panchagnula, K. K. and Palaniyandi, K. (2017). Drilling on fiber reinforced polymer/nanopolymer composite laminates: a review. *Journal of Materials Research and Technology*.

R.D.Pruthviraj. (2014). *A review on recent applications and future prospectus of hybrid composites in various engineering applications*, 3.

Ravindran, P., Manisekar, K., Rathika, P. and Narayanasamy, P. (2013). Tribological properties of powder metallurgy–Processed aluminium self lubricating hybrid composites with SiC additions. *Materials & design*, *45*, 561-570.

Shaffer, S. J. (2013). 101–Introduction to the Basics of Tribology.

Mitrović, S., Babić, M., Stojanović, B., Miloradović, N., Pantić, M. and Džunić, D. (2012). Tribological potential of hybrid composites based on zinc and aluminium alloys reinforced with SiC and graphite particles. *Tribology in Industry*, *34*(4), 177-185.

Palm Biomass Waste Pellet Production Line. (n.d.). Retrieved from http://www.apa.org/helpcenter/recovering-disasters.aspx

Stojanović, B. and Ivanović, L. (2015). Application of aluminium hybrid composites in automotive industry. *Tehnički vjesnik*, *22*(1), 247-251.

Surendran, R., Manibharathi, N. and Kumaravel, A. (2017). Wear properties enhancement of aluminium alloy with addition of nano alumina. *FME Transactions*, *45*(1), 83-88.

Svahn, F., Kassman-Rudolphi, Å. and Wallen, E. (2003). The influence of surface roughness on friction and wear of machine element coatings. *Wear*, *254*(11), 1092-1098.

Tahir, N. A. (2016). *Tribological performances for palm kernel activated carbon epoxy compositE*, 24.

Tahir, N. A. M., Abdollah, M. F. B., Hasan, R. and Amiruddin, H. (2016). The effect of sliding distance at different temperatures on the tribological properties of a palm kernel activated carbon–epoxy composite. *Tribology International*, *94*, 352-359.

Tahir, N. A. M., Abdollah, M. F. B., Hasan, R. and Amiruddin, H. (2015). The effect of temperature on the tribological properties of palm kernel activated carbon-epoxy composite. *Tribology Online*, *10*(6), 428-433.

Tahir, N. A. M., Abdollah, M. F. B., Tamaldin, N., Amiruddin, H. and Mohamad Zin, M. R. B. (2018). A brief review on the wear mechanisms and interfaces of carbon based materials. *Composite Interfaces*, *25*(5-7), 491-513.

Tamás, T. (2016). *Developing of Nanostructured Polymer Composites*. BMe Research Grant. Retrieved from http://doktori.bme.hu/bme_palyazat/2016/honlap/Turcsan_Tamas_gpk_en.html

Uthayakumar, M., Aravindan, S. and Rajkumar, K. (2013). Wear performance of Al–SiC–B4C hybrid composites under dry sliding conditions. *Materials & Design*, *47*, 456-464.

Vasconcelos, P. V., Lino, F. J., Baptista, A. M. and Neto, R. J. (2006). Tribological behaviour of epoxy based composites for rapid tooling. *Wear*, *260*(1-2), 30-39.

Veličković, S., Stojanović, B., Babić, M. and Bobić, I. (2017). Optimization of tribological properties of aluminum hybrid composites using Taguchi design. *Journal of composite materials*, *51*(17), 2505-2515.

Yunxia, C., Wenjun, G. and Rui, K. (2016). Coupling behavior between adhesive and abrasive wear mechanism of aero-hydraulic spool valves. *Chinese Journal of Aeronautics*, *29*(4), 1119-1131.

Yusoff, Z., Jamaludin, S. B. and Noor, M. M. (2012). Physical Properties and Microstructure of Green Aluminium Matrix Composite. In *8 th Asian Australasian Conference on Composite Materials (ACCM-8)* (pp. 6-8).

Yusoff, Z., Jamaludin, S. B., Amin, M. and Zaidi, N. H. A. (2010). Sliding wear properties of hybrid aluminium composite reinforced by particles of palm shell activated carbon and slag. *Journal of Science and Technology*, *2*(1).

Yusoff, Z. The physical and wear properties of hybrid biomass by-product particulates reinforced aluminium matrix composite.

# APPENDICES

# APPENDIX A

Standard test method for wear testing with a pin-on-disk apparatus

## Standard Test Method for
## Wear Testing with a Pin-on-Disk Apparatus[1]

## 1. Scope

1.1 This test method describes a laboratory procedure for determining the wear of materials during sliding using a pin-on-disk apparatus. Materials are tested in pairs under nominally non-abrasive conditions. The principal areas of experimental attention in using this type of apparatus to measure wear are described. The coefficient of friction may also be determined.

1.2 The values stated in SI units are to be regarded as standard.

1.3 *This standard does not purport to address all of the safety concerns, if any, associated with its use. It is the responsibility of the user of this standard to establish appropriate safety and health practices and determine the applicability of regulatory limitations prior to use.*

## 2. Referenced Documents

2.1 *ASTM Standards:*
E 122 Practice for Choice of Sample Size to Estimate a Measure of Quality for a Lot or Process[2]
E 177 Practice for Use of the Terms Precision and Bias in ASTM Test Methods[2]
E 178 Practice for Dealing with Outlying Observations[2]
G 40 Terminology Relating to Wear and Erosion[3]
2.2 *Other Standard:*[4] DIN-50324 Testing of Friction and Wear

## 3. Summary of Test Method

3.1 For the pin-on-disk wear test, two specimens are required. One, a pin with a radiused tip, is positioned perpendicular to the other, usually a flat circular disk. A ball, rigidly held, is often used as the pin specimen. The test machine causes either the disk specimen or the pin specimen to revolve about the disk center. In either case, the sliding path is a circle on the disk surface. The plane of the disk may be oriented either horizontally or vertically.

Note 1DWear results may differ for different orientations.

3.1.1 The pin specimen is pressed against the disk at a specified load usually by means of an arm or lever and attached weights. Other loading methods have been used, such as, hydraulic or pneumatic.

Note 2DWear results may differ for different loading methods.

3.2 Wear results are reported as volume loss in cubic millimetres for the pin and the disk separately. When two different materials are tested, it is recommended that each material be tested in both the pin and disk positions.

3.3 The amount of wear is determined by measuring appropriate linear dimensions of both specimens before and after the test, or by weighing both specimens before and after the test. If linear measures of wear are used, the length change or shape change of the pin, and the depth or shape change of the disk wear track (in millimetres) are determined by any suitable metrological technique, such as electronic distance gaging or stylus profiling. Linear measures of wear are converted to wear volume (in cubic millimetres) by using appropriate geometric relations. Linear measures of wear are used frequently in practice since mass loss is often too small to measure precisely. If loss of mass is measured, the mass loss value is converted to volume loss (in cubic millimetres) using an appropriate value for the specimen density.

3.4 Wear results are usually obtained by conducting a test for a selected sliding distance and for selected values of load and speed. One set of test conditions that was used in an interlaboratory measurement series is given in Table 1 and Table 2 as a guide. Other test conditions may be selected depending on the purpose of the test.

3.5 Wear results may in some cases be reported as plots of wear volume versus sliding distance using different specimens for different distances. Such plots may display non-linear relationships between wear volume and distance over certain portions of the total sliding distance, and linear relationships over other portions. Causes for such differing relationships include initial "break-in" processes, transitions between regions of different dominant wear mechanisms, etc. The extent of such non-linear periods depends on the details of the test system, materials, and test conditions.

3.6 It is not recommended that continuous wear depth data

## G 99

### TABLE 1  Characteristics of the Interlaboratory Wear Test Specimens

Note 1—See Note 4 in 10.4 for information.

| | | Composition (weight%) | Microstructure | Hardness (HV 10) | Roughness[A] | |
|---|---|---|---|---|---|---|
| | | | | | $R_z$(mean) (μm) | $R_a$(mean) (μm) |
| Steel ball (100 Cr6) (AISI 52 | 100][B] | 1.35 to 1.65 Cr | martensitic with minor carbides | 838 6 21 | 0.100 | 0.010 |
| Diameter 10 mm | | ← 0.95 to 1.10 C | and austenite | | | |
| | | 0.15 to 0.35 Si | | | | |
| | | 0.25 to 0.45 Mn | | | | |
| Steel disc (100 Cr6) (AISI 52 | 100][C] | ← <0.030 P | martensitic with minor carbides | 852 6 14 | 0.952 | 0.113 |
| Diameter 40 mm | | <0.030 S | and austenite | | | |
| Alumina ball, diameter 5 10 mm[D] | | ← 95 % Al₂O₃ (with addi- | equi-granular alpha alumina | 1610 6 101 (HV 0.2) | 1.369 | 0.123 |
| | | tives of TiO₂) | with very minor secondary | | | |
| Alumina disc, diameter 5 40.6 mm[D] | | ← MgO and ZnO) | phases | 1599 6 144 (HV 0.2) | 0.968 | 0.041 |

[A] Measured by stylus profilometry. $R_z$ is maximum peak-to-valley roughness. $R_a$ is arithmetic average roughness.
[B] Standard ball-bearing balls (SKF).
[C] Standard spacers for thrust bearings (INA).
[D] Manufactured by Compagnie Industrielle des Ceramiques Electroniques, France.

### TABLE 2  Results of the Interlaboratory Tests[A]

Note 1—See Note 4 in 10.4.
Note 2—Numbers in parentheses refer to all data received in the tests. In accordance with Practice E 178, outlier data values were identified in some cases and discarded, resulting in the numbers without parentheses. The differences are seen to be small.
Note 3—Values preceded by 6 are one standard deviation.
Note 4—Between eleven and twenty laboratories provided these data.
Note 5—Calculated quantities (for example, wear volume) are given as mean values only.
Note 6—Values labeled "NM" were found to be smaller than the reproducible limit of measurement.
Note 7—A similar compilation of test data is given in DIN 50324.

| Results (ball) (disk) | Specimen Pairs | | | |
|---|---|---|---|---|
| | Steel-steel | Alumina-steel | Steel-alumina | Alumina-alumina |
| Ball wear scar diameter (mm) | 2.11 6 0.27 | NM | 2.08 6 0.35 | 0.36 6 0.06 |
| | (2.11 6 0.27) | | (2.03 6 0.41) | (0.3 6 0.06) |
| Ball wear volume (10⁻⁴ mm³) | 198 | | 196 | 0.08 |
| | (198) | | (168) | (0.08) |
| Number of values | 102 | | 60 | 56 |
| | (102) | | (64) | (59) |
| Disk wear scar width (mm) | NM | 0.64 6 0.12 | NM | NM |
| | | (0.64 6 0.12) | | |
| Disk wear volume (10⁻³ mm³) | | 490 | | |
| | | (480) | | |
| Number of values | | 60 | | |
| | | (60) | | |
| Friction coefficient | 0.60 6 0.11 | 0.76 6 0.14 | 0.60 6 0.12 | 0.41 6 0.08 |
| Number of values | 109 | 75 | 64 | 76 |

[A] Test conditions: F 5 10 N; v 5 0.1 ms⁻¹, T 5 23°C; relative humidity range 12 to 78 %; laboratory air; sliding distance 1000 m; wear track (nominal) diameter 5 32 mm; materials: steel 5 AISI 52 100; and alumina 5 a-Al₂O₃.

obtained from position-sensing gages be used because of the complicated effects of wear debris and transfer films present in the contact gap, and interferences from thermal expansion or contraction.

### 4. Significance and Use

4.1 The amount of wear in any system will, in general, depend upon the number of system factors such as the applied load, machine characteristics, sliding speed, sliding distance, the environment, and the material properties. The value of any wear test method lies in predicting the relative ranking of material combinations. Since the pin-on-disk test method does not attempt to duplicate all the conditions that may be experienced in service (for example; lubrication, load, pressure, contact geometry, removal of wear debris, and presence of corrosive environment), there is no ensurance that the test will predict the wear rate of a given material under conditions differing from those in the test.

### 5. Apparatus

5.1 General Description—Fig. 1 shows a schematic drawing of a typical pin-on-disk wear test system, and photographs of two differently designed apparatuses.[5] One type of typical system consists of a driven spindle and chuck for holding the revolving disk, a lever-arm device to hold the pin, and attachments to allow the pin specimen to be forced against the revolving disk specimen with a controlled load. Another type of system loads a pin revolving about the disk center against a stationary disk. In any case the wear track on the disk is a

[5] A number of other reported designs for pin-on-disk systems are given in "A Catalog of Friction and Wear Devices," American Society of Lubrication Engineers (1973). The sole source of supply of commercially built machines known to the committee at this time is Falex Corp., 1020 Airpark Dr., Sugar Grove, IL 60554. If you are aware of alternative suppliers, please provide this information to ASTM Headquarters. Your comments will receive careful consideration at a meeting of the responsible technical committee, [1] which you may attend.

NOTE 1—F is the normal force on the pin, d is the pin or ball diameter, D is the disk diameter, R is the wear track radius, and w is the rotation velocity of the disk.
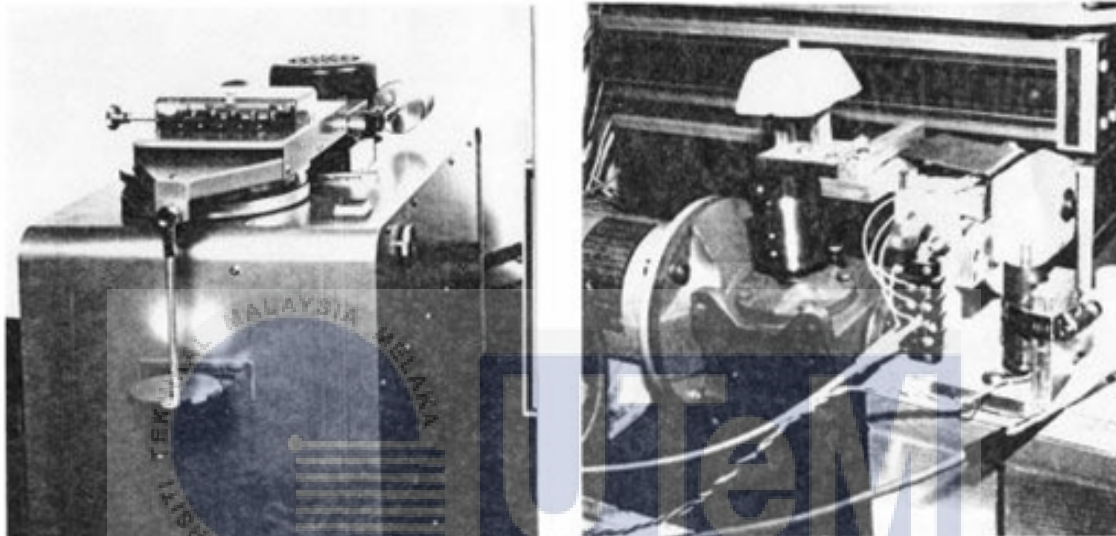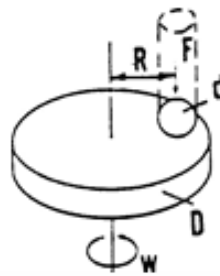
FIG. 1 (a) Schematic of pin-on-disk wear test system. (b) Photographs of two different designs.

circle, involving multiple wear passes on the same track. The system may have a friction force measuring system, for example, a load cell, that allows the coefficient of friction to be determined.

5.2 *Motor Drive*—A variable speed motor, capable of maintaining constant speed (±1 % of rated full load motor speed) under load is required. The motor should be mounted in such a manner that its vibration does not affect the test. Rotating speeds are typically in the range 0.3 to 3 rad/s (60 to 600 r/min).

5.3 *Revolution Counter*—The machine shall be equipped with a revolution counter or its equivalent that will record the number of disk revolutions, and preferably have the ability to shut off the machine after a pre-selected number of revolutions.

5.4 *Pin Specimen Holder and Lever Arm*— In one typical system, the stationary specimen holder is attached to a lever arm that has a pivot. Adding weights, as one option of loading, produces a test force proportional to the mass of the weights applied. Ideally, the pivot of the arm should be located in the plane of the wearing contact to avoid extraneous loading forces

due to the sliding friction. The pin holder and arm must be of substantial construction to reduce vibrational motion during the test.

5.5 *Wear Measuring Systems*—Instruments to obtain linear measures of wear should have a sensitivity of 2.5 µm or better. Any balance used to measure the mass loss of the test specimen shall have a sensitivity of 0.1 mg or better; in low wear situations greater sensitivity may be needed.

## 6. Test Specimens and Sample Preparation

6.1 *Materials*—This test method may be applied to a variety of materials. The only requirement is that specimens having the specified dimensions can be prepared and that they will withstand the stresses imposed during the test without failure or excessive flexure. The materials being tested shall be described by dimensions, surface finish, material type, form, composition, microstructure, processing treatments, and inden-tation hardness (if appropriate).

6.2 *Test Specimens*—The typical pin specimen is cylindrical or spherical in shape. Typical cylindrical or spherical pin

specimen diameters range from 2 to 10 mm. The typical disk specimen diameters range from 30 to 100 mm and have a thickness in the range of 2 to 10 mm. Specimen dimensions used in an interlaboratory test with pin-on-disk systems are given in Table 1.

6.3 *Surface Finish*—A ground surface roughness of 0.8 μm (32 μin.) arithmetic average or less is usually recommended.

NOTE 3—Rough surfaces make wear scar measurement difficult.

6.3.1 Care must be taken in surface preparation to avoid subsurface damage that alters the material significantly. Special surface preparation may be appropriate for some test programs. State the type of surface and surface preparation in the report.

## 7. Test Parameters

7.1 *Load*—Values of the force in Newtons at the wearing contact.

7.2 *Speed*—The relative sliding speed between the contacting surfaces in metres per second.

7.3 *Distance*—The accumulated sliding distance in meters.

7.4 *Temperature*—The temperature of one or both specimens at locations close to the wearing contact.

7.5 *Atmosphere*—The atmosphere (laboratory air, relative humidity, argon, lubricant, etc.) surrounding the wearing contact.

## 8. Procedure

8.1 Immediately prior to testing, and prior to measuring or weighing, clean and dry the specimens. Take care to remove all dirt and foreign matter from the specimens. Use non-chlorinated, non-film-forming cleaning agents and solvents. Dry materials with open grains to remove all traces of the cleaning fluids that may be entrapped in the material. Steel (ferromagnetic) specimens having residual magnetism should be demagnetized. Report the methods used for cleaning.

8.2 Measure appropriate specimen dimensions to the nearest 2.5 μm or weigh the specimens to the nearest 0.0001 g.

8.3 Insert the disk securely in the holding device so that the disk is fixed perpendicular (±1°) to the axis of the resolution.

8.4 Insert the pin specimen securely in its holder and, if necessary, adjust so that the specimen is perpendicular (±1°) to the disk surface when in contact, in order to maintain the necessary contact conditions.

8.5 Add the proper mass to the system lever or bale to develop the selected force pressing the pin against the disk.

8.6 Start the motor and adjust the speed to the desired value while holding the pin specimen out of contact with the disk. Stop the motor.

8.7 Set the revolution counter (or equivalent) to the desired number of revolutions.

8.8 Begin the test with the specimens in contact under load. The test is stopped when the desired number of revolutions is achieved. Tests should not be interrupted or restarted.

8.9 Remove the specimens and clean off any loose wear debris. Note the existence of features on or near the wear scar such as: protrusions, displaced metal, discoloration, microcracking, or spotting.

8.10 Remeasure the specimen dimensions to the nearest 2.5 μm or reweigh the specimens to the nearest 0.0001 g, as appropriate.

8.11 Repeat the test with additional specimens to obtain sufficient data for statistically significant results.

## 9. Calculation and Reporting

9.1 The wear measurements should be reported as the volume loss in cubic millimetres for the pin and disk, separately.

9.1.1 Use the following equations for calculating volume losses when the pin has initially a spherical end shape of radius $R$ and the disk is initially flat, under the conditions that only one of the two members wears significantly:

$$\text{pin (spherical end) volume loss, mm}^3 = \frac{\pi \,(\text{wear scar diameter, mm})^4}{64 \,(\text{sphere radius, mm})} \quad (1)$$

assuming that there is *no significant disk wear*. This is an approximate geometric relation that is correct to 1 % for (wear scar diameter/sphere radius) < 0.3, and is correct to 5 % for (wear scar diameter/sphere radius) < 0.7. The exact equation is given in Appendix X1.

$$\text{disk volume loss, mm}^3 = \frac{\pi \,(\text{wear track radius, mm})(\text{track width, mm})^3}{6 \,(\text{sphere radius, mm})} \quad (2)$$

assuming that there is *no significant pin wear*. This is an approximate geometric relation that is correct to 1 % for (wear track width/sphere radius) < 0.3, and is correct to 5 % for (wear track width/sphere radius) < 0.8. The exact equation is given in Appendix X1.

9.1.2 Calculation of wear volumes for pin shapes of other geometries use the appropriate geometric relations, recognizing that assumptions regarding wear of each member may be required to justify the assumed final geometry.

9.1.3 Wear scar measurements should be done at least at two representative locations on the pin surfaces and disk surfaces, and the final results averaged.

9.1.4 In situations where both the pin and the disk wear significantly, it will be necessary to measure the wear depth profile on both members. A suitable method uses stylus profiling. Profiling is the only approach to determine the exact final shape of the wear surfaces and thereby to calculate the volume of material lost due to wear. In the case of disk wear, the average wear track profile can be integrated to obtain the track cross-section area, and multiplied by the average track length to obtain disk wear volume. In the case of pin wear, the wear scar profile can be measured in two orthogonal directions, the profile results averaged, and used in a figure-of-revolution calculated for pin wear volume.

9.1.5 While mass loss results may be used internally in laboratories to compare materials of equivalent densities, this test method reports wear as volume loss so that there is no confusion caused by variations in density. Take care to use and report the best available density value for the materials tested when calculating volume loss from measured mass loss.

9.1.6 Use the following equation for conversion of mass loss to volume loss.

$$\text{volume loss, mm}^3 = \frac{\text{mass loss, g}}{\text{density, g/cm}^3} \times 1000. \quad (3)$$

70

9.2 If the materials being tested exhibit considerable transfer between specimens without loss from the system, volume loss may not adequately reflect the actual amount or severity of wear. In these cases, this test method for reporting wear should not be used.

9.3 Friction coefficient (defined in Terminology G 40) should be reported when available. Describe the conditions associated with the friction measurements, for example, initial, steady-state, etc.

9.4 Adequate specification of the materials tested is important. As a minimum, the report should specify material type, form, processing treatments, surface finish, and specimen preparation procedures. If appropriate, indentation hardness should be reported.

## 10. Precision and Bias [6]

10.1 The precision and bias of the measurements obtained with this test method will depend upon the test parameters chosen.

10.2 The reproducibility of repeated tests on the same material will depend upon material homogeneity, machine and material interaction, and careful adherence to the specified procedure by the machine operator.

10.3 Normal variations in the procedure will tend to reduce the accuracy of the test method as compared to the accuracy of such material property tests as hardness, density, or thermal expansion rate. Properly conducted tests should, however, maintain a within-laboratory coefficient of variation of 20 % or less for wear loss values. Table 2 contains wear data obtained

from interlaboratory tests (see Note 4). Standard deviation values are given for the measured quantities. Limits of 95 % repeatability can be obtained by multiplying those standard deviation values by the factor 2.8 3. Reproducibility limits (between laboratories) are not available but are estimated to be twice as large as the repeatability limits.

10.4 No bias can be assigned to these results since there are no absolute accepted values for wear.

Note 4—The interlaboratory data given in Table 1 and Table 2 resulted through the cooperation of thirty one institutions in seven countries with the help of national representatives within the Versailles Advanced Materials and Standards (VAMAS) working party on wear test methods.[7]

10.5 In any test series, all data must be considered in the calculation, including outliers (data exceeding the obvious range); they are treated according to Practice E 178.

10.6 While two or more laboratories may develop test data that is within the acceptable coefficient of variation for their own individual test apparatus, the actual data of each laboratory may be relatively far apart. The selection of sample size and the test method for establishing the significance of the difference in averages shall be agreed upon between laboratories and shall be based on established statistical methods of Practice E 122, Practice E 177, and STP 15D.[8]

## 11. Keywords

11.1 ceramic wear; friction; metal wear; non-abrasive; pin-on-disk; wear

[7] Czichos, H., Becker, S., and Lexow, J., *Wear*, Vol 114, 1987, pp 109±130 and *Wear*, Vol 118, 1987, pp 379±380.
[8] *Manual on Quality Control of Materials*, ASTM STP 15D, ASTM, 1951.

## APPENDIX

### (Nonmandatory Information)

### X1. EQUATIONS

| X1.1 Exact equations for determining wear volume loss are as follows for: | Assuming no significant disk wear: |
|---|---|
| | X1.1.2 A disk: |
| X1.1.1 A spherical ended pin: | disk volume loss $= 2\pi R \left[ r^2 \sin^{-1}(d/2r) - (d/4)(4r^2 - d^2)^{1/2} \right]$  (X1.2) |
| pin volume loss $= (\pi h/6)[3d^2/4 + h^2]$,   (X1.1) | |

where:
$h = r - [r^2 - d^2/4]^{1/2}$
$d$ = wear scar diameter, and $r$
= pin end radius.

where:
$R$ = wear track radius, and $d$
= wear track width.
Assuming no significant pin wear.

⟨SID⟩ G 99

# APPENDIX B
## Hardness conversion chart

## Hardness Conversion Charts & Calculator *

### Comparison of Hardness Scales approx. and Tensile Stress Equivalents approx. (maximum value) in imperial and metric units.

| Rockwell | Vickers Diamond Penetrator | Brinell | | | Tensile Stress Equivalents | | | | Shore Scleroscope | Rockwell | | Vickers Diamond Penetrator |
|---|---|---|---|---|---|---|---|---|---|---|---|---|
| 'C' Scale (HRC) | Scale HV10 HV30 | Dia. imp. for 10mm Ball | Carbide Ball | Standard Ball | Tons/in² | 1000lb/in² | kg/mm² | MPa (N/mm²) | Hardness Number | A Scale, 60-kgf (HRA) | 'C' Scale (HRC) | Scale HV10 HV30 |
| 67.7 | 900 | | | | | | | | 96 | 85.6 | 67.7 | 900 |
| 67.0 | 880 | | | | | | | | 95 | 85.0 | 67.0 | 880 |
| 66.3 | 860 | | | | | | | | 98 | 84.7 | 66.3 | 860 |
| 65.5 | 840 | | | | | | | | 92 | 84.2 | 65.5 | 840 |
| 64.9 | 820 | | | | | | | | 90 | 83.6 | 64.8 | 820 |
| 64.0 | 800 | | | | | | | | 88 | 83.4 | 64.0 | 800 |
| 63.3 | 780 | | | | | | | | 87 | 83.0 | 63.3 | 780 |
| 62.5 | 760 | | | | | | | | 86 | 82.6 | 62.8 | 760 |
| 61.7 | 740 | | | | | | | | 84 | 82.2 | 61.7 | 740 |
| 61.0 | 725 | 2.44 | 630 | – | – | – | – | – | 82 | 81.8 | 61.0 | 725 |
| 60.5 | 710 | 2.45 | 627 | – | – | – | – | – | – | 81.5 | 60.5 | 710 |
| 60.0 | 698 | 2.50 | 601 | – | 132 | 295 | 208 | 2039 | 81 | 81.2 | 60.0 | 698 |
| 58.9 | 670 | 2.55 | 578 | – | 127 | 284 | 200 | 1961 | 78 | 80.6 | 58.9 | 670 |
| 57.1 | 650 | 2.60 | 555 | – | 122 | 273 | 192 | 1884 | 75 | 79.6 | 57.1 | 650 |
| 56.1 | 609 | 2.65 | 534 | – | 117 | 262 | 184 | 1807 | 73 | 79.0 | 56.1 | 609 |
| 54.4 | 572 | 2.70 | 514 | – | 112 | 250 | 176 | 1725 | 71 | 78.2 | 54.4 | 572 |
| 51.9 | 532 | 2.75 | 495 | 495 | 108 | 241 | 170 | 1668 | 68 | 76.9 | 51.9 | 532 |
| 50.7 | 517 | 2.80 | 477 | 477 | 105 | 235 | 165 | 1621 | 66 | 76.3 | 50.7 | 517 |
| 49.5 | 497 | 2.85 | 461 | 461 | 101 | 226 | 160 | 1559 | 64 | 75.5 | 49.5 | 497 |
| 47.5 | 470 | 2.90 | 444 | 444 | 98 | 219 | 155 | 1513 | 62 | 74.2 | 47.8 | 470 |
| 46.0 | 452 | 2.95 | 429 | 429 | 95 | 212 | 150 | 1467 | 60 | 73.6 | 46.0 | 452 |
| 44.5 | 437 | 3.00 | 415 | 415 | 92 | 206 | 145 | 1420 | 58 | 73.0 | 44.8 | 437 |
| 43.7 | 422 | 3.05 | 401 | 401 | 88 | 197 | 139 | 1359 | 56 | 72.5 | 43.7 | 422 |
| 42.4 | 408 | 3.10 | 388 | 388 | 85 | 190 | 134 | 1312 | 54 | 71.5 | 42.4 | 408 |
| 41.3 | 395 | 3.15 | 375 | 375 | 82 | 183 | 129 | 1266 | 52 | 71.0 | 41.3 | 395 |
| 39.9 | 381 | 3.20 | 363 | 363 | 80 | 179 | 126 | 1235 | 51 | 70.3 | 39.8 | 381 |
| 38.8 | 370 | 3.25 | 352 | 352 | 77 | 172 | 121 | 1186 | 49 | 69.6 | 38.8 | 370 |
| 37.7 | 359 | 3.30 | 341 | 341 | 75 | 168 | 118 | 1158 | 48 | 69.2 | 37.7 | 359 |
| 36.7 | 349 | 3.35 | 331 | 331 | 73 | 163 | 114 | 1127 | 46 | 68.8 | 36.7 | 349 |
| 35.0 | 337 | 3.40 | 321 | 321 | 71 | 159 | 111 | 1096 | 45 | 68.0 | 35.0 | 337 |
| 34.0 | 327 | 3.45 | 311 | 311 | 68 | 152 | 107 | 1050 | 43 | 67.5 | 34.0 | 327 |
| 33.0 | 318 | 3.50 | 302 | 302 | 66 | 147 | 104 | 1019 | 42 | 66.8 | 33.0 | 318 |
| 32.0 | 308 | 3.55 | 293 | 293 | 64 | 143 | 101 | 988 | 41 | 66.2 | 32.0 | 308 |
| 30.9 | 300 | 3.60 | 285 | 285 | 63 | 141 | 99 | 973 | 40 | 65.7 | 30.9 | 300 |
| 29.8 | 292 | 3.65 | 277 | 277 | 61 | 136 | 96 | 942 | 38 | 65.2 | 29.8 | 292 |
| 29.0 | 284 | 3.70 | 269 | 269 | 59 | 132 | 93 | 911 | 37 | 64.5 | 29.0 | 284 |
| 27.5 | 276 | 3.75 | 262 | 262 | 58 | 130 | 91 | 895 | 36 | 64.0 | 27.5 | 276 |
| 26.6 | 269 | 3.80 | 255 | 255 | 56 | 125 | 89 | 865 | 35 | 63.5 | 26.6 | 269 |
| 25.2 | 261 | 3.85 | 248 | 248 | 55 | 123 | 87 | 849 | 34 | 62.9 | 25.2 | 261 |
| 24.3 | 255 | 3.90 | 241 | 241 | 53 | 118 | 84 | 818 | 33 | 62.6 | 24.3 | 255 |
| 23.0 | 247 | 3.95 | 235 | 235 | 51 | 114 | 81 | 787 | 32 | 62.0 | 23.0 | 247 |
| 22.0 | 241 | 4.00 | 229 | 229 | 50 | 112 | 79 | 772 | 31 | 61.6 | 22.0 | 241 |
| 20.8 | 234 | 4.05 | 223 | 223 | 49 | 110 | 77 | 756 | 30 | 60.7 | 20.8 | 234 |
| | 228 | 4.10 | 217 | 217 | 48 | 107 | 76 | 741 | – | – | | 228 |

| Hardness 'B' Scale HRB | | | | | | | | | | | Hardness 'B' Scale HRB | |
|---|---|---|---|---|---|---|---|---|---|---|---|---|
| 98 | 222 | 4.15 | 212 | 212 | 46 | 103 | 73 | 710 | 29 | – | 98 | 222 |
| 97 | 218 | 4.20 | 207 | 207 | 45 | 101 | 71 | 695 | 28 | – | 97 | 218 |
| 96 | 212 | 4.30 | 197 | 197 | 43 | 97 | 68 | 664 | 27 | – | 96 | 212 |
| 93 | 196 | 4.40 | 187 | 187 | 41 | 92 | 65 | 632 | 25 | – | 93 | 196 |
| 91 | 188 | 4.50 | 179 | 179 | 39 | 88 | 62 | 602 | – | – | 91 | 188 |
| 88.5 | 178 | 4.60 | 170 | 170 | 36 | 81 | 57 | 556 | 24 | – | 88.5 | 178 |
| 86 | 171 | 4.70 | 163 | 163 | 35 | 78 | 55 | 540 | – | – | 86 | 171 |
| 84.2 | 163 | 4.80 | 156 | 156 | 34 | 76 | 54 | 525 | 23 | – | 84.2 | 163 |
| 82 | 156 | 4.90 | 149 | 149 | 32 | 72 | 51 | 494 | – | – | 82 | 156 |
| 80 | 150 | 5.00 | 143 | 143 | 31 | 69 | 49 | 479 | 22 | – | 80 | 150 |
| 77 | 143 | 5.10 | 137 | 137 | 30 | 67 | 48 | 463 | 21 | – | 77 | 143 |
| 75 | 137 | 5.20 | 131 | 131 | 29.5 | 66 | 47 | 455 | 20.5 | – | 75 | 137 |
| 72.5 | 132 | 5.30 | 126 | 126 | 29 | 65 | 46 | 448 | 20 | – | 72.5 | 132 |
| 70 | 127 | 5.40 | 121 | 121 | 28 | 63 | 44 | 432 | – | – | 70 | 127 |
| 67 | 122 | 5.50 | 116 | 116 | 26 | 58 | 42 | 401 | 15 | – | 67 | 122 |

*These charts were prepared using information contained in B.S.860/1967. This standard differs significantly from the superseded standard B.S. 860/1939, and differs slightly from the conversion scales adopted by SAE and ASTM sources.

*** Where hardness acceptance values are specified and a conversion from one scale to another is necessary the source of the conversion data should be stated and understood by the parties involved.

## Hardness Conversion Chart

| Rockwell | | | | | | Rockwell Superficial | | | | Brinell | | Vickers | Shore | |
|---|---|---|---|---|---|---|---|---|---|---|---|---|---|---|
| A | B | C | D | E | F | 15-N | 30-N | 45-N | 30-T | 500 kg | 3000 kg | 136 | | Approx. |
| 60kg Brale | 100kg 1/16" Ball | 150kg Brale | 100kg Brale | 100kg 1/8" Ball | 60kg 1/16" Ball | 15kg Brale | 30kg Brale | 45kg Brale | 30 kg 1/16" Ball | 10mm Ball Steel | 10mm Ball Steel | Diamond Pyramid | Sclero-scope | Tensile Strength (psi) |
| 86.5 | – | 70 | 78.5 | – | – | 94 | 86 | 77.6 | – | – | – | 1076 | 101 | – |
| 86 | – | 69 | 77.7 | – | – | 93.5 | 85 | 76.5 | – | – | – | 1044 | 99 | – |

| | | | | | | | | | | | | | | |
|---|---|---|---|---|---|---|---|---|---|---|---|---|---|---|
| 86 | - | 69 | 77.7 | - | - | 93.5 | 85 | 76.5 | - | - | - | 1044 | 99 | - |
| 85.6 | - | 68 | 76.9 | - | - | 93.2 | 84.4 | 75.4 | - | - | - | 940 | 97 | - |
| 85 | - | 67 | 76.1 | - | - | 92.9 | 83.6 | 74.2 | - | - | - | 900 | 95 | - |
| 84.5 | - | 66 | 75.4 | - | - | 92.5 | 82.8 | 73.2 | - | - | - | 865 | 92 | - |
| 83.9 | - | 65 | 74.5 | - | - | 92.2 | 81.9 | 72 | - | - | 739 | 832 | 91 | - |
| 83.4 | - | 64 | 73.8 | - | - | 91.8 | 81.1 | 71 | - | - | 722 | 800 | 88 | - |
| 82.8 | - | 63 | 73 | - | - | 91.4 | 80.1 | 69.9 | - | - | 705 | 772 | 87 | - |
| 82.3 | - | 62 | 72.2 | - | - | 91.1 | 79.3 | 68.8 | - | - | 688 | 746 | 85 | - |
| 81.8 | - | 61 | 71.5 | - | - | 90.7 | 78.4 | 67.7 | - | - | 670 | 720 | 83 | - |
| 81.2 | - | 60 | 70.7 | - | - | 90.2 | 77.5 | 66.6 | - | - | 654 | 697 | 81 | 320,000 |
| 80.7 | - | 59 | 69.9 | - | - | 89.8 | 76.6 | 65.5 | - | - | 634 | 674 | 80 | 310,000 |
| 80.1 | - | 58 | 69.2 | - | - | 89.3 | 75.7 | 64.3 | - | - | 615 | 653 | 78 | 300,000 |
| 79.6 | - | 57 | 68.5 | - | - | 88.9 | 74.8 | 63.2 | - | - | 595 | 633 | 76 | 290,000 |
| 79 | - | 56 | 67.7 | - | - | 88.3 | 73.9 | 62 | - | - | 577 | 613 | 75 | 282,000 |
| 78.5 | 120 | 55 | 66.9 | - | - | 87.9 | 73 | 60.9 | - | - | 560 | 595 | 74 | 274,000 |
| 78 | 120 | 54 | 66.1 | - | - | 87.4 | 72 | 59.8 | - | - | 543 | 577 | 72 | 266,000 |
| 77.4 | 119 | 53 | 65.4 | - | - | 86.9 | 71.2 | 58.6 | - | - | 525 | 560 | 71 | 257,000 |
| 76.8 | 119 | 52 | 64.6 | - | - | 86.4 | 70.2 | 57.4 | - | - | 500 | 544 | 69 | 245,000 |
| 76.3 | 118 | 51 | 63.8 | - | - | 85.9 | 69.4 | 56.1 | - | - | 487 | 528 | 68 | 239,000 |
| 75.9 | 117 | 50 | 63.1 | - | - | 85.5 | 68.5 | 55 | - | - | 475 | 513 | 67 | 233,000 |
| 75.2 | 117 | 49 | 62.1 | - | - | 85 | 67.6 | 53.8 | - | - | 464 | 498 | 66 | 227,000 |
| 74.7 | 116 | 48 | 61.4 | - | - | 84.5 | 66.7 | 52.5 | - | - | 451 | 484 | 64 | 221,000 |
| 74.1 | 116 | 47 | 60.8 | - | - | 83.9 | 65.8 | 51.4 | - | - | 442 | 471 | 63 | 217,000 |
| 73.6 | 115 | 46 | 60 | - | - | 83.5 | 64.8 | 50.3 | - | - | 432 | 458 | 62 | 212,000 |
| 73.1 | 115 | 45 | 59.2 | - | - | 83 | 64 | 49 | - | - | 421 | 446 | 60 | 206,000 |
| 72.5 | 114 | 44 | 58.5 | - | - | 82.5 | 63.1 | 47.8 | - | - | 409 | 434 | 58 | 200,000 |
| 72 | 113 | 43 | 57.7 | - | - | 82 | 62.2 | 46.7 | - | - | 400 | 423 | 57 | 196,000 |
| 71.5 | 113 | 42 | 56.9 | - | - | 81.5 | 61.3 | 45.5 | - | - | 390 | 412 | 56 | 191,000 |
| 70.9 | 112 | 41 | 56.2 | - | - | 80.9 | 60.4 | 44.3 | - | - | 381 | 402 | 55 | 187,000 |
| 70.4 | 112 | 40 | 55.4 | - | - | 80.4 | 59.5 | 43.1 | - | - | 371 | 392 | 54 | 182,000 |
| 69.9 | 111 | 39 | 54.6 | - | - | 79.9 | 58.6 | 41.9 | - | - | 362 | 382 | 52 | 177,000 |
| 69.4 | 110 | 38 | 53.8 | - | - | 79.4 | 57.7 | 40.8 | - | - | 353 | 372 | 51 | 173,000 |
| 68.9 | 110 | 37 | 53.1 | - | - | 78.8 | 56.8 | 39.6 | - | - | 344 | 363 | 50 | 169,000 |
| 68.4 | 109 | 36 | 52.3 | - | - | 78.3 | 55.9 | 38.4 | - | - | 335 | 354 | 49 | 165,000 |
| 67.9 | 109 | 35 | 51.5 | - | - | 77.7 | 55 | 37.2 | - | - | 327 | 345 | 48 | 160,000 |
| 67.4 | 108 | 34 | 50.8 | - | - | 77.2 | 54.2 | 36.1 | - | - | 319 | 336 | 47 | 156,000 |
| 66.8 | 108 | 33 | 50 | - | - | 76.6 | 53.3 | 34.9 | - | - | 311 | 327 | 46 | 152,000 |
| 66.8 | 108 | 33 | 50 | - | - | 76.6 | 53.3 | 34.9 | - | - | 311 | 327 | 46 | 152,000 |
| 66.3 | 107 | 32 | 49.2 | - | - | 76.1 | 52.1 | 33.7 | - | - | 301 | 318 | 44 | 147,000 |
| 65.8 | 106 | 31 | 48.4 | - | - | 75.6 | 51.3 | 32.5 | - | - | 294 | 310 | 43 | 144,000 |
| 65.3 | 105 | 30 | 47.7 | - | - | 75 | 50.4 | 31.3 | - | - | 286 | 302 | 42 | 140,000 |
| 64.7 | 104 | 29 | 47 | - | - | 74.5 | 49.5 | 30.1 | - | - | 279 | 294 | 41 | 137,000 |
| 64.3 | 104 | 28 | 46.1 | - | - | 73.9 | 48.6 | 28.9 | - | - | 271 | 286 | 41 | 133,000 |
| 63.8 | 103 | 27 | 45.2 | - | - | 73.3 | 47.7 | 27.8 | - | - | 264 | 279 | 40 | 129,000 |
| 63.3 | 103 | 26 | 44.6 | - | - | 72.8 | 46.8 | 26.7 | - | - | 258 | 272 | 39 | 126,000 |
| 62.8 | 102 | 25 | 43.8 | - | - | 72.2 | 45.9 | 25.5 | - | - | 253 | 266 | 38 | 124,000 |
| 62.4 | 101 | 24 | 43.1 | - | - | 71.6 | 45 | 24.3 | - | - | 247 | 260 | 37 | 121,000 |
| 62 | 100 | 23 | 42.1 | - | - | 71 | 44 | 23.1 | 82 | 201 | 240 | 254 | 36 | 118,000 |
| 61.5 | 99 | 22 | 41.6 | - | - | 70.5 | 43.2 | 22 | 81.5 | 195 | 234 | 248 | 35 | 115,000 |
| 61 | 98 | 21 | 40.9 | - | - | 69.9 | 42.3 | 20.7 | 81 | 189 | 228 | 243 | 35 | 112,000 |
| 60.5 | 97 | 20 | 40.1 | - | - | 69.4 | 41.5 | 19.6 | 80.5 | 184 | 222 | 238 | 34 | 109,000 |
| 59 | 96 | 18 | - | - | - | - | - | - | 80 | 179 | 216 | 230 | 33 | 106,000 |
| 58 | 95 | 16 | - | - | - | - | - | - | 79 | 175 | 210 | 222 | 32 | 103,000 |
| 57.5 | 94 | 15 | - | - | - | - | - | - | 78.5 | 171 | 205 | 213 | 31 | 100,000 |
| 57 | 93 | 13 | - | - | - | - | - | - | 78 | 167 | 200 | 208 | 30 | 98,000 |
| 56.5 | 92 | 12 | - | - | - | - | - | - | 77.5 | 163 | 195 | 204 | 29 | 96,000 |
| 56 | 91 | 10 | - | - | - | - | - | - | 77 | 160 | 190 | 196 | 28 | 93,000 |
| 55.5 | 90 | 9 | - | - | - | - | - | - | 76 | 157 | 185 | 192 | 27 | 91,000 |
| 55 | 89 | 8 | - | - | - | - | - | - | 75.5 | 154 | 180 | 188 | 26 | 88,000 |
| 54 | 88 | 7 | - | - | - | - | - | - | 75 | 151 | 176 | 184 | 26 | 86,000 |
| 53.5 | 87 | 6 | - | - | - | - | - | - | 74.5 | 148 | 172 | 180 | 26 | 84,000 |
| 53 | 86 | 5 | - | - | - | - | - | - | 74 | 145 | 169 | 176 | 25 | 83,000 |
| 52.5 | 85 | 4 | - | - | - | - | - | - | 73.5 | 142 | 165 | 173 | 25 | 81,000 |
| 52 | 84 | 3 | - | - | - | - | - | - | 73 | 140 | 162 | 170 | 25 | 79,000 |
| 51 | 83 | 2 | - | - | - | - | - | - | 72 | 137 | 159 | 166 | 24 | 78,000 |
| 50.5 | 82 | 1 | - | - | - | - | - | - | 71.5 | 135 | 156 | 163 | 24 | 76,000 |
| 50 | 81 | 0 | - | - | - | - | - | - | 71 | 133 | 153 | 160 | 24 | 75,000 |
| 49.5 | 80 | - | - | - | - | - | - | - | 70 | 130 | 150 | - | - | 73,000 |
| 49 | 79 | - | - | - | - | - | - | - | 69.5 | 128 | 147 | - | - | - |
| 48.5 | 78 | - | - | - | - | - | - | - | 69 | 126 | 144 | - | - | - |
| 48 | 77 | - | - | - | - | - | - | - | 68 | 124 | 141 | - | - | - |
| 47 | 76 | - | - | - | - | - | - | - | 67.5 | 122 | 139 | - | - | - |
| 46.5 | 75 | - | - | - | 99.5 | - | - | - | 67 | 120 | 137 | - | - | - |
| 46 | 74 | - | - | - | 99 | - | - | - | 66 | 118 | 135 | - | - | - |

| | | | | | | | | | | | | | | |
|---|---|---|---|---|---|---|---|---|---|---|---|---|---|---|
| 47 | 76 | - | - | - | - | - | - | - | 67.5 | 122 | 138 | - | - | - |
| 46.5 | 75 | - | - | - | 99.5 | - | - | - | 67 | 120 | 137 | - | - | - |
| 46 | 74 | - | - | - | 99 | - | - | - | 66 | 118 | 135 | - | - | - |
| 45.5 | 73 | - | - | - | 98.5 | - | - | - | 65.5 | 116 | 132 | - | - | - |
| 45 | 72 | - | - | - | 98 | - | - | - | 65 | 114 | 130 | - | - | - |
| 44.5 | 71 | - | - | 100 | 97.5 | - | - | - | 64.2 | 112 | 127 | - | - | - |
| 44 | 70 | - | - | 99.5 | 97 | - | - | - | 63.5 | 110 | 125 | - | - | - |
| 43.5 | 69 | - | - | 99 | 96 | - | - | - | 62.8 | 109 | 123 | - | - | - |
| 43 | 68 | - | - | 98 | 95.5 | - | - | - | 62 | 107 | 121 | - | - | - |
| 42.5 | 67 | - | - | 97.5 | 95 | - | - | - | 61.4 | 106 | 119 | - | - | - |
| 42 | 66 | - | - | 97 | 94.5 | - | - | - | 60.5 | 104 | 117 | - | - | - |
| 41.8 | 65 | - | - | 96 | 94 | - | - | - | 60.1 | 102 | 116 | - | - | - |
| 41.5 | 64 | - | - | 95.5 | 93.5 | - | - | - | 59.5 | 101 | 114 | - | - | - |
| 41 | 63 | - | - | 95 | 93 | - | - | - | 58.7 | 99 | 112 | - | - | - |
| 40.5 | 62 | - | - | 94.5 | 92 | - | - | - | 58 | 98 | 110 | - | - | - |
| 40 | 61 | - | - | 93.5 | 91.5 | - | - | - | 57.3 | 96 | 108 | - | - | - |
| 39.5 | 60 | - | - | 93 | 91 | - | - | - | 56.5 | 95 | 107 | - | - | - |
| 39 | 59 | - | - | 92.5 | 90.5 | - | - | - | 55.9 | 94 | 106 | - | - | - |
| 38.5 | 58 | - | - | 92 | 90 | - | - | - | 55 | 92 | 104 | - | - | - |
| 38 | 57 | - | - | 91 | 89.5 | - | - | - | 54.6 | 91 | 102 | - | - | - |
| 37.8 | 56 | - | - | 90.5 | 89 | - | - | - | 54 | 90 | 101 | - | - | - |
| 37.5 | 55 | - | - | 90 | 88 | - | - | - | 53.2 | 89 | 99 | - | - | - |
| 37 | 54 | - | - | 89.5 | 87.5 | - | - | - | 52.5 | 87 | - | - | - | - |
| 36.5 | 53 | - | - | 89 | 87 | - | - | - | 51.8 | 86 | - | - | - | - |
| 36 | 52 | - | - | 88 | 86.5 | - | - | - | 51 | 85 | - | - | - | - |
| 35.5 | 51 | - | - | 87.5 | 86 | - | - | - | 50.4 | 84 | - | - | - | - |
| 35 | 50 | - | - | 87 | 85.5 | - | - | - | 49.5 | 83 | - | - | - | - |
| 34.8 | 49 | - | - | 86.5 | 85 | - | - | - | 49.1 | 82 | - | - | - | - |
| 34.5 | 48 | - | - | 85.5 | 84.5 | - | - | - | 48.5 | 81 | - | - | - | - |
| 34 | 47 | - | - | 85 | 84 | - | - | - | 47.7 | 80 | - | - | - | - |
| 33.5 | 46 | - | - | 84.5 | 83 | - | - | - | 47 | 79 | - | - | - | - |
| 33 | 45 | - | - | 84 | 82.5 | - | - | - | 46.2 | 79 | - | - | - | - |
| 32.5 | 44 | - | - | 83.5 | 82 | - | - | - | 45.5 | 78 | - | - | - | - |
| 32 | 43 | - | - | 82.5 | 81.5 | - | - | - | 44.8 | 77 | - | - | - | - |
| 31.5 | 42 | - | - | 82 | 81 | - | - | - | 44 | 76 | - | - | - | - |
| 31 | 41 | - | - | 81.5 | 80.5 | - | - | - | 43.4 | 75 | - | - | - | - |
| 30.8 | 40 | - | - | 81 | 79.5 | - | - | - | 43 | 74 | - | - | - | - |
| 30.5 | 39 | - | - | 80 | 79 | - | - | - | 42.1 | 74 | - | - | - | - |
| 30 | 38 | - | - | 79.5 | 78.5 | - | - | - | 41.5 | 73 | - | - | - | - |
| 29.5 | 37 | - | - | 79 | 78 | - | - | - | 40.7 | 72 | - | - | - | - |
| 29 | 36 | - | - | 78.5 | 77.5 | - | - | - | 40 | 71 | - | - | - | - |
| 28.5 | 35 | - | - | 78 | 77 | - | - | - | 39.3 | 71 | - | - | - | - |
| 28 | 34 | - | - | 77 | 76.5 | - | - | - | 38.5 | 70 | - | - | - | - |
| 27.8 | 33 | - | - | 76.5 | 75.5 | - | - | - | 37.9 | 69 | - | - | - | - |
| 27.5 | 32 | - | - | 76 | 75 | - | - | - | 37.5 | 68 | - | - | - | - |
| 27 | 31 | - | - | 75.5 | 74.5 | - | - | - | 36.6 | 68 | - | - | - | - |
| 26.5 | 30 | - | - | 75 | 74 | - | - | - | 36 | 67 | - | - | - | - |
| 26 | 29 | - | - | 74 | 73.5 | - | - | - | 35.2 | 66 | - | - | - | - |
| 25.5 | 28 | - | - | 73.5 | 73 | - | - | - | 34.5 | 66 | - | - | - | - |
| 25 | 27 | - | - | 73 | 72.5 | - | - | - | 33.8 | 65 | - | - | - | - |
| 24.5 | 26 | - | - | 72.5 | 72 | - | - | - | 33.1 | 65 | - | - | - | - |
| 24.2 | 25 | - | - | 72 | 71 | - | - | - | 32.4 | 64 | - | - | - | - |
| 24 | 24 | - | - | 71 | 70.5 | - | - | - | 32 | 64 | - | - | - | - |
| 23.5 | 23 | - | - | 70.5 | 70 | - | - | - | 31.1 | 63 | - | - | - | - |
| 23 | 22 | - | - | 70 | 69.5 | - | - | - | 30.4 | 63 | - | - | - | - |
| 22.5 | 21 | - | - | 69.5 | 69 | - | - | - | 29.7 | 62 | - | - | - | - |
| 22 | 20 | - | - | 68.5 | 68.5 | - | - | - | 29 | 62 | - | - | - | - |
| 21.5 | 19 | - | - | 68 | 68 | - | - | - | 28.1 | 61 | - | - | - | - |
| 21.2 | 18 | - | - | 67.5 | 67 | - | - | - | 27.4 | 61 | - | - | - | - |
| 21 | 17 | - | - | 67 | 66.5 | - | - | - | 26.7 | 60 | - | - | - | - |
| 20.5 | 16 | - | - | 66.5 | 66 | - | - | - | 26 | 60 | - | - | - | - |
| 20 | 15 | - | - | 65.5 | 65.5 | - | - | - | 25.3 | 59 | - | - | - | - |
| - | 14 | - | - | 65 | 65 | - | - | - | 24.6 | 59 | - | - | - | - |
| - | 13 | - | - | 64.5 | 64.5 | - | - | - | 23.9 | 58 | - | - | - | - |
| - | 12 | - | - | 64 | 64 | - | - | - | 23.5 | 58 | - | - | - | - |
| - | 11 | - | - | 63.5 | 63.5 | - | - | - | 22.6 | 57 | - | - | - | - |
| - | 10 | - | - | 62.5 | 63 | - | - | - | 21.9 | 57 | - | - | - | - |
| - | 9 | - | - | 62 | 62 | - | - | - | 21.2 | 56 | - | - | - | - |
| - | 8 | - | - | 61.5 | 61.5 | - | - | - | 20.5 | 56 | - | - | - | - |
| - | 7 | - | - | 61 | 61 | - | - | - | 19.8 | 56 | - | - | - | - |
| - | 6 | - | - | 60.5 | 60.5 | - | - | - | 19.1 | 55 | - | - | - | - |
| - | 5 | - | - | 60 | 60 | - | - | - | 18.4 | 55 | - | - | - | - |
| - | 4 | - | - | 59 | 59.5 | - | - | - | 18 | 55 | - | - | - | - |
| - | 3 | - | - | 58.5 | 59 | - | - | - | 17.1 | 54 | - | - | - | - |
| - | 2 | - | - | 58 | 58 | - | - | - | 16.4 | 54 | - | - | - | - |
| - | 1 | - | - | 57.5 | 57.5 | - | - | - | 15.7 | 53 | - | - | - | - |
| - | 0 | - | - | 57 | 57 | - | - | - | 15 | 53 | - | - | - | - |

Click for the ASTM E140 - 07 document: Standard Hardness Conversion Tables for Metals Relationship Among Brinell Hardness, Vickers Hardness, Rockwell Hardness, Superficial Hardness, Knoop Hardness, and Scleroscope Hardness

Hardness

74

Alumina material properties datasheet

| 99.5% Aluminum Oxide | | | |
|---|---|---|---|
| **Mechanical** | **Units of Measure** | **SI/Metric** | **(Imperial)** |
| Density | gm/cc (lb/ft$^3$) | 3.89 | (242.8) |
| Porosity | % (%) | 0 | (0) |
| Color | — | ivory | — |
| Flexural Strength | MPa (lb/in$^2$x10$^3$) | 379 | (55) |
| Elastic Modulus | GPa (lb/in$^2$x10$^6$) | 375 | (54.4) |
| Shear Modulus | GPa (lb/in$^2$x10$^6$) | 152 | (22) |
| Bulk Modulus | GPa (lb/in$^2$x10$^6$) | 228 | (33) |
| Poisson's Ratio | — | 0.22 | (0.22) |
| Compressive Strength | MPa (lb/in$^2$x10$^3$) | 2600 | (377) |
| Hardness | Kg/mm$^2$ | 1440 | — |
| Fracture Toughness K$_{IC}$ | MPa·m$^{1/2}$ | 4 | — |
| Maximum Use Temperature (no load) | °C (°F) | 1750 | (3180) |
| **Thermal** | | | |
| Thermal Conductivity | W/m°K (BTU·in/ft$^2$·hr·°F) | 35 | (243) |
| Coefficient of Thermal Expansion | 10$^{-6}$/°C (10$^{-6}$/°F) | 8.4 | (4.7) |
| Specific Heat | J/Kg·°K (Btu/lb·°F) | 880 | (0.21) |
| **Electrical** | | | |
| Dielectric Strength | ac-kv/mm (volts/mil) | 16.9 | (420) |
| Dielectric Constant | @ 1 MHz | 9.8 | (9.8) |
| Dissipation Factor | @ 1 kHz | 0.0002 | (0.0002) |
| Loss Tangent | @ 1 kHz | — | — |
| Volume Resistivity | ohm·cm | >10$^{14}$ | — |

PKAC+AL/E (50/50)

PKAC/E (50/50)



AL/E 50/50

PKAC+AL/E (60/40)



PKAC/E (60/40)

AL/E (60/40)

PKAC+AL/E (70/30)                          PKAC/E (70/30)



AL/E (70/30)                               SK2 Carbon Steel Disc
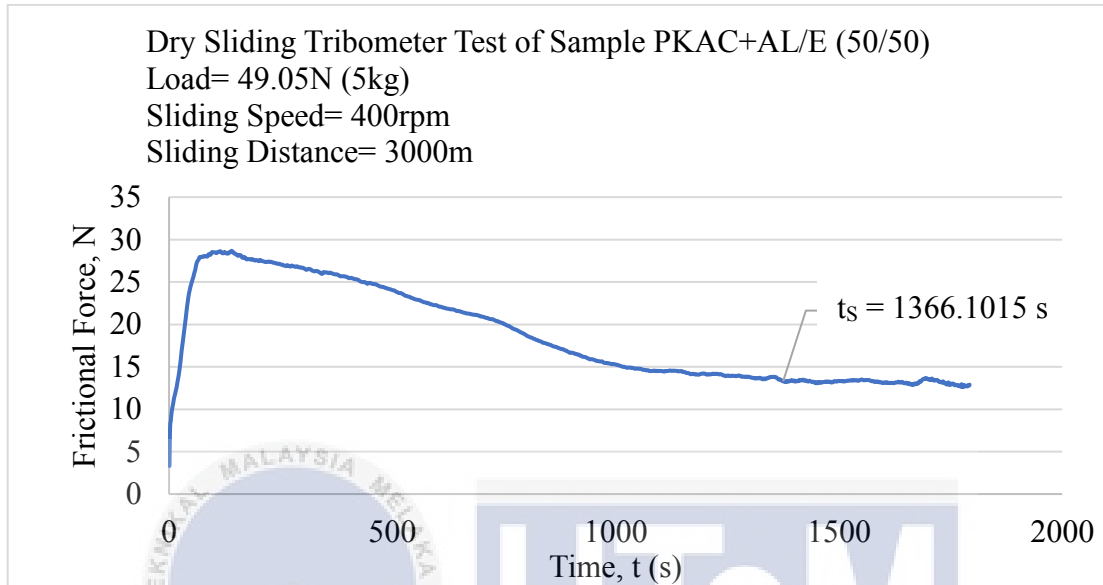
1. Palm Kernel Activated Carbon (PKAC)
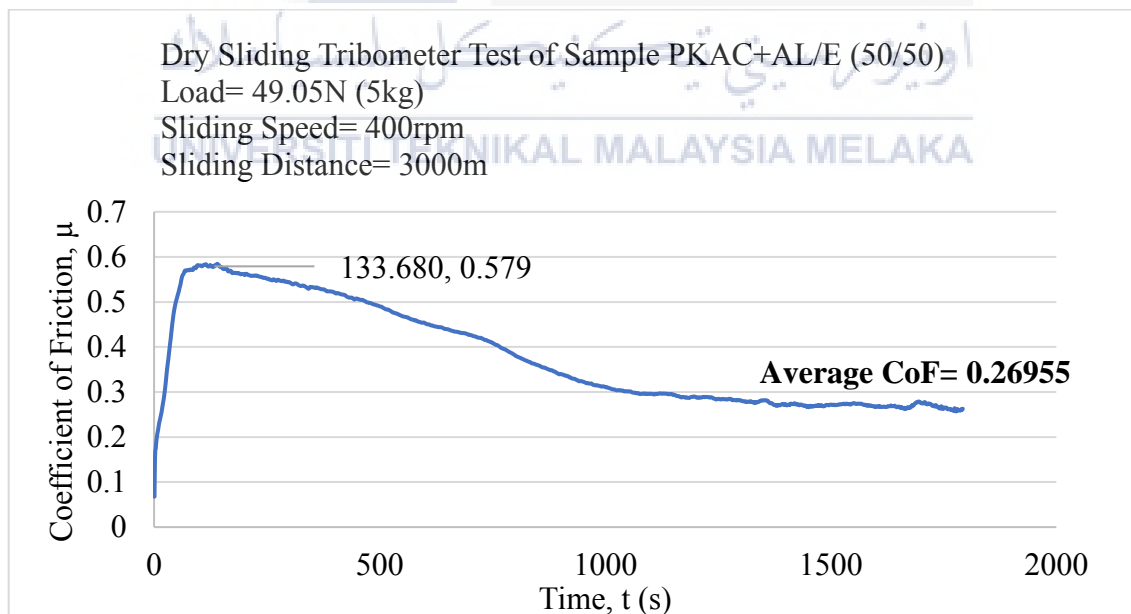


2. Alumina, $AL_2O_3$



3. Carbon chromium steel ball

Frictional force and coefficient of friction (CoF) against time graphs

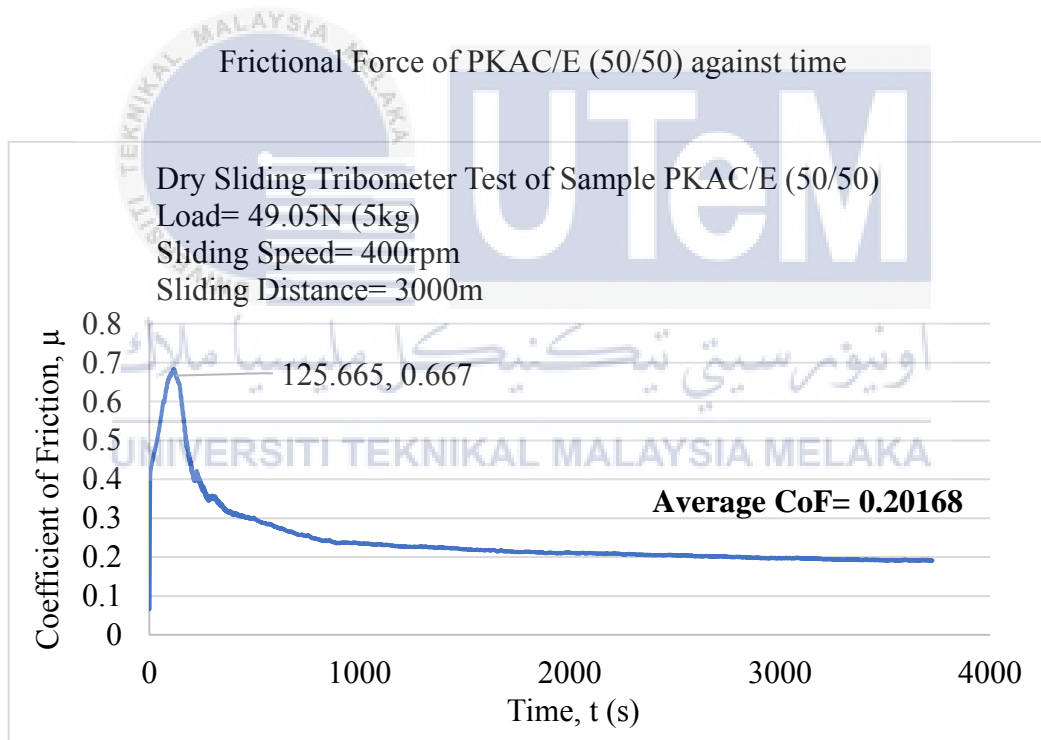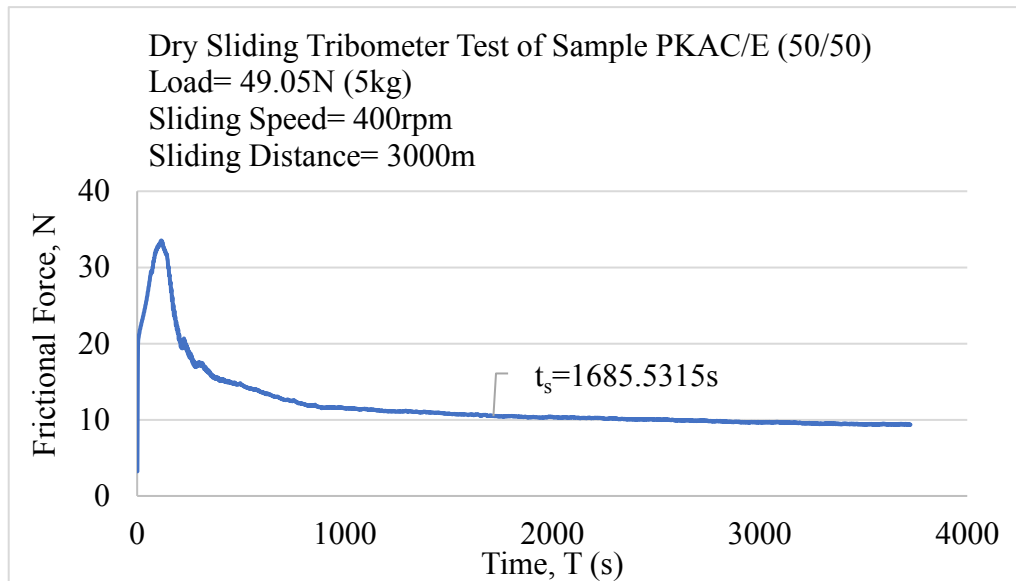1. Frictional force and coefficient of friction (CoF) results for PKAC+AL/E (50/50)



Dry Sliding Tribometer Test of Sample PKAC+AL/E (50/50)
Load= 49.05N (5kg)
Sliding Speed= 400rpm
Sliding Distance= 3000m

$t_S = 1366.1015$ s

Frictional force of PKAC+AL/E (50/50) against time



Dry Sliding Tribometer Test of Sample PKAC+AL/E (50/50)
Load= 49.05N (5kg)
Sliding Speed= 400rpm
Sliding Distance= 3000m
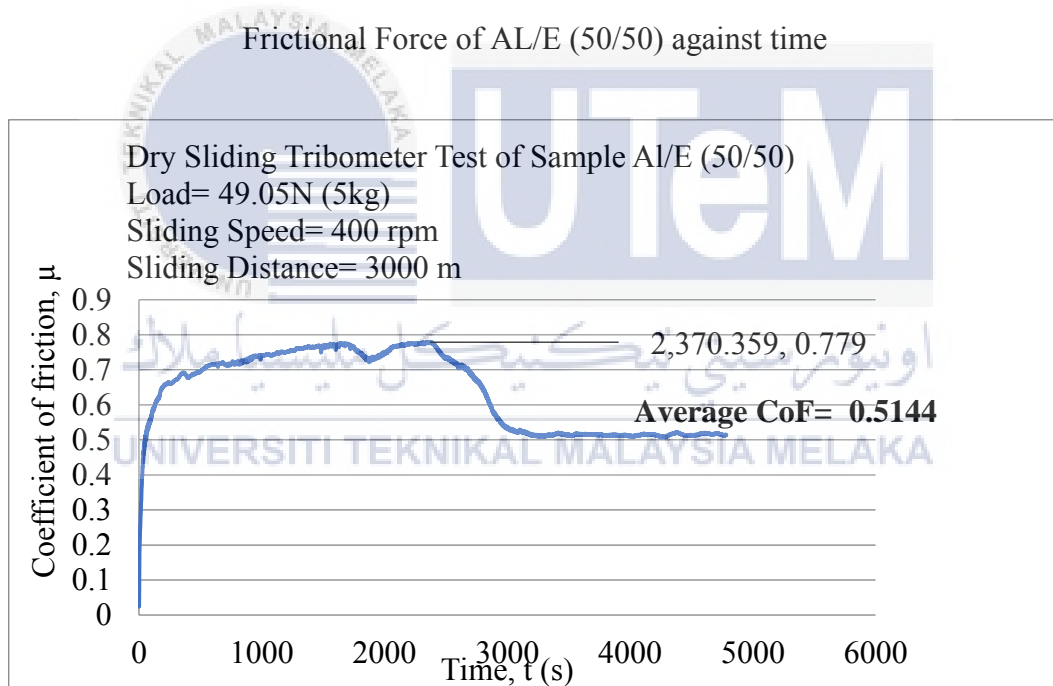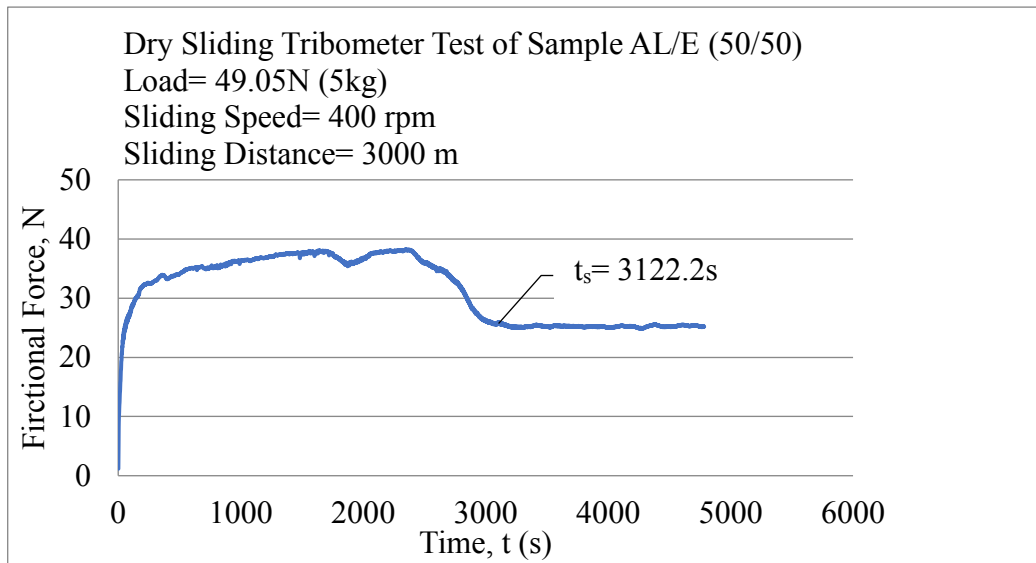
133.680, 0.579

**Average CoF= 0.26955**

Coefficient of Friction of PKAC+AL/E (50/50) against time

2. Frictional force and coefficient of friction (CoF) results for PKAC/E (50/50)

Dry Sliding Tribometer Test of Sample PKAC/E (50/50)
Load= 49.05N (5kg)
Sliding Speed= 400rpm
Sliding Distance= 3000m



$t_s$=1685.5315s

Frictional Force of PKAC/E (50/50) against time

Dry Sliding Tribometer Test of Sample PKAC/E (50/50)
Load= 49.05N (5kg)
Sliding Speed= 400rpm
Sliding Distance= 3000m
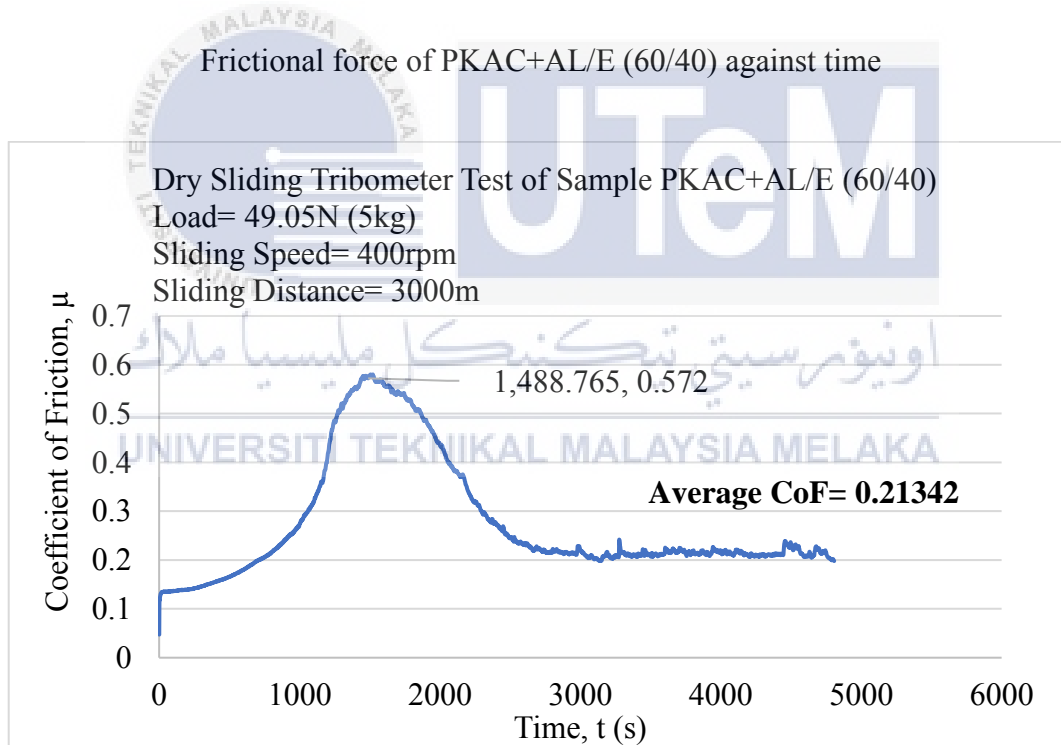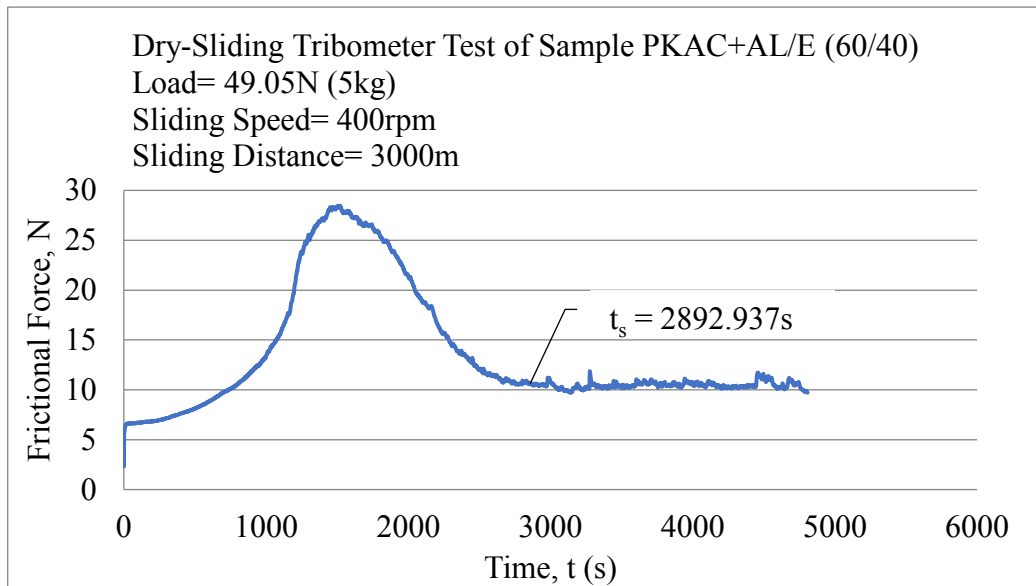


125.665, 0.667

**Average CoF= 0.20168**

Coefficient of Friction of PKAC/E (50/50) against time

3. Frictional force and coefficient of friction (CoF) results for AL/E (50/50)



Dry Sliding Tribometer Test of Sample AL/E (50/50)
Load= 49.05N (5kg)
Sliding Speed= 400 rpm
Sliding Distance= 3000 m

$t_s$= 3122.2s

Frictional Force of AL/E (50/50) against time



Dry Sliding Tribometer Test of Sample Al/E (50/50)
Load= 49.05N (5kg)
Sliding Speed= 400 rpm
Sliding Distance= 3000 m
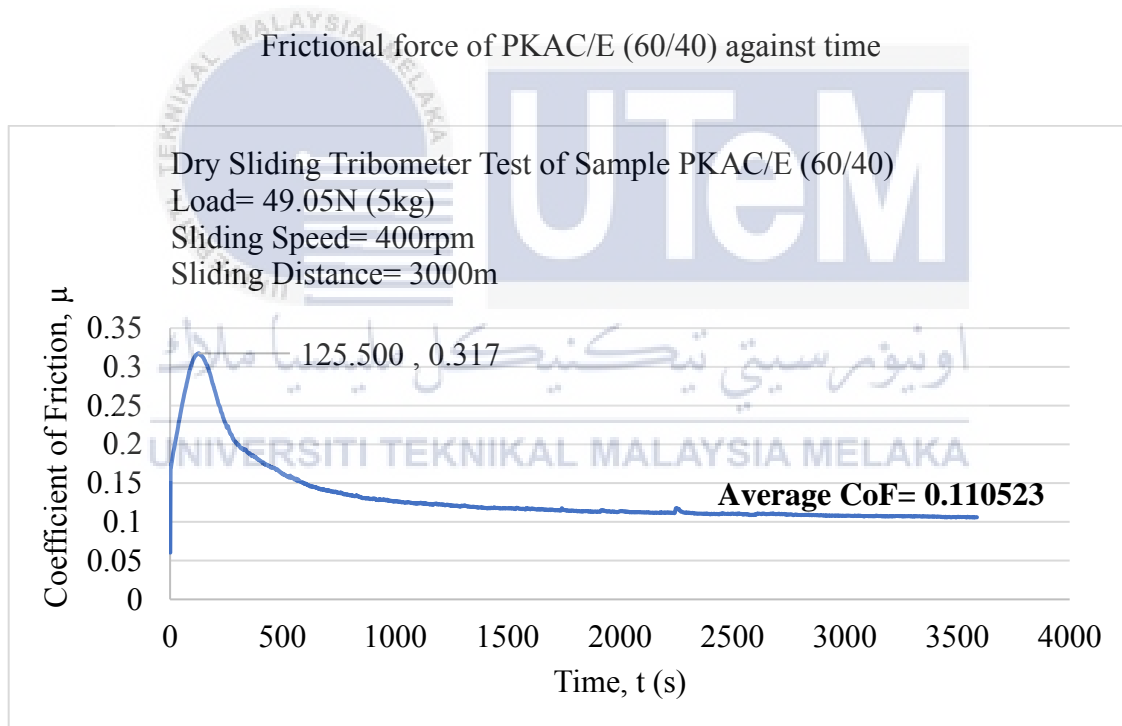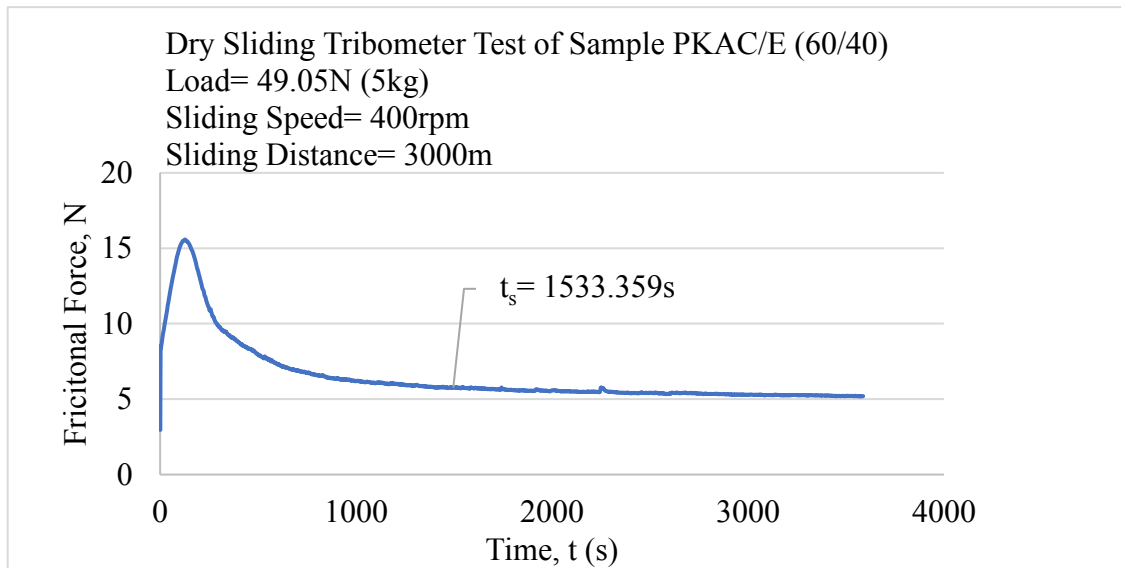
2,370.359, 0.779

**Average CoF= 0.5144**

Coefficient of Friction of AL/E (50/50) against time

4. Frictional force and coefficient of friction (CoF) results for PKAC+AL/E (60/40)

Dry-Sliding Tribometer Test of Sample PKAC+AL/E (60/40)
Load= 49.05N (5kg)
Sliding Speed= 400rpm
Sliding Distance= 3000m



$t_s = 2892.937s$

Frictional force of PKAC+AL/E (60/40) against time

Dry Sliding Tribometer Test of Sample PKAC+AL/E (60/40)
Load= 49.05N (5kg)
Sliding Speed= 400rpm
Sliding Distance= 3000m



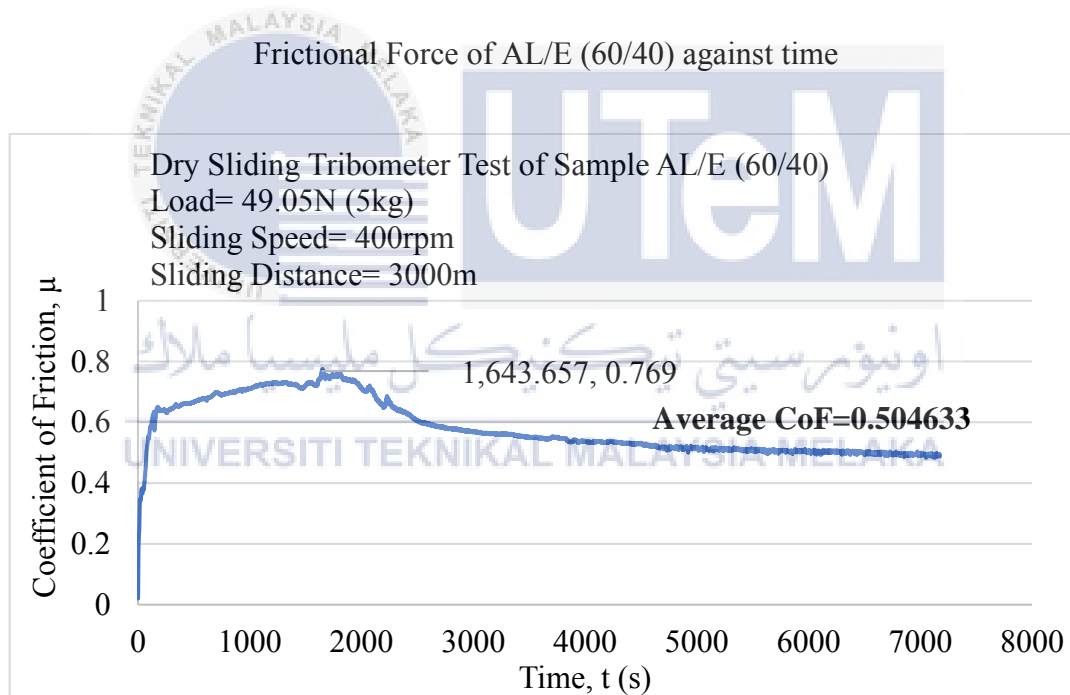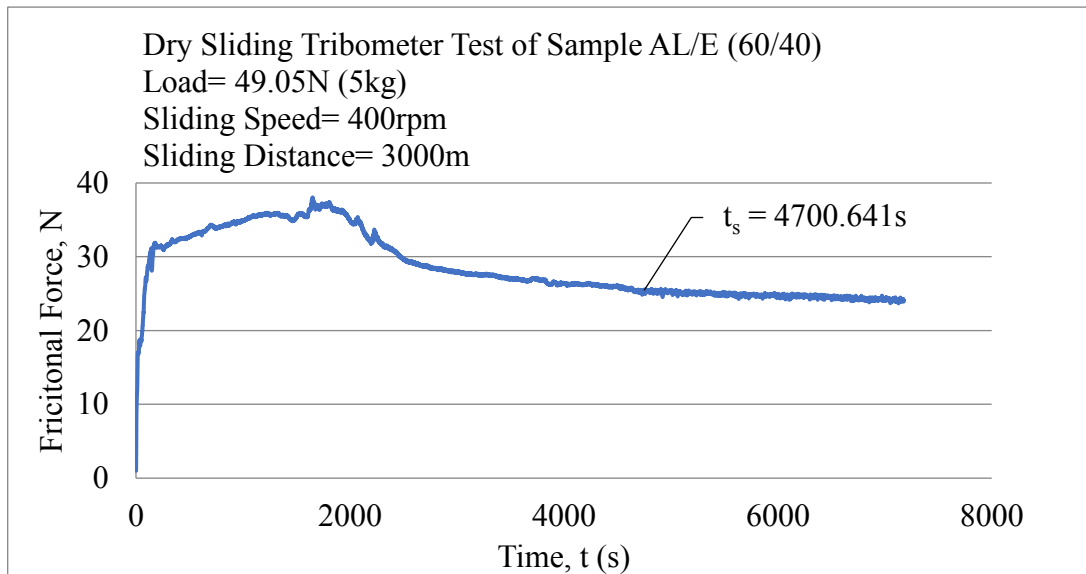1,488.765, 0.572

**Average CoF= 0.21342**

Coefficient of Friction of PKAC+AL/E (60/40) against time

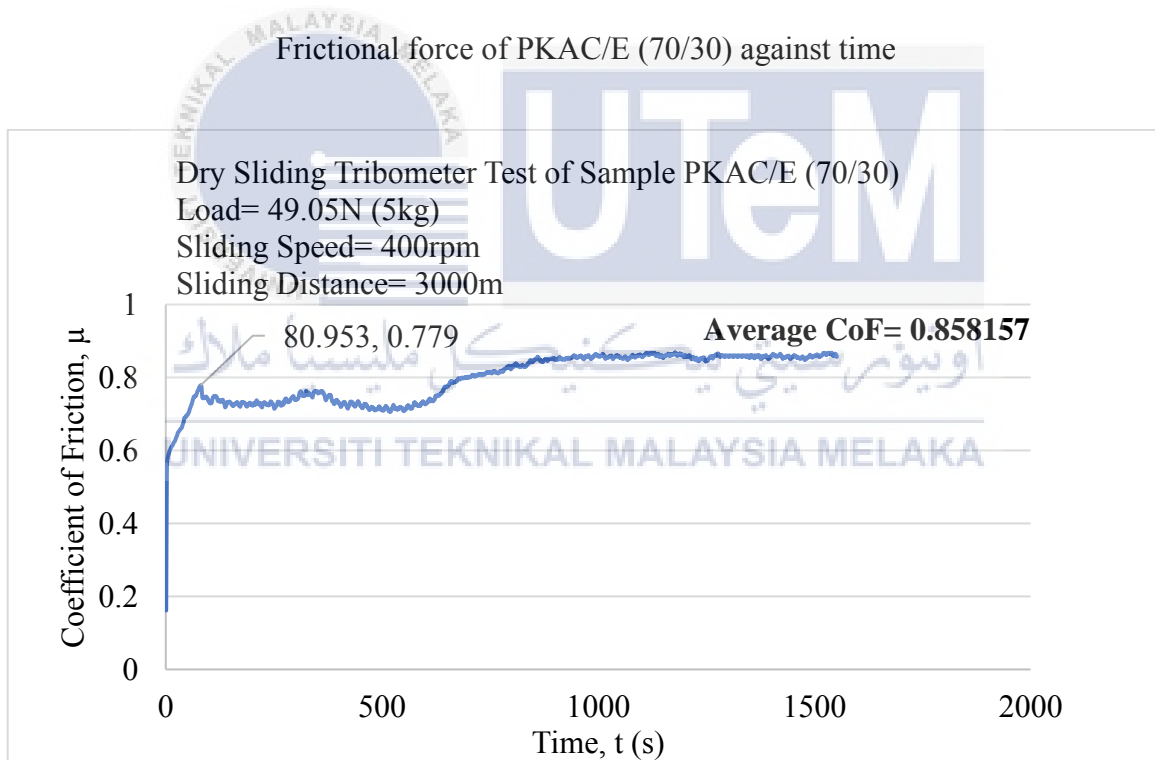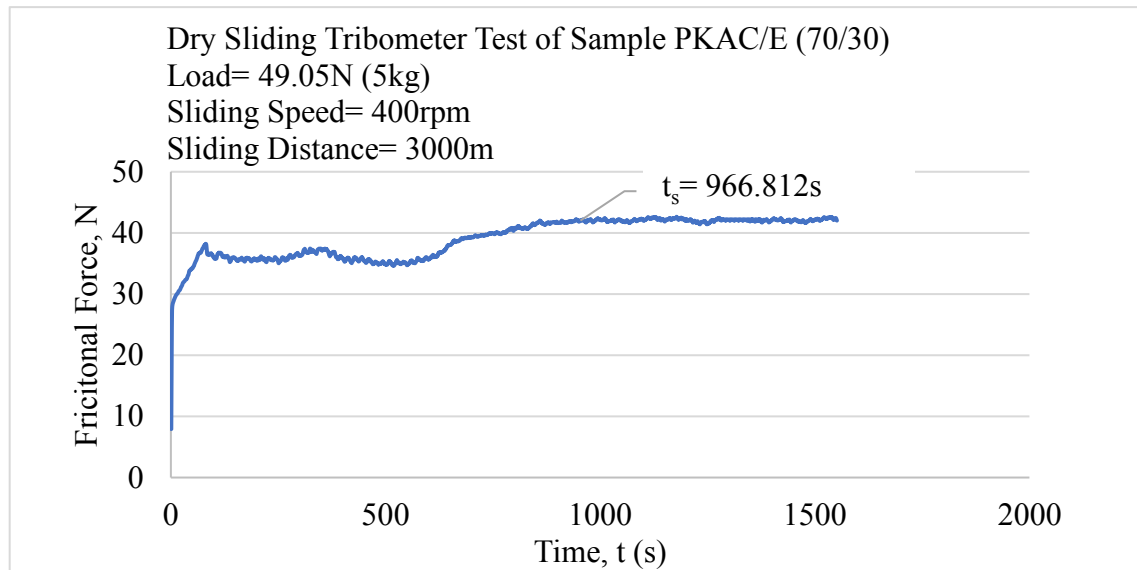5. Frictional force and coefficient of friction (CoF) results for PKAC/E (60/40)



Dry Sliding Tribometer Test of Sample PKAC/E (60/40)
Load= 49.05N (5kg)
Sliding Speed= 400rpm
Sliding Distance= 3000m

$t_s$= 1533.359s

Frictional force of PKAC/E (60/40) against time



Dry Sliding Tribometer Test of Sample PKAC/E (60/40)
Load= 49.05N (5kg)
Sliding Speed= 400rpm
Sliding Distance= 3000m

125.500 , 0.317

**Average CoF= 0.110523**

Coefficient of Friction of PKAC/E (60/40) against time

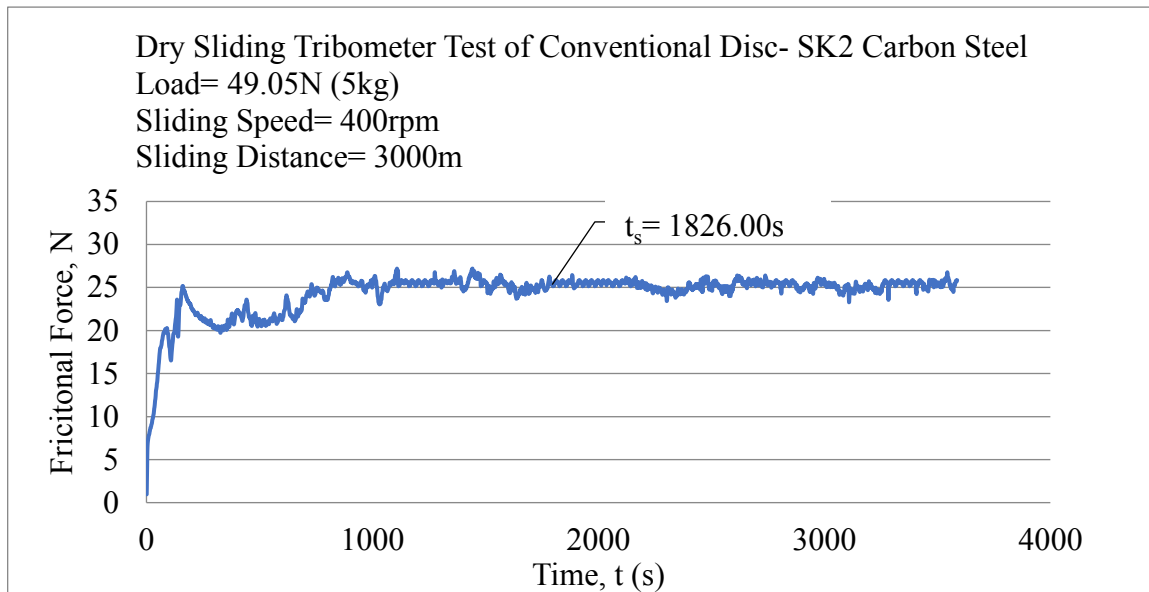6. Frictional force and coefficient of friction (CoF) results for AL/E (60/40)



Dry Sliding Tribometer Test of Sample AL/E (60/40)
Load= 49.05N (5kg)
Sliding Speed= 400rpm
Sliding Distance= 3000m

$t_s$ = 4700.641s

Frictional Force of AL/E (60/40) against time



Dry Sliding Tribometer Test of Sample AL/E (60/40)
Load= 49.05N (5kg)
Sliding Speed= 400rpm
Sliding Distance= 3000m

1,643.657, 0.769

**Average CoF=0.504633**

Coefficient of Friction of AL/E (60/40) against time

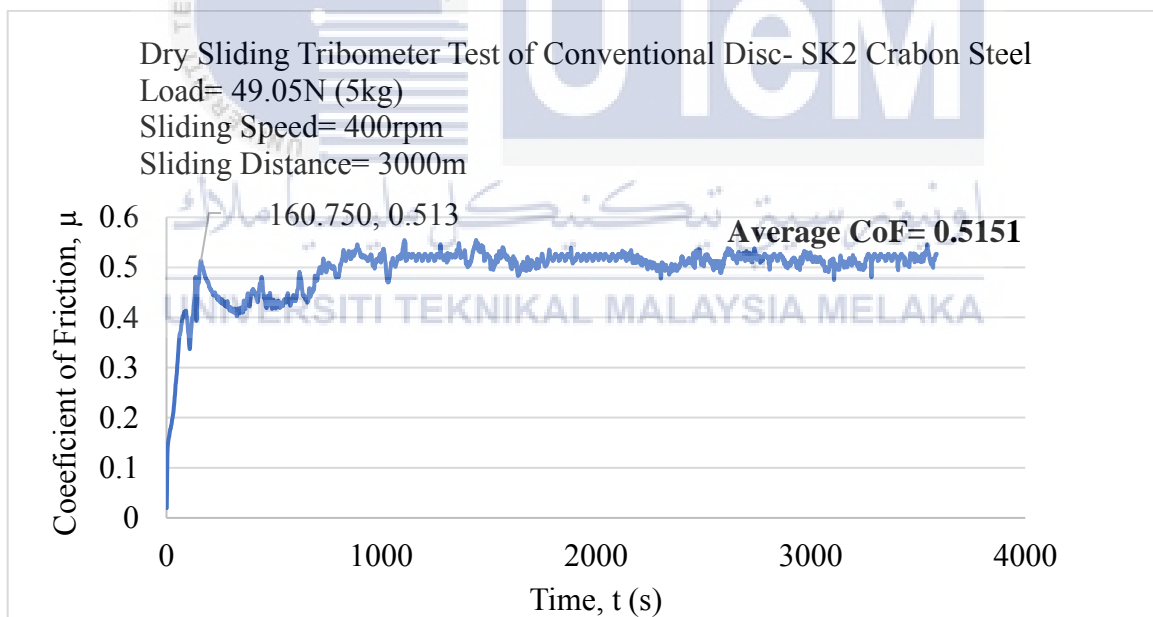7. Frictional force and coefficient of friction (CoF) results for PKAC/E (70/30)



Dry Sliding Tribometer Test of Sample PKAC/E (70/30)
Load= 49.05N (5kg)
Sliding Speed= 400rpm
Sliding Distance= 3000m

$t_s$= 966.812s

Frictional force of PKAC/E (70/30) against time



Dry Sliding Tribometer Test of Sample PKAC/E (70/30)
Load= 49.05N (5kg)
Sliding Speed= 400rpm
Sliding Distance= 3000m

80.953, 0.779

**Average CoF= 0.858157**

Coefficient of Friction of PKAC/E (70/30) against time

**8.** Frictional force and coefficient of friction (CoF) results for SK2 Carbon Steel



Dry Sliding Tribometer Test of Conventional Disc- SK2 Carbon Steel
Load= 49.05N (5kg)
Sliding Speed= 400rpm
Sliding Distance= 3000m

$t_s$= 1826.00s

**Frictional force of SK2 Carbon Steel against time**



Dry Sliding Tribometer Test of Conventional Disc- SK2 Crabon Steel
Load= 49.05N (5kg)
Sliding Speed= 400rpm
Sliding Distance= 3000m

160.750, 0.513

**Average CoF= 0.5151**

**Coefficient of Friction of SK2 Carbon Steel against time**

Specific wear rate calculations

1. Specific Wear Rate Calculation of PKAC+AL/E (50/50)

Parameters used in specific wear rate calculation of PKAC+AL/E (50/50)

| | PKAC+AL/E (50/50) |
|---|---|
| Mass before sliding test, $M_b$(g) | 33.515 |
| Mass after sliding test, $M_a$ (g) | 33.417 |
| Radius of Disc Sample, r (mm) | 37 |
| Thickness of Disc Sample, t (mm) | 5 |
| Load Applied, W (N) | 49.05 |
| Sliding Distance, L (mm) | $3\times10^6$ |

a) Volume of PKAC+AL/E (50/50), $V_{PA(50/50)} = \pi r^2 t$

$$= \pi (37)^2 (5)$$

$$= 2.150 \times 10^4 \, mm^3$$

b) Density of PKAC+AL/E (50/50), $\rho_{PA(50/50)} = \dfrac{Mass\ before\ sliding\ test}{Volume}$

$$= \frac{33.515}{2.150 \times 10^{\wedge}4}$$

$$= 1.559 \times 10^{-3} \, g/mm^3$$

c) Loss of mass of PKAC+AL/E (50/50) after sliding test, $M_{loss\ PA(50/50)}$

$$= 33.515 - 33.417$$

$$= 0.098g$$

d) Loss of Volume of PKAC+AL/E (50/50), $V_{loss\ PA(50/50)} = \dfrac{M_{loss\ PA(50/50)}}{\rho}$

$$= \frac{0.098}{1.559 \times 10^{-3}}$$

$$= 62.861\ mm^3$$

e) Specific Wear Rate of PKAC+AL/E (50/50), $k_{PA(50/50)} = \dfrac{V_{loss\ PA(50/50)}}{W \times L}$

$$= \frac{62.861}{49.05 \times 3000000}$$

$$= 4.272 \times 10^{-7}\ mm^3/Nmm$$

The specific wear rate calculated for PKAC+AL/E (50/50) is $4.272 \times 10^{-7}$ mm$^3$/Nmm.
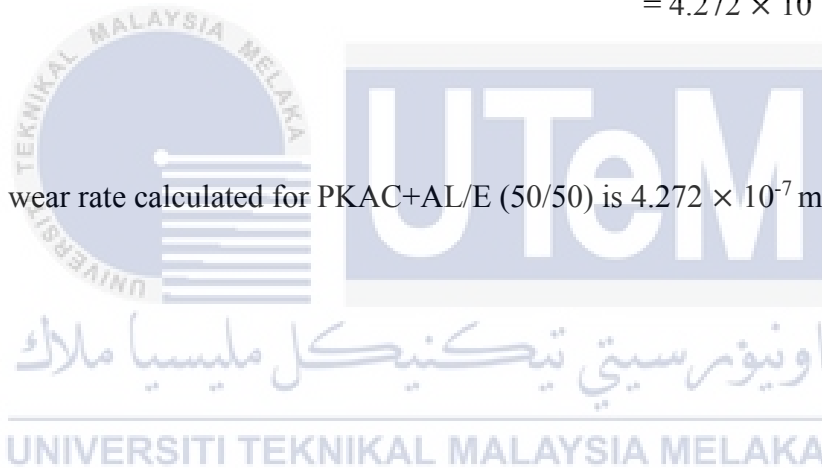
2. Specific Wear Rate Calculation of PKAC/E (50/50)

Parameters used in specific wear rate calculation of PKAC/E (50/50)

|  | PKAC/E (50/50) |
|---|---|
| Mass before sliding test, $M_b$(g) | 27.272 |
| Mass after sliding test, $M_a$ (g) | 27.244 |
| Radius of Disc Sample, r (mm) | 37 |
| Thickness of Disc Sample, t (mm) | 4.5 |
| Load Applied, W (N) | 49.05 |
| Sliding Distance, L (mm) | $3 \times 10^6$ |

a) Volume of PKAC/E (50/50), $V_{P(50/50)} = \pi r^2 t$

$$= \pi (37)^2 (4.5)$$

$$= 1.935 \times 10^4 \, mm^3$$

b) Density of PKAC/E (50/50), $\rho_{P(50/50)} = \dfrac{\text{Mass before sliding test}}{\text{Volume}}$

$$= \frac{27.272}{1.935 \times 10^{\wedge}4}$$

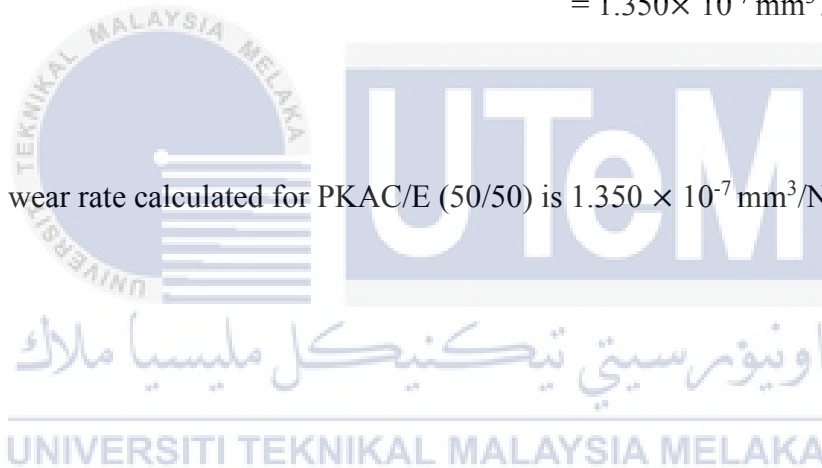$$= 1.409 \times 10^{-3} \, g/mm^3$$

c) Loss of mass of PKAC/E (50/50) after sliding test, $M_{loss \, P(50/50)} = 27.272 - 27.244$

$$= 0.028g$$

d) Loss of Volume of PKAC/E (50/50), $V_{loss\ P(50/50)} = \dfrac{M_{loss\ P(50/50)}}{\rho}$

$$= \frac{0.028}{1.409 \times 10^{-3}}$$

$$= 19.872 \text{ mm}^3$$

e) Specific Wear Rate of PKAC/E (50/50), $k_{P(50/50)} = \dfrac{V_{loss\ P(50/50)}}{W \times L}$

$$= \frac{19.872}{49.05 \times 3000000}$$

$$= 1.350 \times 10^{-7} \text{ mm}^3/\text{Nmm}$$

The specific wear rate calculated for PKAC/E (50/50) is $1.350 \times 10^{-7}$ mm$^3$/Nmm.

3. Specific Wear Rate Calculation of AL/E (50/50)

Parameters used in specific wear rate calculation of AL/E (50/50)

|  | AL/E (50/50) |
|---|---|
| Mass before sliding test, $M_b$(g) | 29.990 |
| Mass after sliding test, $M_a$ (g) | 29.790 |
| Radius of Disc Sample, r (mm) | 37 |
| Thickness of Disc Sample, t (mm) | 4.5 |
| Load Applied, W (N) | 49.05 |
| Sliding Distance, L (mm) | $3 \times 10^6$ |

a) Volume of AL/E (50/50), $V_{A(50/50)} = \pi r^2 t$

$$= \pi (37)^2 (4.5)$$

$$= 1.935 \times 10^4 \, mm^3$$

b) Density of AL/E (50/50), $\rho_{A(50/50)} = \dfrac{\text{Mass before sliding test}}{\text{Volume}}$

$$= \frac{29.990}{1.935 \times 10^{\wedge}4}$$
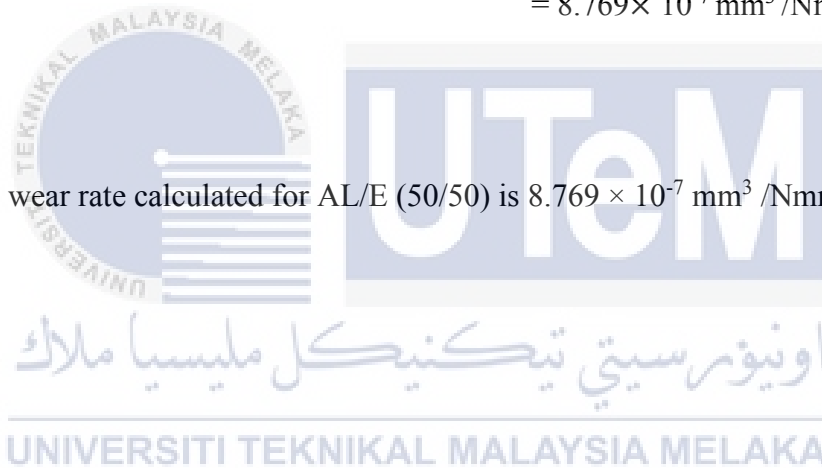
$$= 1.550 \times 10^{-3} \, g/mm^3$$

c) Loss of mass of AL/E (50/50) after sliding test, $M_{loss \, A(50/50)} = 29.990 - 29.790$

$$= 0.200g$$

91

d) Loss of Volume of AL/E (50/50), $V_{loss\ A(50/50)} = \dfrac{M\ loss\ A(50/50)}{\rho}$

$$= \dfrac{0.200}{1.550 \times 10^{-3}}$$

$$= 129.032\ mm^3$$

e) Specific Wear Rate of AL/E (50/50), $k_{A(50/50)} = \dfrac{Vloss\ A(50/50)}{W \times L}$

$$= \dfrac{129.032}{49.05 \times 3000000}$$

$$= 8.769 \times 10^{-7}\ mm^3\ /Nmm$$

The specific wear rate calculated for AL/E (50/50) is $8.769 \times 10^{-7}\ mm^3\ /Nmm$.

4. Specific Wear Rate Calculation of PKAC+AL/E (60/40)

Parameters used in specific wear rate calculation of PKAC+AL/E (60/40)

|  | PKAC+AL/E (60/40) |
|---|---|
| Mass before sliding test, $M_b$(g) | 36.938 |
| Mass after sliding test, $M_a$ (g) | 36.776 |
| Radius of Disc Sample, r (mm) | 37 |
| Thickness of Disc Sample, t (mm) | 4 |
| Load Applied, W (N) | 49.05 |
| Sliding Distance, L (mm) | $3 \times 10^6$ |

a) Volume of PKAC+AL/E (60/40), $V_{PA(60/40)} = \pi r^2 t$

$$= \pi (37)^2 (4)$$

$$= 1.720 \times 10^4 \text{ mm}^3$$

b) Density of PKAC+AL/E (60/40), $\rho_{PA(60/40)} = \dfrac{\text{Mass before sliding test}}{\text{Volume}}$

$$= \dfrac{36.938}{1.720 \times 10^{\wedge}4}$$

$$= 2.148 \times 10^{-3} \text{ g/mm}^3$$

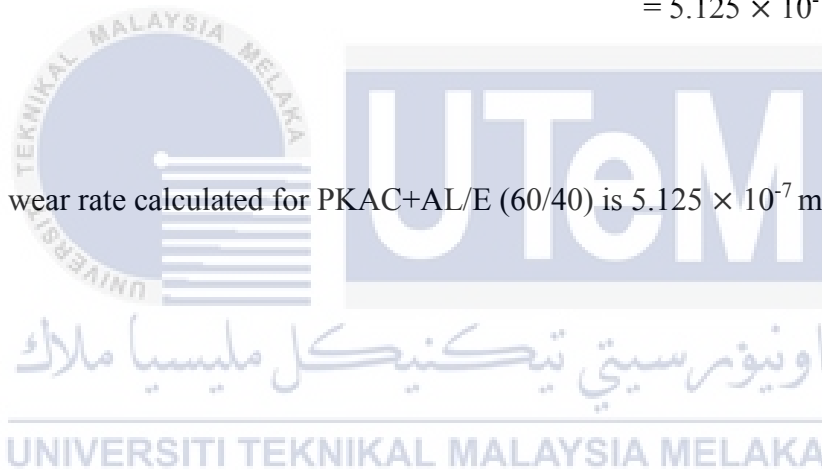c) Loss of mass of PKAC+AL/E (60/40) after sliding test, $M_{loss\ PA(60/40)}$

$$= 36.938 - 36.776$$

$$= 0.162\text{g}$$

d) Loss of Volume of PKAC+AL/E (60/40), $V_{\text{loss PA(60/40)}} = \dfrac{M_{\text{loss PA(60/40)}}}{\rho}$

$$= \dfrac{0.162}{2.148 \times 10^{-3}}$$

$$= 75.419 \text{ mm}^3$$

e) Specific Wear Rate of PKAC+AL/E (60/40), $k_{\text{PA(60/40)}} = \dfrac{V_{\text{loss PA(60/40)}}}{W \times L}$

$$= \dfrac{75.419}{49.05 \times 3000000}$$

$$= 5.125 \times 10^{-7} \text{ mm}^3/\text{Nmm}$$

The specific wear rate calculated for PKAC+AL/E (60/40) is $5.125 \times 10^{-7}$ mm$^3$/Nmm.

5. Specific Wear Rate Calculation of PKAC/E (60/40)

Parameters used in specific wear rate calculation of PKAC/E (60/40)

|  | PKAC/E (60/40) |
|---|---|
| Mass before sliding test, $M_b$(g) | 22.966 |
| Mass after sliding test, $M_a$ (g) | 22.926 |
| Radius of Disc Sample, r (mm) | 37 |
| Thickness of Disc Sample, t (mm) | 4 |
| Load Applied, W (N) | 49.05 |
| Sliding Distance, L (mm) | $3 \times 10^6$ |

a) Volume of PKAC/E (60/40), $V_{P(60/40)} = \pi r^2 t$

$$= \pi (37)^2 (4)$$

$$= 1.720 \times 10^4 \, mm^3$$

b) Density of PKAC/E (60/40), $\rho_{P(60/40)} = \dfrac{Mass\ before\ sliding\ test}{Volume}$

$$= \dfrac{22.966}{1.720 \times 10^{\wedge}4}$$

$$= 1.335 \times 10^{-3} \, g/mm^3$$

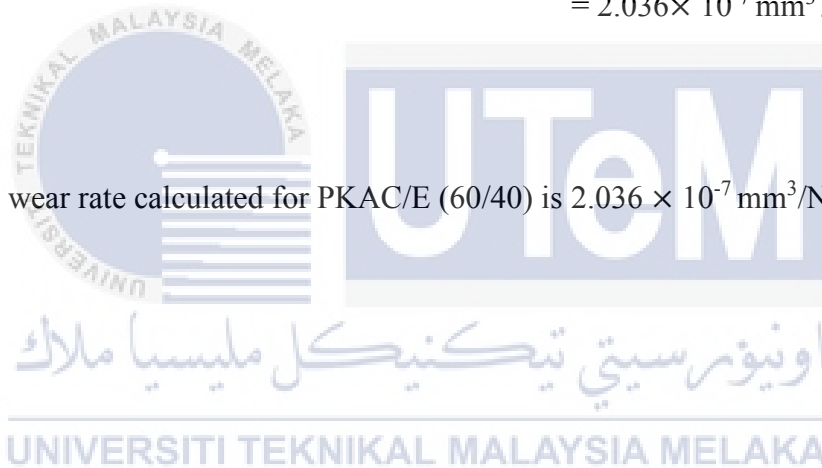c) Loss of mass of PKAC/E (60/40) after sliding test, $M_{loss\ P(60/40)} = 22.966 - 22.926$

$$= 0.039g$$

95

d) Loss of Volume of PKAC/E (60/40), $V_{\text{loss P}(60/40)} = \dfrac{M_{\text{loss P}(60/40)}}{\rho}$

$$= \dfrac{0.039}{1.335 \times 10^{-3}}$$

$$= 29.957 \text{ mm}^3$$

e) Specific Wear Rate of PKAC/E (60/40), $k_{\text{P}(60/40)} = \dfrac{V_{\text{loss P}(60/40)}}{W \times L}$

$$= \dfrac{29.957}{49.05 \times 3000000}$$

$$= 2.036 \times 10^{-7} \text{ mm}^3 / \text{Nmm}$$

The specific wear rate calculated for PKAC/E (60/40) is $2.036 \times 10^{-7}$ mm$^3$/Nmm.

6. Specific Wear Rate Calculation of AL/E (60/40)

Parameters used in specific wear rate calculation of AL/E (60/40)

|  | AL/E (60/40) |
|---|---|
| Mass before sliding test, $M_b$(g) | 38.240 |
| Mass after sliding test, $M_a$ (g) | 37.980 |
| Radius of Disc Sample, r (mm) | 37 |
| Thickness of Disc Sample, t (mm) | 5 |
| Load Applied, W (N) | 49.05 |
| Sliding Distance, L (mm) | $3 \times 10^6$ |

a) Volume of AL/E (60/40), $V_{A(60/40)} = \pi r^2 t$

$$= \pi (37)^2 (5)$$

$$= 2.150 \times 10^4 \, mm^3$$

b) Density of AL/E (60/40), $\rho_{A(60/40)} = \dfrac{\text{Mass before sliding test}}{\text{Volume}}$

$$= \frac{38.240}{2.150 \times 10^{\wedge}4}$$
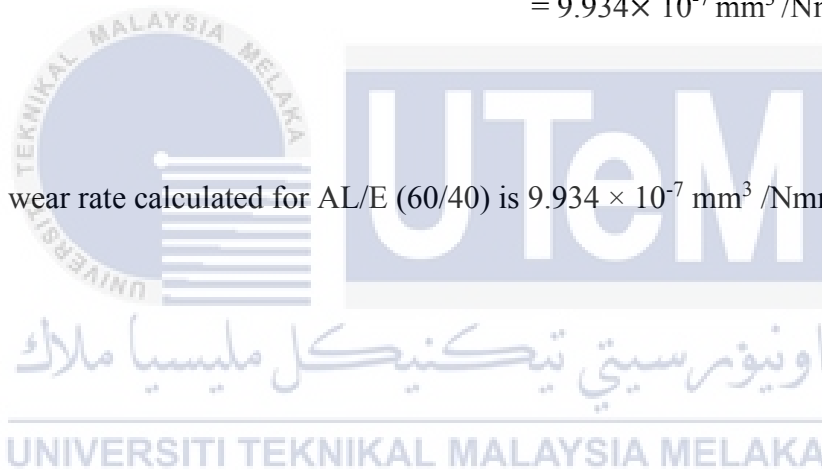
$$= 1.779 \times 10^{-3} \, g/mm^3$$

c) Loss of mass of AL/E (60/40) after sliding test, $M_{loss\ A(60/40)} = 38.240 - 37.980$

$$= 0.260g$$

97

d) Loss of Volume of AL/E (60/40), $V_{loss\ A(60/40)} = \dfrac{M\ loss\ A(60/40)}{\rho}$

$$= \dfrac{0.260}{1.779 \times 10^{-3}}$$

$$= 146.182\ mm^3$$

e) Specific Wear Rate of AL/E (60/40), $k_{A(60/40)} = \dfrac{Vloss\ A(60/40)}{W \times L}$

$$= \dfrac{146.182}{49.05 \times 3000000}$$

$$= 9.934 \times 10^{-7}\ mm^3\ /Nmm$$

The specific wear rate calculated for AL/E (60/40) is $9.934 \times 10^{-7}\ mm^3$ /Nmm.

7. Specific Wear Rate Calculation of PKAC/E (70/30)



Parameters used in specific wear rate calculation of PKAC/E (70/30)

|  | PKAC/E (70/30) |
|---|---|
| Mass before sliding test, $M_b$(g) | 24.612 |
| Mass after sliding test, $M_a$ (g) | 24.577 |
| Radius of Disc Sample, r (mm) | 37 |
| Thickness of Disc Sample, t (mm) | 5 |
| Load Applied, W (N) | 49.05 |
| Sliding Distance, L (mm) | $1.3 \times 10^6$ |

a) Volume of PKAC/E (70/30), $V_{P(70/30)} = \pi r^2 t$

$$= \pi (37)^2 (5)$$

$$= 2.150 \times 10^4 \, mm^3$$

b) Density of PKAC/E (70/30), $\rho_{P(70/30)} = \dfrac{\text{Mass before sliding test}}{\text{Volume}}$

$$= \dfrac{24.612}{2.150 \times 10^\wedge 4}$$
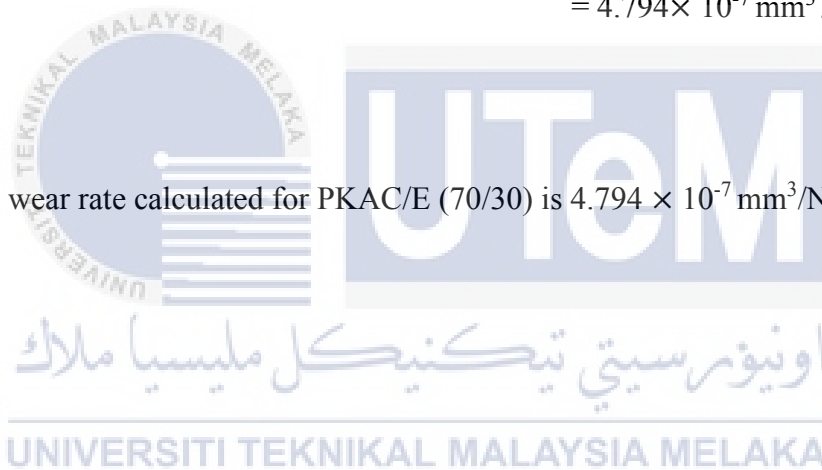
$$= 1.145 \times 10^{-3} \, g/mm^3$$

c) Loss of mass of PKAC/E (70/30) after sliding test, $M_{loss\ P(70/30)} = 24.612 - 24.577$

$$= 0.035g$$

d) Loss of Volume of PKAC/E (70/30), $V_{loss\ P(70/30)} = \dfrac{M_{loss\ P(70/30)}}{\rho}$

$$= \dfrac{0.035}{1.145 \times 10\char`\^-3}$$

$$= 30.568 \text{ mm}^3$$

e) Specific Wear Rate of PKAC/E (70/30), $k_{P(70/30)} = \dfrac{V_{loss\ P(70/30)}}{W \times L}$

$$= \dfrac{30.568}{49.05 \times 1300000}$$

$$= 4.794 \times 10^{-7} \text{ mm}^3 \text{/Nmm}$$

The specific wear rate calculated for PKAC/E (70/30) is $4.794 \times 10^{-7}$ mm$^3$/Nmm.

8. Specific Wear Rate Calculation of SK2 Carbon Steel Disc

Parameters used in specific wear rate calculation of SK2 Carbon Steel Disc

|  | SK2 Carbon Steel Disc |
| --- | --- |
| Mass before sliding test, $M_b$(g) | 131.500 |
| Mass after sliding test, $M_a$ (g) | 131.380 |
| Radius of Disc Sample, r (mm) | 37 |
| Thickness of Disc Sample, t (mm) | 4 |
| Load Applied, W (N) | 49.05 |
| Sliding Distance, L (mm) | $1.3 \times 10^6$ |

a) Volume of SK2 Carbon Steel Disc, $V_{SK2} = \pi r^2 t$

$$= \pi (37)^2 (4)$$

$$= 1.720 \times 10^4 \, mm^3$$

b) Density of SK2 Carbon Steel Disc, $\rho_{SK2} = \dfrac{\text{Mass before sliding test}}{\text{Volume}}$

$$= \frac{131.500}{1.720 \times 10^4}$$

$$= 7.644 \times 10^{-3} \, g/mm^3$$

Loss of mass of SK2 Carbon Steel Disc after sliding test, $M_{loss \, SK2} = 131.500 - 131.380$

$$= 0.120g$$

c) Loss of Volume of SK2 Carbon Steel Disc, $V_{loss\ SK2} = \dfrac{M\ loss\ P(70/30)}{\rho}$

$$= \frac{0.120}{7.644 \times 10^{-3}}$$
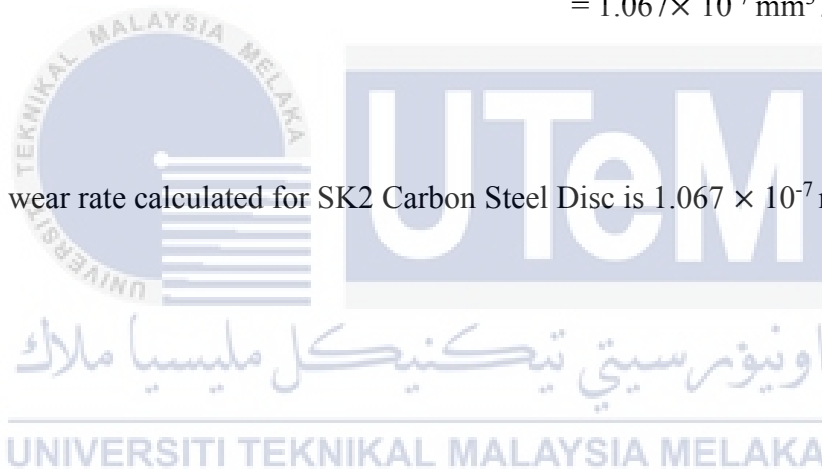
$$= 15.699\ mm^3$$

d) Specific Wear Rate of SK2 Carbon Steel Disc, $k_{SK2} = \dfrac{V\ loss\ P(70/30)}{W \times L}$

$$= \frac{15.699}{49.05 \times 3000000}$$

$$= 1.067 \times 10^{-7}\ mm^3\ /Nmm$$

The specific wear rate calculated for SK2 Carbon Steel Disc is $1.067 \times 10^{-7}$ mm$^3$/Nmm.

Project timeline Gantt Chart for PSM 1

| No | Task | Week | | | | | | | | | | | | | | |
|---|---|---|---|---|---|---|---|---|---|---|---|---|---|---|---|---|
| | | 1 | 2 | 3 | 4 | 5 | 6 | 7 | 8 | 9 | 10 | 11 | 12 | 13 | 14 | 15 |
| 1 | Collect Information | █ | █ | █ | █ | █ | █ | █ | █ | █ | █ | █ | █ | █ | █ | █ |
| 2 | Project Planning | █ | █ | | | | | | | | | | | | | |
| 3 | Preparation of Chapter 1 Introduction | █ | █ | █ | | | | | | | | | | | | |
| 4 | Literature Study | █ | █ | █ | █ | | | | | | | | █ | █ | █ | █ |
| 5 | Preparation of Chapter 2 Literature Review | | | █ | █ | █ | | | | | | | | | | |
| 6 | Methodology Planning | | | | | █ | █ | | | | | | | | | |
| 7 | Preparation of Chapter 3 Methodology | | | | | | █ | █ | █ | | | | | | | |
| 8 | Preparation of Specimens | | | | | | █ | █ | █ | █ | █ | █ | █ | █ | | |
| 9 | Preliminary Tribometer Test | | | | | | | | | | █ | █ | █ | █ | | |
| 10 | Preparation of Chapter 4 Preliminary Results and Discussions | | | | | | | | | | █ | █ | █ | █ | | |
| 11 | PSM 1 Draft Report Submission | | | | | | | | | | | | | | █ | |
| 12 | PSM 1 Presentation | | | | | | | | | | | | | | | █ |

Project timeline Gantt Chart for PSM 2

| No | Task | Week | | | | | | | | | | | | | | |
|---|---|---|---|---|---|---|---|---|---|---|---|---|---|---|---|---|
| | | 1 | 2 | 3 | 4 | 5 | 6 | 7 | 8 | 9 | 10 | 11 | 12 | 13 | 14 | 15 |
| 1 | Collect Information | █ | █ | █ | █ | █ | █ | █ | █ | █ | █ | █ | █ | █ | █ | █ |
| 2 | Preparation and Correction of Chapter 3 Methodology | █ | █ | | | | | | | | | | | | | |
| 3 | Preparation of Specimens | █ | █ | █ | | | | | | | | | | | | |
| 4 | Literature Study | █ | █ | █ | █ | █ | █ | █ | █ | █ | █ | █ | █ | █ | █ | █ |
| 5 | Ball-on-Disc Tribometer Test | | | | █ | █ | █ | █ | █ | █ | █ | █ | | | | |
| 6 | 3D Surface Morphology | | | | | | | | | | | | █ | | | |
| 7 | Preparation of Chapter 4 Results and Discussions | | | | █ | █ | █ | █ | █ | █ | █ | █ | █ | █ | | |
| 8 | Preparation of Chapter 5 Conclusion and Recommendations | | | | | | | | | █ | █ | █ | █ | █ | | |
| 9 | Review PSM 2 Draft Report | | | | | | | | | | | █ | █ | █ | | |
| 11 | PSM 2 Draft Report Submission | | | | | | | | | | | | | | █ | |
| 12 | PSM 2 Presentation | | | | | | | | | | | | | | | █ |